SEROTONIN TRANSPORTERS IN DEPRESSION

Sudhakar Selvaraj



St Catherine's College, Oxford

&

University Department of Psychiatry, Oxford

This thesis is submitted to the University of Oxford for the degree of Doctor of Philosophy

Trinity term 2010

Abstract

SEROTNIN TRANSPORTERS IN DEPRESSION

Sudhakar Selvaraj, St Catherine's College, Oxford

Submitted for the degree of Doctor of Philosophy, University of Oxford, Trinity term 2010.

Major depression is a common, recurrent and severe mental illness and is a leading cause of medical disability worldwide. The pathophysiology of depression is not well understood but evidence strongly suggests that dysfunction in brain serotonin (5-HT) neurons may play a significant role. The serotonin transporter (5-HTT) recycles released 5-HT back into neurons and is a key regulator of 5-HT neurotransmission. Abnormality in the 5-HTT has been proposed as an important mechanism in the etiopathophysiology and in the treatment of depression. Using positron emission tomography (PET) in conjunction with [^{11}C] DASB, a selective 5-HTT radiotracer, it is now possible to measure the 5-HTT in the living human brain. The aim of this thesis was to study 5-HTT binding in major depression and also to identify the effect of a 5-HTT genetic polymorphism on 5-HTT binding and brain morphology.

Unmedicated, acutely depressed patients had diminished availability of the 5-HTT in several brain regions including the brain stem, thalamus, caudate, putamen, anterior cingulate cortex and frontal cortex. However, there was no significant difference in 5-HTT availability between unmedicated recovered depressed patients and healthy comparison subjects in any of the brain regions studied. There was no significant difference in brain 5-HTT availability in healthy controls with different 5-HTT polymorphic variations. However, brain morphological analysis revealed reduced brain gray matter volume in S' allele carriers vs L'L' homozygotes in several brain regions including anterior cingulate cortex.

The results suggest at least in a subgroup of patients, acute depression is associated with decreased availability of the 5-HTT as measured by ligand PET. The results indicate that this abnormality is a state marker of depression but this needs to be confirmed by future studies following the *same* group of patients through depression, treatment and its resolution. The findings also suggest that if the 5-HTT promoter polymorphism exerts a reliable effect on the risk of depression it is not mediated through changes in the 5-HTT but more probably through modifications in brain morphology perhaps of neurodevelopmental origin.

Declaration

The chapters described in this study have been published as the following papers. I confirm that I was the principal researcher in each of the studies which were conducted in collaboration with a number of colleagues. Although other co-researchers (Dr Zubin Bhagwagar and Dr Venkatesha Naga Murthy) involved in the study recruited part of the study subjects, I recruited most of the healthy subjects and patients involved in the study. Furthermore, I carried out data collection, PET image analysis, statistical analysis of the results, writing up of scientific papers and also project-related administration work.

Chapter 3 is published as Hinz R, Selvaraj S, Murthy NV, Bhagwagar Z, Taylor M, Cowen PJ, Grasby PM. Effects of citalopram infusion on the serotonin transporter binding of [11C]DASB in healthy controls. J Cereb Blood Flow Metab. 2008 Aug;28(8):1478-90. I recruited 3 out of 4 subjects who were studied. I did the image analysis, PET modeling and statistical analysis with the help of Dr Rainer Hinz.

Chapter 4 is published as *Selvaraj S, * Venkatesha Murthy N, Bhagwagar Z, Bose SK, Hinz R, Grasby PM, Cowen PJ. Diminished brain 5-HT transporter binding in major depression: a positron emission tomography study with [(11)C]DASB. Psychopharmacology (Berl). 2009 Sep 16. [Epub ahead of print]. I recruited 15 out of 24 healthy volunteers and 9 out of 12 patients while Dr Venkatesha Naga Murthy recruited the remaining subjects. I have shared 1st authorship with Dr Venkatesha Naga Murthy.

Chapter 5 is published as Bhagwagar Z, Murthy N, Selvaraj S, Hinz R, Taylor M, Fancy S, Grasby P, Cowen P. 5-HTT binding in recovered depressed patients and healthy volunteers: a positron emission tomography study with [11C]DASB. Am J Psychiatry. 2007 Dec;164(12). I recruited 14 out of 24 patients in this study. I did the image analysis, PET modeling, statistical analysis and writing up with the help of other co-researchers.

Chapter 6 is published as * Murthy NV, * Selvaraj S, Cowen PJ, Bhagwagar Z, Riedel WJ, Peers P, Kennedy JL, Sahakian BJ, Laruelle MA, Rabiner EA,

Grasby PM. Serotonin transporter polymorphisms (SLC6A4 insertion/deletion and rs25531) do not affect the availability of 5-HTT to [11C] DASB binding in the living human brain. Neuroimage. 2010 Aug 1;52(1):50-4. I recruited 23 out of 63 subjects and the rest were recruited by Dr Venkatesha NagaMurthy for another study looking at vulnerability markers in healthy subjects with a family risk of depression. Dr Venkatesha Naga Murthy and I shared the image analysis, PET modeling, statistical analysis and writing up and I have shared 1st authorship with him.

Chapter 7 is published as Selvaraj S, Godlewska BR, Norbury R, Bose S, Turkheimer F, Stokes P, Rhodes R, Howes O, Cowen PJ. Decreased regional gray matter volume in S' allele carriers of the 5-HTTLPR triallelic polymorphism. Mol Psychiatry. 2010 Nov 2. [Epub ahead of print].

Acknowledgement

This thesis would not have been possible without the support and guidance of Professor Philip Cowen. He has not only provided regular day-to-day supervision but also taught me intellectual curiosity and a humble attitude toward research. I would like to thank many colleagues who have helped me accomplish this thesis. Professor Paul Grasby was the day-to-day scientific mentor at the MRC Cyclotron unit and I liked his meticulous approach to science. Professor Guy Goodwin has provided overall departmental support for this work. Professor Paul Harrison was inspirational to me and to others in the department and was always willing to offer advice. I would like to acknowledge Zubin Bhagwagar who was my early mentor and co-investigator for his encouragement and support. Venkatesha Murthy, Rainer Hinz, Ray Norbury, Beata Godlewska and Matthew Taylor are colleagues at MRC Cyclotron unit and Oxford who have worked on some of the projects and were instrumental in completing the work.

MRC Cyclotron unit staff members were critical in successfully running the project. I would like to thank the radiographers (Andy Blyth, Hope McDevitt, Andrea Williams), mathematical modellers (Rainer Hinz, Federico Turkheimer), chemistry (Shaun Creasey) and blood analysis team (Safiye Osman, Noora Ali), image reconstruction team (Len), physicist (Terry Spinks), Medical Radiation expert (Melvyn Meyers) and other General Electric IMANET staff. I would like to especially thank Subrata Bose for his technical and computing expertise and Jamie Swingland for stimulating scientific discussions. I would like to thank Linda Carter, Rena Hockney, Pam Taylor and Shazi Singh for administrative support which undoubtedly made my work easier.

The study projects would not have been possible without the patience and enthusiasm of the study volunteers and patients who took part in the studies.
I have learned how arduous a task is to manage a clinical research project.

I would like to thank my wife Birundha for her patience (even forgoing holidays) and support which kept me in balance and motivated me to complete my work. Finally, I could not have come to this level in my career without my parents and family to whom I am eternally indebted.

List of Chapters

Abstract 2

Declaration 4

Acknowledgement 6

List of Chapters 7

Table of Contents 8

List of Figures 14

List of Tables 16

Glossary of Abbreviation 17

1 Introduction 18

2 General Methods 63

3 Effects of Citalopram Infusion on 5-HTT Binding ..... ……116

4 5-HTT Binding in Major Depression 150

5 5-HTT Binding in Recovered Depressed Patients 168

6 5-HTT Polymorphisms and [^{11}C] DASB Binding 186

7 5-HTTLPR Triallelic Polymorphism and Brain Morphometry 200

8 Summary and Discussion 215

References 229

Table of Contents

Abstract 2

Declaration 4

Acknowledgement 6

List of Chapters 7

Table of Contents 8

List of Figures 14

List of Tables 16

Glossary of Abbreviation 17

1 Introduction 18

1.1 Depression 19

1.1.1 Clinical Features and Diagnosis 19

1.1.2 Stages of Illness 21

1.1.3 Epidemiology 22

1.1.4 Clinical Course 24

1.1.5 Treatment 25

1.1.6 Etiology of Depression 28

1.2 Serotonin (5-HT) System 30

1.2.1 Background 30

1.2.2 5-HT Synthesis 31

1.2.3 5-HT Neurobiology 31

1.2.4 5-HT Transporter (5-HTT) 35

1.3 5-HT in Depression 35

1.3.1 5-HT Metabolism in Depression 36

1.3.2 5-HT Neuroendocrine Challenge Tests 37

1.3.3 Tryptophan Depletion Test 37

1.3.4 Post Mortem 5-HT_{1A} And 5-HT_{2A} Studies in Depression 38
1.3.5 Positron Emission Tomography Studies in Depression 40
1.4 5-HTT Studies in Depression 45
1.4.1 Platelet 5-HTT Binding in Depression 45
1.4.2 Post-Mortem Brain 5-HTT Binding in Depression 46
1.4.3 5-HTT Imaging Studies in Depression 47
1.4.3.1 Single Photon Emission Tomography (SPET) Studies 47
1.4.3.2 Positron Emission Tomography (PET) Studies 48
1.5 Quantification of [^{11}C]DASB Binding 56
1.6 5-HTT Genetic Polymorphism and 5-HTT Binding 57
1.6.1 5-HTT Gene and Function 57
1.6.2 5-HTTLPR and 5-HTT Binding in Platelets and Post-Mortem Brain ……..58
1.6.3 5-HTTLPR and 5-HTT Binding using Brain Imaging 59
1.7 5-HTTLPR and Brain Structure 60
1.8 Aims of the Thesis 62
2 General Methods 63
2.1 Approval for Studies 64
2.2 Participants 64
2.2.1 Recruitment 64
2.2.2 Study Participant Screening Interview 65
2.2.3 Inclusion Criteria for Controls 66
2.2.4 Exclusion Criteria for Controls 66
2.2.5 Inclusion Criteria for Recovered Depressed Patients 66
2.2.6 Inclusion Criteria for Depressed Patients 67
2.2.7 Exclusion Criteria for Acute and Recovered Depressed Patients . 68
2.3 Psychological Questionnaires 68
2.4 Positron Emission Tomography (PET) Imaging - Background and Principle 69
2.4.1 The Fundamentals of PET Physics 70

2.4.2 PET Camera 71
2.4.3 Coincidence Detection 72
2.4.4 Sources of Error in PET Data Acquisition 72
2.4.5 PET Image Reconstruction 73
2.5 Principles of Radiotracer 75
2.5.1 Radiotracer For 5-HTT 76
2.5.2 [^{11}C]DASB Synthesis 78
2.5.3 In-Vitro and In-Vivo Characteristics 78
2.5.4 Bio-Distribution and Dosimetry 79
2.5.5 [^{11}C]DASB Brain Distribution 79
2.6 PET Data Analysis 80
2.6.1 Basic Tracer Pharmacokinetics 80
2.6.2 PET Quantification 82
2.6.3 Compartmental Modelling 84
2.6.3.1 Binding Potential and Affinity 88
2.6.3.2 Volume of Distribution 90
2.6.4 Methods of Data Analysis 91
2.6.4.1 Kinetic Modelling 91
2.6.4.2 Graphical Analysis 91
2.6.4.3 Reference Tissue Models 92
2.6.4.4 Spectral Analysis 92
2.6.4.5 Equilibrium Method 93
2.7 Test Retest Reliability of [^{11}C]DASB 93
2.8 The Limitations of PET Imaging 94
2.9 MRI and Brain Morphology 95
2.9.1 Region of Interest (ROI) Analysis 96
2.9.2 Voxel-Based Morphometry 96
2.9.3 VBM Methodology 97
2.9.4 VBM Limitations 99

2.10 Experimental Procedure for Participants undergoing PET Scans With [^{11}C]DASB 100

2.10.1 Pet Scan Acquisition 100

2.10.2 [^{11}C]DASB Synthesis 102

2.10.3 [^{11}C]DASB Injection 103

2.10.4 Arterial Input Function 103

2.10.5 MRI Scans and Regions of Interest (ROI) Definition 104

2.10.6 Generation of the Plasma Input Function 108

2.10.7 Quantification of the Ligand Binding in Tissue 111

2.11 Statistical Methods 114

3 Effects of Citalopram infusion on 5-HTT Binding 116

3.1 Introduction 117

3.2 Materials and Methods 120

3.2.1 Subjects and Medication 120

3.2.2 Positron Emission Tomography Scan Acquisition 121

3.2.3 MRI Scans and Definition of Regions of interest……123

3.2.3.2 Generation of the Plasma Input Function 123

3.2.3.3 Quantification of the Ligand Binding in Tissue 124

3.3 Results 125

3.3.1 Input Function 125

3.3.2 Tissue Response 131

3.4 Discussion 142

4 5-HTT Binding in Major Depression 150

4.1 Introduction 151

4.2 Methods and Materials 153

4.2.1 Participants 153

4.2.2 PET Scanning 154

4.2.3 MRI Scans and Definition of Volumes of Interest 155

4.2.4 Quantification of DASB Binding 156

4.3 Statistical Analysis 158

4.4 Results 158
4.5 Discussion 163
4.5.1 Modelling Methods in Ligand Imaging 164
5 5-HTT Binding in Recovered Depressed Patients 168
5.1 Introduction 169
5.2 Methods 170
5.2.1 Participants 170
5.2.2 PET Scanning 171
5.2.3 Radiotracer 171
5.2.4 MRI Scans and Definition of Regions of Interest 172
5.2.5 Input Function 173
5.2.6 Quantification of DASB Binding 173
5.3 Statistical Analysis 174
5.4 Results 174
5.5 Discussion 180
5.5.1 Relationship of Low 5-HTT Binding and Clinical Symptomatology…... 183
6 5-HTT Polymorphisms and [^{11}C] DASB Binding 186
6.1 Introduction 187
6.2 Materials and Methods 189
6.2.1 Participants 189
6.2.2 Genotyping 190
6.2.3 Statistical Analysis 191
6.3 Results 191
6.4 Discussion 194
7 5-HTTLPR Triallelic Polymorphism and Brain Morphometry 200
7.1 Introduction 201
7.2 Methods 203
7.2.1 Study Participants 203

7.2.2 MRI Acquisition 204
7.2.3 Regions of Interest (ROI) Analysis 204
7.2.4 VBM Preprocessing 204
7.2.5 Genotyping 205
7.2.6 Statistics 206
7.3 Results 206
7.4 Discussion 207
8 Summary and Discussion 215
8.1 Summary of Main Findings 216
8.1.1 Study 1: 216
Aim 216
Results 216
8.1.2 Study 2: 217
Aim 217
Results 217
8.1.3 Study 3: 217
Aim 217
Results 217
8.1.4 Study 4: 218
Aim 218
Results 218
8.1.5 Study 5: 218
Aim 218
Results 219
8.2 Discussion 219
8.2.1 5-HTT in Depression 219
8.2.2 Future Directions 221
8.2.3 PET Methodological Issues 222
8.2.4 5-HTT Transporter Gene, 5-HTT and Brain Morphology 224
8.2.5 Conclusion 227
References 229

List of Figures

Figure 1-1: 5-HT metabolism 32

Figure 1.2: 5-HT innervation in the human brain..... 33

Figure 2-1– Positron emission and annihilation 71

Figure 2-2– Coincidence event in a PET camera 74

Figure 2-3 – Sources of error in PET acquisition 75

Figure 2-4: Chemical structure of [^{11}C]DASB..... 78

Figure 2.4a & 2.4b: Blood and tissue time-activity curve respectively 84

Figure 2-5: PET Compartment model 86

Figure 2-6: Overview of Voxel-Based Morphometry pre-processing..... 98

Figure 2-7: Flow chart of standard and optimised Voxel-based morphometry (VBM)..... 99

Figure 2-8: [^{11}C]DASB scan with frame information and total count rate per frame from a healthy participant 102

Figure 2-9: [^{11}C]DASB Image analysis flow chart 106

Figure 2-10: Fraction of unmetabolized parent [^{11}C]DASB compound in arterial plasma over time..... 109

Figure 2.11: Ratio of plasma activity concentration over whole blood activity over the scan duration from a healthy participant 110

Figure 2-12: [^{11}C]DASB Logan plot from a healthy participant showing brain stem (Top) and cerebellum (bottom) 112

Figure 3-1: Mean plasma citalopram concentrations (±SEM) following 10 mg, 20 mg and 40 mg infusions..... 121

Figure 3-2: Ratio of plasma activity concentration over whole blood activity concentration after placebo infusion or citalopram infusion. 127

Figure 3-3: Fraction of unmetabolised parent compound in arterial plasma after placebo infusion or citalopram infusion. 128

Figure 3-5: Relative bias of the estimated slope from the Logan plot analysis as a function of the threshold time t*. 135

Figure 3-6 Oblique slice through parametric images of the total volume of distribution V_T from the same subject as in Figure 3-4 generated with spectral analysis after placebo infusion (A) and after citalopram infusion (B) 141

Figure 4-1: MRI and [^{11}C]DASB summated image from a representative control subject in the left and middle column, respectively and [^{11}C]DASB summated image from a acute depressed (right most column) 163

Figure 5-1: Mean [^{11}C]DASB VD (volume of distribution) images obtained from parametric maps generated with spectral analysis of healthy volunteers (N=20, left) and recovered depressed patients (N=24, right) in the coronal, sagittal and transverse views respectively. 178

Figure 5-2: Scatter plots of individual BP estimates of [^{11}C]DASB in the regions of interest (ROIs). 179

Figure 7-1: Displayed are axial, coronal and sagittal images depicting significantly reduced gray matter volume in S' allele carriers vs L'L' homozygotes in right inferior frontal gyrus. 213

Figure 7-2: Axial and coronal depicting significantly reduced gray matter volume in S' allele carriers vs L'L' homozygotes in (a) left anterior cingulate and (b) superior temporal gyrus 214

List of Tables

Table 1-1 DSM-4 diagnostic criteria for Dysthymia 21

Table 1-2: 5-HT receptor type and physiology 34

Table 1-3: 5-HT_{1A} and 5-HT_{2A} ligand imaging studies in depression 41

Table 1-4: 5-HTT Imaging studies in depression..... 50

Table 3-2: Parameter estimates from the graphical analysis of reversible binding regional tissue time-activity curves 139

Table 3-3 Parameter estimated from sampling of parametric maps of V_T generated with spectral analysis 140

Table 4-1: Clinical characteristics of the participants and Radiochemical parameters 159

Table 4-2: Binding potential (BP_P) (ml.cm-3) and BP_{ND} of [^{11}C]DASB in control subjects and medication-free acute depressed patients. 162

Table 6-1: Mean (SD) [^{11}C] DASB binding potential in different brain regions by 5-HTTLPR biallelic genotypes..... 193

Table 6-2: Mean (SD) [^{11}C] DASB binding potential in different brain regions by 5-HTTLPR gain of function triallelic genotypes 193

Table 7-1: Characteristics of Regions of Interest (ROI) based studies..... 211

Table 7-2: Characteristics of Voxel-based morphometry (VBM) based studies……212

Glossary of Abbreviation

[^{11}C]DASB	[^{11}C]N,N-dimethyl-2-(2-amino-4-cynophenylthio)benzylamine
5-HT	5-hydroxy tryptamine or Serotonin
5-HTT	5- hydroxy tryptamine transporter
ANOVA	Analysis of variance
BDI	Beck depression inventory
BP	Binding potential
DAS	Dysfunctional attitude scale
DSM	Diagnostic and statistical manual of mental disorders
HAM-D	Hamilton depression rating scale
K_D	Dissociation constant
MRI	Magnetic resonance imaging
PET	Positron emission tomography
RMMANOVA	Repeated measures of analysis of variance
ROI	Region of interest
SCID	Structured clinical interview for DSM-IV disorders
SD	Standard deviation
SEM	Standard error of the mean
SPET	Single photon emission tomography
SSRI	Selective serotonin reuptake inhibitor
VBM	Voxel-based Morphometry

1 INTRODUCTION

1.1 DEPRESSION

Depression is a common, recurrent and severe mental illness associated with substantial long-term disability. It is characterised by symptoms such as depressed or irritable mood, tiredness, lack of interest in pleasurable activities, poor sleep and appetite, low self-esteem, cognitive difficulties and suicidal thoughts.

1.1.1 Clinical features and Diagnosis

The diagnosis of depression is essentially clinical and is currently made by the use of reliable diagnostic schedules such as the Diagnostic and Statistical Manual of Mental Disorders or DSM-IV (Table 1-1) and the International Classification of Diseases (ICD-10). The American Psychiatric Association has specified criteria for Major Depressive Disorder (MDD) in the DSM-IV which is as follows;

A. Five (or more) of the following symptoms have been present during the same 2-week period and represent a change from previous functioning; at least one of the symptoms is either (1) depressed mood or (2) loss of interest or pleasure.

1. Depressed mood most of the day, nearly every day
2. Markedly diminished interest or pleasure in all, or almost all, activities most of the day, nearly every day
3. Significant weight loss when not dieting or weight gain (e.g., a change of

more than 5% of body weight in a month), or decrease or increase in appetite nearly every day.

4. Insomnia or hypersomnia nearly every day

5. Psychomotor agitation or retardation nearly every day

6. Fatigue or loss of energy nearly every day

7. Feelings of worthlessness or excessive or inappropriate guilt (which may be delusional) nearly every day

8. Diminished ability to think or concentrate, or indecisiveness, nearly every day

9. Recurrent thoughts of death (not just fear of dying), recurrent suicidal ideation without a specific plan, or a suicide attempt or a specific plan for committing suicide

B. The symptoms do not meet criteria for a Mixed Episode

C. The symptoms cause clinically significant distress or impairment in social, occupational, or other important areas of functioning

D. The symptoms are not due to the direct physiological effects of a substance or a general medical condition

E. The symptoms are not better accounted for by Bereavement

Major depression is classified as mood disorder and is conventionally distinguished from bipolar disorder in which episodes of mania as well as depression occur. The precise boundary between major depression and bipolar disorder is a matter of active current research but patients who suffer from hypomania (but not mania) are now classified as bipolar II disorder and there is uncertainty as to whether the presence of lesser degrees of mood elevation in

patients with major depression should lead to a diagnosis of bipolar spectrum disorder (Akiskal et al., 2000; Angst, 1998). DSM-IV also contains a category for milder but persistent depression (Dysthymia) which does not reach the threshold for major depression (Table 1-1).

Table 1-1 DSM -4 diagnostic criteria for Dysthymia

Chronic depression symptoms with depressed mood present almost daily for atleast 2 years or more, a) Has two or more of symptoms (1) increased or decreased appetite (2) fatigue or loss of energy (3) insomnia or hypersomnia (4) Poor self-image (5) feelings of hopelessness (6) diminished ability to think or concentrate, or indecisiveness b) Symptoms was not severe enough to meet the criteria for MDD c) Symptoms never absent longer than 2 consecutive months. c) Not had a major depressive episode d) Symptoms cause clinically important distress or impair work, social or personal functioning.

1.1.2 Stages of illness

The MDD can be single episode or recurrent depressive disorder if there are

two or more major depressive episodes. To classify two separate episodes, there must be an interval of at least 2 consecutive months in which criteria are not met for a major depressive episode. In addition, the Macarthur foundation research network on the psychobiology of depression (Frank et al., 1991) recommended the use of following terms:

Episode is the occurrence of a certain number of symptoms for a certain period of time

Remission is a period of time in which the individual does not meet the criteria for the disorder

Recovery is when full remission has lasted a defined period of time and conceptually implies the end of an episode

Relapse is the return of symptoms sufficient to satisfy the criteria for an episode before recovery

Recurrence is the return of symptomatology satisfying the criteria for an episode which occurs after the start of the recovery period implying a new episode.

1.1.3 Epidemiology

The life-time prevalence of MDD in US-European population varies between 13-16% (Alonso et al., 2004; Kessler et al., 2003) with a 12 month prevalence of 2-5%. Patients with MDD are at higher risk of suicide than general population and the life time risk is about 12-15% (Harris and Barraclough, 1998) although the degree of risk varies depending on the patient population sampled.

According to the World Health Organisation, after perinatal conditions, lower respiratory infections and HIV/AIDS, MDD is the fourth leading cause of disability worldwide (about 12.7% of total years lived with disability) (Murray and Lopez, 1997; Ustun et al., 2004). MDD is a highly co-morbid condition commonly associated with anxiety disorders, obsessive-compulsive disorder, substance misuse, and somatoform disorders.

The median age of onset of major depression is around 27 years and rates of major depression are about twice as great in women as men across different cultures (Piccinelli and Wilkinson, 2000; Weissman et al., 1993; Weissman et al., 1996; Weissman and Olfson, 1995). The reasons for the higher rates of depression among women are uncertain. The increase starts to be apparent at puberty (Angold et al., 1998) and could be due in part to a greater readiness in women to admit depressive symptoms (Gijsbers van Wijk et al., 1999); however, such selective reporting is unlikely to be the whole explanation. A number of other possible explanations (which are not of course, mutually exclusive) have been advanced, for example,

- Some depressed men who misuse alcohol and exhibit interpersonal hostility are misdiagnosed (Davidson and Ritson, 1993).
- Gender-related neurobiological differences (for example, in the organisation of central of 5-HT pathways) might make women biochemically more likely to experience stress-related mood disorders (Cahill, 2006).
- In most societies women are exposed to greater social disadvantage

than men and, for example, are more likely than men to experience sexual abuse and domestic violence (Heise L et al., 1999).

Whilst it used to be thought that the risk of depressive disorders increased with age, recent surveys suggest that major depression is most prevalent in the 18–44 age groups (Kessler et al., 2005). A number of studies have suggested that people born since 1945 in industrialized countries have both a higher lifetime risk of major depression and an earlier age of onset (Hagnell et al., 1982; Robins et al., 1984). These studies have mainly been retrospective and it is possible that the apparent increased rate of major depression in young people is because older people forget (or do not reveal) that they have been depressed (Murphy et al., 2000; Paykel, 2000).

1.1.4 Clinical course

The average length of a depressive episode is about 6 months but about 25% of patients have episodes of more than a year and about 10–20% develop a chronic unremitting course (Piccinelli and Wilkinson, 1994). After recovery at least 50% patients with major depression will experience further episodes (that is, have recurrent major depression) (Keller et al., 1992) and over a 25-year follow-up, on average, patients with recurrent major depression experience about five further episodes (Mueller and Leon, 1996). Furthermore a high proportion of depressed patients (at least one third) do not achieve complete symptom remission between episodes (Piccinelli and Wilkinson, 1994). Overall only about 25% of patients with recurrent depression achieve a period of 5

years clinical stability with good social and occupational performance (Maj et al., 1992; Mueller and Leon, 1996). This recurrent and chronic course is an important reason for the high morbidity of major depression.

1.1.5 Treatment

A wide range of treatments is available for major depression but the two classes of therapies that have been most thoroughly evaluated are pharmacological approaches (antidepressant medication) and cognitive behaviour therapy, a structured psychotherapy based on Beck's cognitive theory of depression.

Antidepressant medications are the mainstay of the management of major depression of moderate and greater clinical severity. The first classes of compounds to be introduced were the tricyclic antidepressants (TCAs) and the monoamine oxidase inhibitors (MAOIs), the antidepressant effects of which were first discovered about 50 years ago. Subsequently it became apparent that MAOIs were associated with potentially dangerous food and drug interactions; also a major trial conducted by the Medical Research Council questioned their efficacy (Medical Research Council, 1965). TCAs therefore became the most widely used antidepressants.

Investigations in experimental animals suggest that the therapeutic effect of TCAs was mediated by their ability to potentiate the brain neurotransmitters, noradrenaline and serotonin. This effect was achieved through blockade of a

reuptake pump located on the cell membrane of the neuron from which the transmitters were released (Snyder et al., 1965). Therefore TCAs and related drugs are known as “reuptake inhibitors”. While TCAs are undoubtedly helpful drugs in the treatment of depression a substantial minority of patients (about 30%) do not respond to treatment while many others have difficulty in tolerating a therapeutic dose (about 125 to 150 mg daily) because of adverse effects (Anderson, 2000; Anderson et al., 2008).

The adverse effects of TCAs were believed to be due to pharmacological actions other than noradrenaline and serotonin reuptake blockade. For example blockade by TCAs of acetylcholine receptors caused so called “anticholinergic effects” which were subjectively experienced as dry mouth, constipation, blurred vision and urinary hesitancy (Gelder et al., 2006). The ability of TCAs to block noradrenaline alpha1 receptors was associated with drowsiness and postural hypotension. Most seriously the membrane stabilising effect of TCAs predisposed to cardiac arrhythmias, which could have fatal consequences in even modest overdoses (for example, the acute ingestion of only one weeks’ supply of medication) (Gelder et al., 2006; Goldberg et al., 1985).

The problems with TCAs led drug companies to develop antidepressant drugs whose sole pharmacological action at therapeutic dose was the inhibition of serotonin (5-HT) reuptake; subsequently drugs with this pharmacological property were classified as “selective serotonin reuptake inhibitors (SSRIs)” (Healy, 1997). The first such agent licensed in the UK in 1982 was zimelidine

and while at its introduction this agent seemed effective and well tolerated it was withdrawn subsequently because of an association with a rare autoimmune syndrome (Healy, 1997). The next SSRI to be introduced, fluvoxamine, was licensed in 1983 but did not produce a great impact in terms of the treatment of depression perhaps because it was perceived by clinicians to be poorly tolerated, an impression borne out by some but not all subsequent meta-analytic reviews (Cipriani et al., 2009; Edwards and Anderson, 1999; Gartlehner et al., 2008). Over the next five years five other SSRIs were introduced to the UK market, fluoxetine (1989), sertraline (1990), paroxetine, (1991), citalopram (1995) and escitalopram (2002). A further drug, venlafaxine, introduced in the UK in 1995, is often considered with the SSRIs because at standard doses it behaves as a selective inhibitor of serotonin reuptake while at higher doses it probably inhibits the reuptake of noradrenaline as well (Gelder et al., 2006). Venlafaxine is classified as a serotonin and noradrenaline re-uptake inhibitor (SNRI) and has been regarded as slightly more effective than SSRIs in some but not all meta-analyses (Anderson et al., 2008).

Over the last 15 years SSRIs have gradually become regarded as first line treatment for the pharmacological management of depression. SSRIs are not more effective than tricyclic antidepressants and in the most severely depressed patients, for example, depressed inpatients, might be a little less effective (Anderson et al., 2008). However they are moderately better tolerated and safer in overdose than TCAs. The National Institute for Health and Clinical Excellence (NICE) produced an extensive, evidence-based guideline for the

treatment of depression in 2004 (NICE, 2004). In its advice to practitioners about prescribing, NICE recommended SSRIs as first line treatment. “When an antidepressant is to be prescribed in routine care, it should be a selective serotonin reuptake inhibitor (SSRI), because SSRIs are as effective as tricyclic antidepressants and are less likely to be discontinued because of side effects.” It is clearly of great theoretical interest that drugs whose sole acute pharmacological effect is essentially confined to blockade of the 5-HT transporter can be effective antidepressants and emphasises the role of the transporter in antidepressant action and, perhaps, in the pathophysiology of depression. The updated NICE guidelines (2009) continue to recommend SSRIs as first line drug treatment for depression of moderate and greater severity (NICE and Guidelines, 2009).

1.1.6 Etiology of depression

The aetiology of depression is clearly multifactorial and is usually considered under a number of headings such as genetics, early life experiences, personality and life stress. Many risk factors for depression are well established. For example, depression clearly runs in families and twin and adoption studies have shown that this can be accounted for in some measure by genetic factors (Kendler et al., 2006a; Kendler and Prescott, 1999; Sullivan et al., 2000), though heritability estimates (37%) are substantially less than those for bipolar disorder (85%) and schizophrenia (83%) (Bienvenu et al., 2010). Progress in identifying specific genes predisposing to depression through association and linkage studies has been limited.

The genetic findings suggest that environment plays an important role in the etiology of depression and childhood adversity, particularly sexual abuse (Bifulco et al., 1991), has been linked to the later development of depression as has the personality characteristic of neuroticism (Kendler et al., 2006b). Depression is often precipitated by adverse life events, particularly losses and by current life stresses and a diminished supportive social network (Kendler et al., 1999; Kessler, 1997). Of importance to the present study is the fact that a previous history of depression is a high risk factor for the development of future episodes (Kendler et al., 2001).

The biochemical pathophysiology of depression is not well understood and indeed one of the main approaches is based on the discoveries of the pharmacological effects of the antidepressant drugs outlined above. Because TCAs and MAOIs potentiate the actions of noradrenaline and serotonin, the monoamine hypothesis suggests that depression itself is caused by a functional deficiency of noradrenaline (Bunney and Davis, 1965; Schildkraut, 1965; Schildkraut and Kety, 1967) and/or serotonin function in the CNS (Coppen et al., 1965; Coppen, 1969; Lapin and Oxenkrug, 1969). As noted above, the finding that SSRIs, a class of compounds whose acute effects are limited to potentiation of serotonin function, are also effective antidepressants has focused much attention on the serotonin hypothesis of depression. The evidence for serotonin abnormalities in unmedicated depressed patients will be discussed below after a review of the neurobiology of the brain serotonin system.

1.2 SEROTONIN (5-HT) SYSTEM

Serotonin or 5-Hydroxytryptamine (5-HT) is an extensively studied neurotransmitter that is involved in the regulation of diverse physiological functions and behaviour such as appetite, temperature, energy homeostasis, mood, sleep-wake cycle cognition and pain. Drugs that act selectively upon 5-HT receptors and binding sites are now successfully used in the treatment of many central nervous system (CNS) illnesses, including depression, anxiety, migraine and nausea and vomiting.

1.2.1 Background

The 5-HT was first extracted from gut mucosa by Vittorio Erspamer and Vialli in 1937 and was named as ‘Enteramine’ (Whitaker-Azmitia, 1999). In a separate research on vasoconstrictive substances in blood, Maurice Rapport, Irvine Page and Arda Green isolated, purified and isolated 5-HT from bovine serum and named it as Serotonin (Rapport et al., 1948a, b). In 1953, high concentrations of 5-HT were first found in brain (Twarog et al., 1953). Gaddum and Hammeed (1954) (Gaddum, 1953) and Woolley and Shaw (1954) (Woolley and Shaw, 1954) later found that the hallucinogenic effects of lysergic acid diethylamide (LSD) might result from an antagonism of 5-HT in the central nervous system and this led the research into link between 5-HT and behaviour (Aghajanian and Marek, 1999).

Almost 95% of 5-HT is present in gastrointestinal enterochromaffin and enteric

neuronal cells (Kim and Camilleri, 2000). The remainder of 5-HT is present in brain, lungs, kidneys, adrenal glands and other body systems. 5-HT is stored in blood platelets and takes part in platelet aggregation and blood coagulation.

1.2.2 5-HT synthesis

Brain 5-HT is synthesised in 5-HT neurones from the amino acid precursor l-tryptophan via hydroxylation and decarboxylation enzymatic steps (Figure 1-1). The synthesised 5-HT is stored in presynaptic vesicles to protect it from metabolism by monoamine oxidase. 5-Hydroxyindoleacetic acid (5-HIAA) is the main metabolite of serotonin and is excreted in urine. Peripheral 5-HT cannot cross the blood-brain-barrier and therefore brain 5-HT stores are dependent on the transport of tryptophan across the blood-brain-barrier.

1.2.3 5-HT neurobiology

5-HT neuronal cell bodies are located in the mid-brain-brainstem raphe complex which sends projection fibres to the brain and spinal cord (Hornung, 2003) and 5-HT axons innervate almost every area of the brain (Figure 1-2). Raphe 5-HT neurones are characterised by a slow, regular and spontaneous firing pattern which is tightly regulated. 5-HT neuronal firing results in 5-HT being released from the 5-HT nerve terminal into the synapse where it acts upon several biochemically distinct pre and post –synaptic receptors before being recycled back into the nerve terminal by the 5-HT transporter. Current molecular biological, pharmacological and behavioural research has identified

15 distinct 5-HT receptor subtypes (Barnes and Sharp, 1999; Hoyer et al., 2002). Except for 5-HT_3 receptor, which is linked directly to a ligand gated ion channel, all 5-HT receptors are G-protein coupled transmembrane metabotropic receptors (Table 1-3).

Figure 1-1: 5-HT metabolism

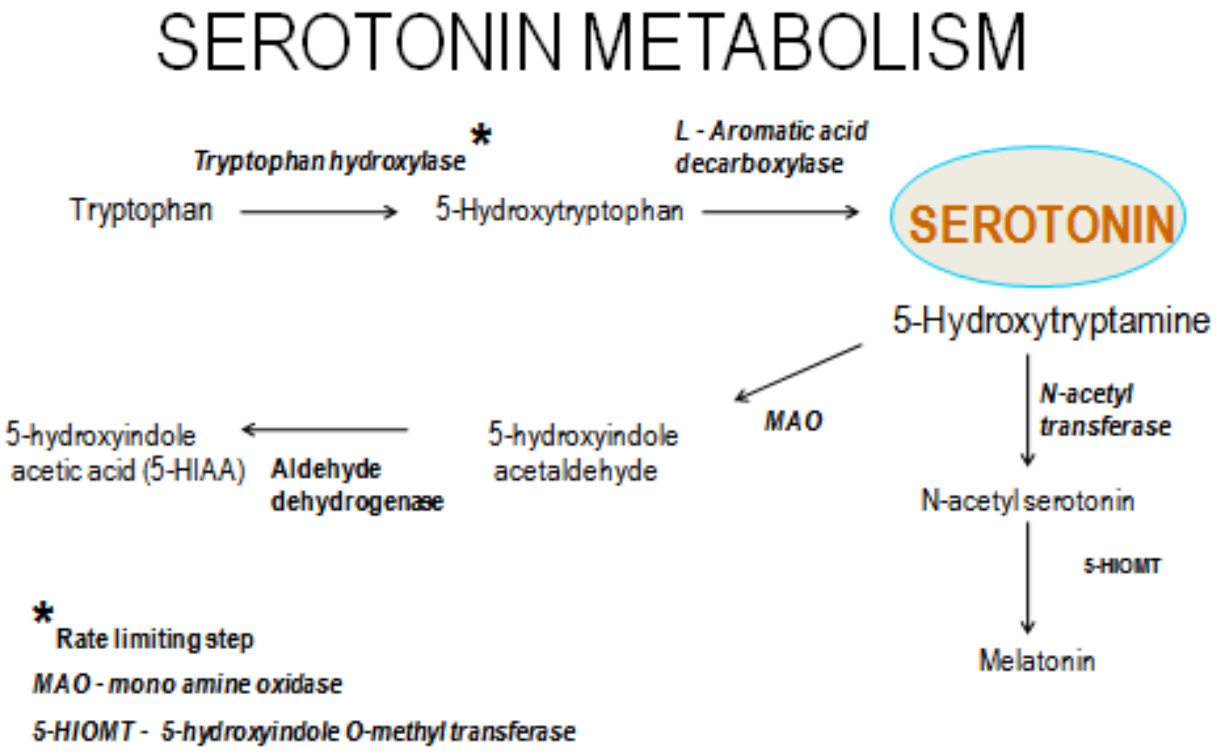


Figure 1.2: 5-HT innervation in the human brain

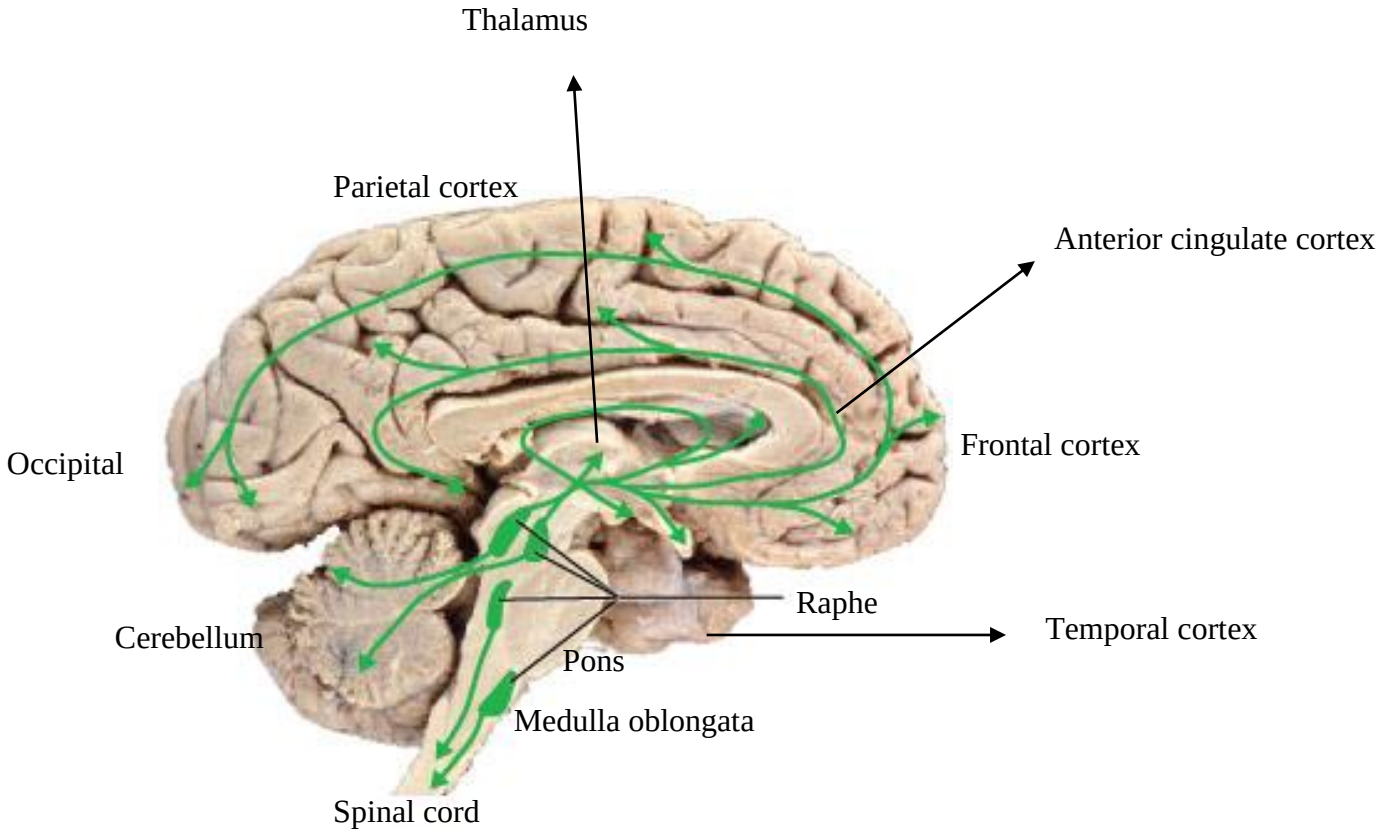


Image Source:

http://learn.genetics.utah.edu/content/addiction/reward/pathways.html

28th may 2009 – labelled by author

Table 1-2: 5-HT receptor type and physiology

5-HT system	Receptors	Action on post-synaptic neurone	Molecular action
5-HT_1	1A, 1B, 1D, 1G, 1F	inhibitory	G-protein coupled decreases cellular levels of cAMP
5-HT_2	2A, 2B, 2C	excitatory	G-protein coupled increases cellular levels of IP3 and DAG
5-HT_3		excitatory	ligand-gated Na+ and K+ cation channel depolarises cell membrane
5-HT_4		excitatory	G-protein coupled increases cellular levels of cAMP
5-HT_5	5A, 5B	inhibitory	G-protein coupled decreases cellular levels of cAMP
5-HT_6		excitatory	G-protein coupled increases cellular levels of cAMP
5-HT_7		excitatory	G-protein coupled increases cellular levels of cAMP

cAMP – cyclic Adenosine monophosphate; IP3 – Inositol triphosphate; DAG – Diacylglycerol

1.2.4 5-HT transporter (5-HTT)

Because the 5-HTT is a key target for antidepressant drugs, its structure and function have been intensively studied in animals and humans. The 5-HTT is encoded by a single-copy gene (SLC6A4) located on chromosome 17q12. The gene spans about 24 kb and contains 13 exons; (Ramamoorthy et al., 1993). The 5-HTT is a 630 amino acid protein with 12 transmembrane segments located on 5-HT neurons. An Na(+)- and Cl(-)-coupled serotonin transporter is expressed on human neuronal, platelet, placental, and pulmonary membranes (Ramamoorthy et al., 1993). The 5-HTT terminates the action of 5-HT within the synapse by transporting the neurotransmitter back inside the nerve terminal. Blockade of the 5-HTT is the primary site of action of the SSRIs and also an important site of action for TCAs.

1.3 5-HT IN DEPRESSION

Various methodologies have been employed to examine the status of 5-HT in unmedicated patients meeting standardised criteria for major depression. Generally earlier studies used indirect measures of central 5-HT, for example by assaying peripheral biochemical compounds or easily accessible blood cells such as the platelet. More recent investigations have made use of technological advances to measure specific 5-HT receptors in the living human brain. Changes in the 5-HTT in depression are the focus of this thesis and will be discussed in detail below. Here I summarise other changes in 5-HT activity that have been identified in depressed patients.

1.3.1 5-HT metabolism in depression

There is reliable evidence that levels of tryptophan, the amino acid precursor of 5-HT, are lowered in depressed patients (Coppen et al., 1973; Cowen et al., 1989). Since the synthesis of brain 5-HT is dependent on the availability of tryptophan from plasma this would be expected to lower brain 5-HT synthesis to some extent. However, a similar reduction in plasma tryptophan can be seen in people who lose weight by dieting which suggests that the low tryptophan seen in depressed patients might be a consequence of decrease appetite and weight loss rather than a primary abnormality (Anderson et al., 1990).

There have been numerous studies of levels of 5-HIAA in cerebrospinal fluid in depressed patients but no clear consensus has emerged. Generally it believed that if low 5-HIAA is present it is likely to be confined to a subgroup of depressed individuals who have made violent suicide attempts (Asberg et al., 1976a; Asberg et al., 1976b). Similar findings have been reported in other diagnostic categories such as schizophrenia (Ninan et al., 1984), and low CSF 5-HIAA has also been reported in people with personality disorders who have behaved aggressively to others (Stanley et al., 2000). Therefore low CSF 5-HIAA seems to be associated with a tendency to exhibit aggressive behaviours to self or others rather than a particular diagnostic category (Brown et al., 1982).

1.3.2 5-HT neuroendocrine challenge tests

More consistent changes have been reported in neuroendocrine investigations where the prolactin response to 5-HT challenge is lowered, particularly in drugs that enhance 5-HT function through facilitating pre-synaptic 5-HT release (Cowen and Charig, 1987; Heninger et al., 1984). Thus the prolactin response to intravenous clomipramine and citalopram are reliably lowered in depressed patients (Anderson et al., 1992; Golden et al., 1992; Kapitany et al., 1999). The mechanism that underlies this abnormality is not clear but it does not seem to reflect a generalised lowering in prolactin release in depression. For example, the prolactin response to dopamine receptor blockade is not lowered in depression (Anderson and Cowen, 1991) It is not clear, however, whether this abnormality in prolactin release is specific for depression, as opposed, for example anxiety disorders. In addition, the prolactin response to intravenous citalopram remains blunted even when depressed patients have recovered and been withdrawn from drug treatment (Bhagwagar et al., 2002b). This suggests that impaired 5-HT-mediated prolactin release may be associated with vulnerability to depression but is not necessarily associated with the symptomatic state of depression (Bhagwagar et al., 2002b).

1.3.3 Tryptophan depletion test

Another approach to elucidating the role of 5-HT in depression is to find a means of lowering brain 5-HT function and then examining its clinical and neuropsychological effects The technique employed, “tryptophan depletion”

(TRD), takes advantage of the fact that is possible to lower plasma and brain tryptophan by administering an amino-acid mixture free of the 5-HT precursor, tryptophan. Because the conversion of tryptophan to 5-hydroxytryptophan by tryptophan hydroxylase is the rate-limiting step in 5-HT synthesis (see above), TRD is able to produce a transient lowering of brain 5-HT activity (Biggio et al., 1974; Young et al., 1985).

In healthy volunteers with no vulnerability factors for the development of depression, TRD does not produce consistent changes in mood. This suggests that lowering brain 5-HT is not of itself sufficient to cause clinical depressive symptomatology (Booij et al., 2002). However, in recovered depressed patients withdrawn from medication, TRD causes, in a high proportion of participants, a transient but striking return of a full range of depressive symptomatology (Delgado et al., 1990; Smith et al., 1997). This suggests that in those with risk factors for depression, lowering brain 5-HT function can indeed cause clinical depressive symptomatology (Booij et al., 2002). This supports the notion that low brain 5-HT may be involved in the pathophysiology of the acute clinical syndrome.

1.3.4 Post mortem 5-HT_{1A} and 5-HT_{2A} studies in depression

Post mortem brain tissues provide high spatial resolution to study 5-HT receptors and their associated mRNA. However there are several limitations to post-mortem studies (Stockmeier, 2003): a) post-mortem brain changes due to asphyxia and other causes of death may be difficult to control; b) suicide and suicidal behaviour may have specific neurochemical abnormalities and

complicate the results of depression studies; c) retrospective ascertainment of diagnosis may be a potential bias; c) unknown effects of medication and other psychoactive substances are not controlled; d) limited availability of tissue samples mainly from selective regions such as cortex and brain stem; e) lack of control for potential confounders such as age, gender, smoking status, post-mortem interval, brain hemisphere or regions studied.

The results of the post-mortem studies investigating 5-HT_{1A} and 5-HT_{2A} receptors in depression and suicide are mixed (Stockmeier, 2003). Thus while some studies using selective 5-HT_{1A} agonist (8-OH-DPAT) in suicide victims with or without depression reported increased binding in cortical areas (Arango et al., 1995; Matsubara et al., 1991) and hippocampus (Joyce et al., 1993), other investigations reported no change in these regions (Arranz et al., 1994; Dillon et al., 1991; Lowther et al., 1997; Stockmeier et al., 1997) or brain stem raphe (Arango et al., 2001); in mid-brain raphe, however, 5-HT_{1A} binding was reported increased (Stockmeier et al., 1998).

In 5-HT_{2A} studies in suicide victims with or without depression 5-HT_{2A} receptor binding is increased in dorsal prefrontal cortex in some (Arango et al., 1990; Arora and Meltzer, 1989b; Hrdina et al., 1993; Laruelle et al., 1993a; Mann et al., 1986; Stanley and Mann, 1983; Turecki et al., 1999) but not all studies (Arranz et al., 1994; Crow et al., 1984; Gross-Isseroff et al., 1990; Owen et al., 1986; Rosel et al., 2000; Stockmeier et al., 1997). In other brain regions such as hippocampus, rostral part of frontal cortex or brain stem results are also inconsistent with reports of either increased 5-HT_{2A} receptor binding or no

change (see review (Stockmeier, 2003)). Finally, Pandey et al. (2002) reported increased levels of 5-HT_{2A} receptors, 5-HT_{2A} receptor protein and mRNA expression in the prefrontal cortex (areas 8, 9) in teenage suicide victims with different psychiatric illnesses. The authors also showed that the increase might be restricted to certain cortical layers, with increased binding of 5-HT_{2A} in layer 5 but not 3 or 6.

1.3.5 Positron emission tomography studies in depression

Technological developments have enabled the measurement of 5-HT receptor binding in the living human brain using ligand imaging in conjunction with positron emission tomography (PET) and single photon emission tomography (SPET). There is reasonably consistent evidence that the binding density of 5-H_{1A} receptors shows a widespread decrease in depressed patients (Table 2). However, as with the prolactin response to citalopram, the binding appears to remain low in recovered depressed patients suggesting that it is not a marker of the acute depressive state (Bhagwagar et al., 2004). In addition, 5-HT_{1A} receptor binding is also lowered in patients with panic disorder (Neumeister et al., 2004); however, these patients usually have high rates of co-morbid depression. It should also be noted; however, that one group has reported increases in 5-HT_{1A} receptor binding in both acutely depressed (Parsey et al., 2006d) and recovered depressed patients (Miller et al., 2009). The reason for this discrepancy is controversial but might reflect methodological differences in terms of the use of an arterial input method to quantify non-specific binding and choice of cerebellar grey or white matter as reference region.

Certain other 5-HT receptors, for example the 5-HT_{2A} receptor (Table 1-4) and the 5-HT transporter (Table 1-5), have also been widely studied in imaging investigations in depressed patients. However, the data from this work are contradictory showing that even the use of state of the art imaging to measure 5-HT receptors in unmedicated patients, classified with reliable diagnostic systems, can be insufficient to overcome clinical heterogeneity or technical variability between different laboratories. The findings on the 5-HT transporter are discussed in detail below.

Table 1-3: 5-HT_{1A} and 5-HT_{2A} ligand imaging studies in depression

5-HT_{1A} Studies	Radiotracer	Subjects unmedicated	Findings
Drevets et al (1999) (Drevets et al., 2007)	[^{11}C]WAY-100635	12 both MDD and Bipolar disorder	Decrease raphe and mesial-temporal cortex
Sargent et al (2000) (Sargent et al., 2000)	[^{11}C]WAY-100635	15 MDD + 10 medicated	Decrease in frontal, temporal, and limbic cortex
Bhagwagar et al (2004) (Bhagwagar et al., 2004)	[^{11}C]WAY-100635	14 MDD remitted	Decrease in cortical and limbic areas

Meltzer et al (2004) (Meltzer et al., 2004)	[^{11}C]WAY-100635	17 MDD elderly	Decrease in raphe
Parsey et al (2006) (Parsey et al., 2006d)	[^{11}C]WAY-100635	28 MDD	Increase in drug naïve subgroup
Drevets et al (2007) (Drevets et al., 2007) replication	[^{11}C]WAY-100635	16 MDD	Decrease in medial temporal cortex and raphe
Hirvonen et al (2008) (Hirvonen et al., 2008)	[^{11}C]WAY-100635	21 MDD	Decrease in most regions
Miller et al (2009)(Miller et al., 2009)	[^{11}C]WAY-100635	15 MDD remitted	Increase in most brain regions
5-HT2A Studies	Ligand	Subjects	Findings
Attar-Lévy et al (1999) (Attar-Levy et al., 1999)	[^{18}F]setoperone	7 MDD	No change - ? small decrease in frontal cortex
Meyer et al (1999) (Meyer et al., 1999)	[^{18}F]setoperone	14 MDD	No change in prefrontal cortex
Yatham et al	[^{18}F]setoperone	20 MDD	Decrease in

(2000) (Yatham et al., 2000)			cortical areas
Meyer et al (2003) (Meyer et al., 2003)	[^{18}F]setoperone	22 MDD	Subgroup with high DAS[1] had high binding potential
Biver et al 1997 (Biver et al., 1997)	[^{18}F]altanserin	8 MDD	Decrease in Right posterolateral orbitofrontal cortex and the anterior insular cortex
Meltzer et al 1999 (Meltzer et al., 1999)	[^{18}F]altanserin	11 elderly MDD	No change
Larisch et al (2001) (Larisch et al., 2001)	[^{18}F]altanserin	12 FH+ve MDD Med+unmed	Decrease
Mintun et al (2004) (Mintun et al., 2004)	[^{18}F]altanserin	46 MDD	Decrease in hippocampus
Sheline et al 2004	[^{18}F]altanserin	16 elderly MDD	Decrease in

(Sheline et al., 2004)			hippocampus
Bhagwagar Z (2004) (Bhagwagar et al., 2006)	[11C]MDL	20 remitted MDD	Increase in cortex
Messa C (2003) (Messa et al., 2003)	[^{18}F]FESP	19 MDD (drug naïve)	Decrease in cortex and anterior cingulate cortex
D'haenen et al (1992) (D'Haenen et al., 1992)	2-^{123}I-ketanserin	19 MDD	?no change and Increase in parietal cortex
Schins et al (2005) (Schins et al., 2005)	^{123}I-5-I-R91150	9 post-Myocardial Infarction MDD	Increase

DAS[1] – Dysfunctional Attitude Scale

1.4 5-HTT STUDIES IN DEPRESSION

1.4.1 Platelet 5-HTT binding in depression

The human brain 5-HTT and platelet 5-HTT are encoded by the same gene, on chromosome 17 (Lesch et al., 1993). Platelets are the carrier and storage sites for 5-HT in plasma but cannot synthesise 5-HT. Platelet 5-HTT takes up 5-HT that has been released from gut, lungs and other areas and, stores it in vesicle ready for use as a vasoconstrictor (Vanhoutte, 1991). Brain and platelet 5-HTT share common physiological and biochemical properties and the platelet has been proposed as a peripheral model to study central 5-HT function (Stahl, 1977).

Early reports showed impaired 5-HT transport through the platelet membrane (Coppen et al., 1978; Meltzer et al., 1981). Imipramine was used as a marker for platelet 5-HTT binding and initial studies showed reduced imipramine platelet binding in depression (Briley et al., 1980; Paul et al., 1981). A majority of studies have confirmed the finding of decreased imipramine platelet binding in depression, however there are several inconsistencies probably due to differences in the ligands, laboratory methods and study sample sizes (Ellis and Salmond, 1994; Schneider and Lyness, 1995). The contradictory results of lowered B_{MAX} of [^{3}H]imipramine compared to the more selective [^{3}H]paroxetine binding to platelets in depression may be due to the differences in their binding sites (Marcusson and Ross, 1990).

Direct in-vivo brain measures of 5-HTT binding are needed to validate the

results of platelet studies in depression. It is possible that the platelet and neuronal 5-HTT activity may be differentially regulated due to differences in the transcriptional and post transcriptional mechanisms. Moreover, empirically, changes in the platelet and brain 5-HTT in depression may not correlate (Malison et al., 1998; Uebelhack et al., 2006). For instance, Malison et al (Malison et al., 1998) measured brain 5-HTT using the SPET ligand βCIT and platelet binding using [^{3}H] paroxetine and did not find any significant correlation between both binding measures across individuals.

1.4.2 Post-mortem brain 5-HTT binding in depression

5-HTT binding studies have also been carried out in post-mortem tissue mainly in patients with a diagnosis of depression who have died by suicide. The results of these investigations as far as 5-HTT binding is concerned have been mixed and inconclusive with majority of studies reporting either decreased binding in frontal cortex (Arango et al., 1995; Gross-Isseroff et al., 1989; Joyce et al., 1993; Laruelle et al., 1993a; Mann et al., 2000; Perry et al., 1983; Stanley et al., 1982) or no change in cortex (Arora and Meltzer, 1989a; Crow et al., 1984; Hrdina et al., 1993; Lawrence et al., 1990; Leake et al., 1991; Little et al., 1997; Owen et al., 1986) or brain stem areas (Arango et al., 2001; Bligh-Glover et al., 2000; Klimek et al., 2003; Little et al., 1997)(see Stockmeier 2003 for full review). There are, however, several important differences between the studies; use of different ligands with varied specificity ([^{3}H]imipramine or the more selective [^{3}H]citalopram, [^{3}H]paroxetine or [^{3}H]cyanoimipramine); sampling of different brain regions; differences in diagnostic criteria and case

ascertainment, and variable sample size among studies.

Austin et al (2002) studied other 5-HTT parameters and found decreases in length of 5-HTT-positive axons in layer 6 in Area 46, dorsolateral prefrontal cortex (DLPFC) in depressed suicide victims. In addition, Arango et al found decreases in dorsal raphe neurons expressing 5-HTT mRNA in depressed suicide patients (Arango et al., 2001).

1.4.3 5-HTT Imaging studies in depression

1.4.3.1 Single Photon Emission Tomography (SPET) studies

In the first successful SPET study using [^{123}I]-βCIT, Malison et al (1998) showed low brain stem and thalamus 5-HTT binding potential (BP) in depressed patients compared with healthy controls (Malison et al., 1998). Other SPET studies using [^{123}I]-βCIT or [^{123}I]-nor-βCIT (more selective to 5-HTT than βCIT) or [^{123}I]-ADAM, generally show decreased binding potential (BP) of the 5-HTT in thalamus and midbrain-brain stem complex in depressed patients (Joensuu et al., 2007; Lehto et al., 2006; Newberg et al., 2005; Staley et al., 2006; Willeit et al., 2000)(see Table 1). However, not all studies agree; Dahlstrom et al (2000) found increased 5-HTT BP in hypothalamus/midbrain of depressed adolescents while Herold et al (2006) and Ruhe et al (2009) found no difference in 5-HTT in these regions. However Ruhe et al (2009) found decreased 5-HTT in a subgroup of male subjects.

A limitation of studies with the βCIT SPET ligand is that it has similar affinity for the dopamine transporter (DAT) and the 5-HTT (Laruelle et al., 1994) and also it is not possible to image the 5-HTT in other cortico-limbic brain areas relevant to depression such as amygdala, anterior cingulate cortex (ACC) and hippocampus.

1.4.3.2 Positron Emission Tomography (PET) studies

The two PET radioligands, which have been most widely used in the last decade, are the [^{11}C](+)McN5652 (Suehiro et al., 1993) and [^{11}C]DASB (Houle et al., 2000). In a comparative evaluation of these two 5-HTT radioligands, [^{11}C]DASB compared favourably to [^{11}C](+)McN5652, both in non-human primates (Szabo et al., 2002) and humans (Frankle et al., 2004) with the critical advantage of having higher specific to non-specific binding. In addition, it is difficult to reliably measure the plasma free fraction f_P of [^{11}C]McN5652 and as a result Binding Potential (BP_F) (see 2.3.3.4 Compartment model) which is a measure of f_P $BP_P = f_P * B_{avail} / K_D$. f_P is the plasma free fraction and the concentration of tracer available for transport into tissue. It is difficult to interpret conditions that show differences in brain distribution volumes if f_P is not measurable (Ikoma et al., 2002). This issue is discussed in detail in methods chapter 2.

Both [^{11}C] McN5652 and [^{11}C] DASB allow quantification of the 5-HTT in brain regions outside the brain stem and midbrain (Szabo et al., 1995; Wilson et al., 2002). [^{11}C](+)McN5652 and [^{11}C]DASB have been widely used to study the

5-HTT in various neuropsychiatric diseases such as major depression, anxiety disorders, obsessive-compulsive disorder, schizophrenia, eating disorders, Alzheimer's dementia and Parkinson's disease. It should be noted, however, that [^{11}C]DASB is not really effective for the measurement of 5-HTT in regions of relatively low binding density such as cortex because it has s relatively low specific binding in these areas.. Two novel PET tracers [^{11}]C MADAM (Lundberg et al., 2006) and [^{11}C]AFM, a novel tracer seems to have advantage in this area and initial results from human studies are promising (Huang et al., 2002).

PET studies of the 5-HTT in acutely depressed patients reveal more inconsistent results than SPET (Table 3). Overall, a few studies show decreased 5-HTT BP in depressed patients, however others found either no change or increased 5-HTT BP in certain brain regions. Given the inconsistent nature of 5-HTT PET imaging findings, it is very important to find out from where the variance in results might emerge. Relevant factors are likely to include subject heterogeneity, methodological differences in ligand modelling, disease factors (effects of weight loss, insomnia, for example), medication status of the subjects, and genetic differences in the 5-HTT (see below).

One approach to tackling some of these variables is to identify relatively enduring abnormalities in brain 5 HTT mechanisms in people at risk of recurrent illness by studying those who have suffered from depression but who are fully recovered and off medication. An advantage of this approach is that any changes seen are unlikely to be attributable to epiphenomena of acute

depressive illness or its treatment. Studies of this nature have been successful in delineating persistent PET neuroimaging changes in depression (Bhagwagar and Cowen, 2008). For instance, Bhagwagar and colleagues (2004) found that recovered depressed patients exhibit diminished cortical BP of 5-HT1A receptors measured by [^{11}C]-WAY 100635 while cortical 5 HT2A receptor BP, measured by [^{11}C] MDL 100,907, was increased (Bhagwagar et al., 2006).

The second approach is to find out whether the results of PET studies in depression are due to differences in analysis methods employed. For instance, some of the studies have used arterial blood samples which will help estimate the free and non-specific binding of the ligand, while others do not use these measures (Table 3). There are also key differences in the use of reference regions, methods of analysis etc.

Table 1-4: 5-HTT Imaging studies in depression

Studies	Radioligand	Subjects N=depressed subjects	Results	Other findings	PET methodology
SPET STUDIES					
Malison 1998(Malison et al., 1998)	[^{123}I]-βCIT	MDD (n=12)	DECREASED in brain stem BP	First SPET imaging study on	N/A

				5-HTT in depression	
Willeit et al 2000 (Willeit et al., 2000)	[^{123}I]-βCIT	Seasonal affective disorder with depression (n=11)	DECREASED in Thalamus and hypothalamus	no change midbrain-pons	N/A
Dahlstrom et al 2000 (Dahlstrom et al., 2000)	[^{123}I]-βCIT	children-adolescents (n=31)	INCREASED in midbrain-hypothalamus in	ROI includes (the raphe nuclei, substantia nigra and the colliculi)	N/A
Staley et al 2006 (Staley et al., 2006)	[^{123}I]-βCIT	MDD (n=32)	DECREASED BP in diencephalon in female subgroup	no change in striatal or brainstem	N/A
Lehto et al 2006 (Lehto et al., 2006)	[^{123}I]-nor-βCIT	MDD (n=29)	DECREASED in midbrain	Atypical symptoms scores of HAM-D-29 were inversely correlated with SERT densities in the	N/A

				midbrain.	
Joensuu et al 2007 (Joensuu et al., 2007)	[^{123}I]-nor-βCIT	MDD (n=29)	DECREASED in midbrain		N/A
Newberg et al 2005 (Newberg et al., 2005)	[^{123}I]ADAM	MDD (n=7)	DECREASED in midbrain	decrease correlating negatively with the severity of depressive symptoms and age	N/A
Herold et al 2006 (Herold et al., 2006)	[^{123}I]ADAM	MDD (n=21)	NO CHANGE	however male subjects had trend level low BP in midbrain	N/A
Ruhe et al 2009 (Ruhe et al., 2009)	[^{123}I]-βCIT	MDD (N=49)	NO CHANGE	Subgroup of male subjects had low BP in midbrain and diencephalon	N/A

PET STUDIES					
Ichimiya et al 2002 (Ichimiya et al., 2002)	[^{11}C](+)McN5652	MDD and Bipolar disorder vs Controls (n=13 MDD (7))	INCREASED BP in thalamus	no change midbrain Also included euthymic subjects	Logan graphical analysis with cerebellum as reference region No arterial input function
Reivich et al 2004 (Reivich et al., 2004)	[^{11}C](+)McN5652	MDD (n=4)	INCREASED Distribution Volume Ratio (DVR) in R ACC and L frontal	No change in midbrain/pons	Simplified reference tissue model with cerebellum as reference region No arterial input function
Parsey et al 2006 (Parsey et al., 2006b)	^{11}C-(+)McN5652	MDD (n=25)	DECREASED BP in amygdala-midbrain		Likelihood estimation in a graphical approach with cerebellum

					as reference region. Arterial input used Natural log-transformed data – not multiple comparison corrected
Oquendo et al 2007 (Oquendo et al., 2007)	[^{11}C](+)McN5652	Bipolar depressed Vs controls (n=18)	DECREASED BP in amygdala, midbrain, hippocampus, thalamus, putamen and ACC	Lower cerebellar binding in BD compared to controls	Same as Parsey et al 2006
Meyer et al 2004 (Meyer et al., 2004a)	[^{11}C]DASB	MDD (n=20)	NO CHANGE in any ROI including Midbrain	Subgroup with high DAS score had high 5-HTT BP in all ROI except midbrain	Logan analysis without arterial input and Cerebellum as reference region
Cannon et	[^{11}C]DAS	Bipolar	INCREASED	DECREA	MRTM2

al 2006 (Cannon et al., 2006)	B	depressed (n=18)	BP in ROI analysis thalamus, dorsal cingulate, insula and caudate-	SED BP only in brain stem	method of Ichise et al. (2003) Cerebellum as reference region No arterial input function
Cannon et al 2007 (Cannon et al., 2007)	[^{11}C]DASB	Bipolar depressed BD (n=18) Vs MDD (n=18) Vs controls	INCREASED 5-HTT BP in thalamus, insula, PAG) and striatum in MDD. Elevated 5-HTT BP in DCC in BD VS controls - no change in midbrain	Depression-severity correlated negatively with 5-HTT BP in the thalamus in MDD-subjects.	MRTM2 method of Ichise et al. (2003) Cerebellum as reference region No arterial input function
Reimold et al 2008 (Reimold et al., 2008)	[^{11}C]DASB	MDD (n=10)	DECREASED BP Thalamus – ROI analysis	Anxiety scores negatively correlated with thalamus, amygdala and midbrain	MRTM2 method of Ichise et al. (2003) Cerebellum as reference region No arterial input function

1.5 QUANTIFICATION OF [11C] DASB BINDING

In general, the quantification of the specific binding in brain PET and SPET studies is based on two assumptions regarding the use of a reference region (Cunningham and Lammertsma, 1995a). First, the reference region should effectively be devoid of specific binding. Second, the free and nonspecific binding of the radioligand should be uniform across the entire brain such that the binding estimate in the reference region can be used as a measure of the free and nonspecific binding in the other parts of the brain. However, in studies of PET radioligand binding to the 5-HTT, a growing amount of evidence suggests that these assumptions may not be fully met (Ikoma et al., 2002; Kish et al., 2005; Suehiro et al., 1993; Szabo et al., 2002). For instance, Parsey et al (2006c) reported a 33% reduction of the [^{11}C]DASB distribution volume in cerebellar grey matter after daily oral sertraline treatment in healthy volunteers (Parsey et al., 2006c). The differences observed in the reference region cerebellum may either over or underestimate the study results in terms of calculated specific binding.

Also, there are some uncertainties about the best way to quantify ligand binding (i.e. the use of a reference tissue model or arterial input function). As the cerebellum is believed to have a very low or even negligible concentration of 5-HTT (however, see Parsey et al 2006c above), some authors have suggested that it could be used as reference region. Nevertheless, it has been reported that there are differences in the amount of 5-HTT availability in the grey and white matter of the cerebellum, with lowest 5-HTT densities observed in the

white matter (Kish et al., 2005). These findings need to be carefully validated for potential pitfalls.

1.6 5-HTT GENETIC POLYMORPHISM AND 5-HTT BINDING

1.6.1 5-HTT gene and function

As noted above, the human 5-HTT gene is located on chromosome 17q12 (Ramamoorthy et al., 1993). The transcription of the gene is modulated by a 44-bp length variation in its upstream regulatory region, termed short (S) versus long (L) 5-HTTLPR, which results in differential transcription of the 5-HTT in vitro, with the L form being associated with higher 5-HTT expression levels (Lesch et al., 1996). More recently the 5-HTTLPR has been shown to exist in a triallelic form because the L allele itself has two functional variants (L_A and L_G) with the L_G form exhibiting similar levels of 5 HTT expression in vitro as the S allele (Hu et al., 2005). Theoretically lower expression of the 5-HTT in S carriers could to lead differences in functional measures of 5-HT function and also in measures of 5-HTT ligand binding where it would be predicted that S carriers would have lower 5-HTT binding.

An example of a difference in functional responses with different 5-HTT genotypes is provided by functional magnetic resonance imaging (fMRI) studies which have measured the activity of the amygdala in response to negative emotional stimuli (Hariri et al., 2005; Munafo et al., 2008; Rhodes et al., 2007). Across a range of tasks and stimulus types, carriers of an S allele of the 5-

HTTPLR reportedly show greater amygdala activation. Because 5-HT pathways play an important role in modulating amygdala excitability such an effect of 5-HTTPLR genotype has some biological plausibility (Hariri et al., 2006). However, the robustness of the genotype effect has been questioned because of a decrease in the reported effect size of this observation over recent years and the possibility of publication bias in more recent studies (Munafo et al., 2008).

In addition, there are clinically-orientated investigations suggesting, for example, that carriers of the S allele are at greater risk of experiencing depression when exposed to stressful life events (Caspi et al., 2003) and less likely when depressed to respond to treatment with SSRIs (Serretti et al., 2007). However both these findings are controversial (Kraft et al., 2007; Risch et al., 2009; Taylor et al., 2010).

1.6.2 5-HTTLPR and 5-HTT binding in platelets and post-mortem brain

From the point of view of PET ligand binding studies of the 5-HTT is important to find out whether the 5-HTT gene variants influence the expression of 5-HTT protein. Early studies used platelet 5-HTT binding and activity to study the functional effect of the 5-HTT gene variant. Greenberg BD (1999) found that the 'L' variant was associated with more rapid initial platelet 5-HT uptake (V_{MAX}), but 5-HTTLPR genotype had no effect on platelet [3H]paroxetine binding (B_{MAX}), affinity for [^{3}H]5-HT or [^{3}H]paroxetine, or 5-HT content (Greenberg et al.,

1999). Similarly, Preuss et al (2000) did not find an effect of 5-HTTLPR on [^{3}H]paroxetine binding sites in platelets in healthy subjects. Using post-mortem brain tissue, Mann et al (2000) reported no correlation between 5-HTTLPR and 5-HTT binding. Similarly Lim et al (2006) found no effect of 5-HTTLPR on post mortem brain stem 5-HTT mRNA.

1.6.3 5-HTTLPR and 5-HTT binding using brain imaging

Despite these mixed findings it is possible that 5-HTTLPR genotype might affect expression of the 5 HTT in the human brain in-vivo. If it does this would have important implications for understanding the discrepant PET findings of the 5-HTT in depression, as well as the role of individual variation of the 5-HTTLPR in the pathophysiology of emotional disorders (Uher and McGuffin, 2008). However, the results to date of SPET and PET investigations have been inconsistent probably as a consequence of relatively modest sample sizes and ligands of varying specificity for the 5-HTT.

Using [^{123}I]-βCIT with SPET in 96 healthy subjects, van Dyck et al (van Dyck et al., 2004) reported higher 5 HTT binding in brainstem and striatum among carriers of the SS genotype when compared with heterozygote SL carriers, but this result was not confirmed in two smaller investigations also using [^{123}I]-βCIT (Jacobsen et al., 2000; Willeit et al., 2001). Using [^{11}C] McN5652, Shioe et al (2003) found no effect of the triallelic polymorphism on 5-HTT binding, a finding which was confirmed by Parsey et al (2006a) who found no effect of the triallelic polymorphism on 5-HTT binding in 42 healthy subjects and 25 acutely

depressed patients. However Praschak-Rieder et al (2007) using [^{11}C] DASB in 43 healthy subjects reported increased 5-HTT in putamen specifically in those with an L_A/L_A genotype and Reimold et al (2007), showed a similar effect in midbrain in 19 healthy volunteers with L_A/L_A genotype. It is again unclear whether the discrepant results are due to differences in radioligands, analysis methods, type 1 error or other unknown confounding effects.

1.7 5-HTTLPR AND BRAIN STRUCTURE

Given the complexity of brain circuitry and network activity, it is possible that the effect of the 5-HTTLPR in functional MRI studies of emotional processing may be explained by mechanisms other than a genotype-mediated change in 5-HTT receptor expression. One hypothesis is that 5-HTTLPR genotype may be important in development so that effects of genotype on brain function in adults are likely attributable to earlier neurodevelopmental changes. This view is supported by the observation that carriers of the S allele have reduced Grey Matter (GM) volume in both anterior cingulate and amygdala (Pezawas et al., 2005) and decreased functional connectivity between these brain regions (Heinz et al., 2005; Pezawas et al., 2005). Pezawas et al (2005) also found decreased volume in perigenual anterior cingulate and amygdala in the S carriers in 114 controls (L'L'= 35, S'= 79) classified according to the bialleleic promoter polymorphism. In contrast, Canli et al (2005) studying 41 healthy controls (L'L= 13, S'= 28) found widespread reductions in gray matter in S' carriers (insula, left middle frontal gyrus and gyrus rectus, right inferior temporal

gyrus, anterior cingulate, and cerebellum). Frodl et al (2008) using the tri-allelic polymorphism in 77 healthy controls, also found rather more widespread reductions in gray matter in S' carriers (left amygdala, right hippocampus, left anterior cingulate cortex and bilateral dorsolateral prefrontal cortex). However, in the latter study the morphometric comparisons appear to have been restricted to L'L' (n= 10) and S'S' (n= 23) homozygotes. Finally, a recent study in non-human primates (4 L'L' vs 4 L'S'), reported widespread reductions in gray matter volume in S' carriers in anterior cingulate, medial prefrontal and orbitofrontal cortex as well as the amygdala (Jedema et al., 2010).

The above studies show that neuroanatomical correlates may underlie the different functional reactions in S carriers to probes of neural circuitry regulating emotion. These findings may be relevant in the neurobiology of MDD; for instance, Frodl et al (2008) found that while healthy subjects carrying the S- or L_G-allele had smaller grey matter volumes than those with the L_A-allele, depressed patients with the L_A-allele had reduced GM volumes, suggesting that patients are more vulnerable for morphological changes during depressive episodes. However, these studies, though of interest, require confirmation. In addition, there are differences in the study findings in the brain regions that showed correlations between 5-HTT genotype and brain structure. These differences may be due to technical factors or due to sample size. Pezawas et al (2005) and Frodl et al (2005) used low resolution 1.5 Tesla MRI and Pezawas et al (2005) and Canli et al (2005) studied the biallelic genotype and not the more recently described triallelic genotype.

1.8 AIMS OF THE THESIS

The main aim of the thesis was to study 5-HTT binding in Major Depressive Disorder using PET in conjunction with [^{11}C] DASB. First, I conducted a methodological experiment to characterise the blockade of SERT binding sites after citalopram infusion in healthy human volunteers using [^{11}C]DASB to validate the use of [^{11}C]DASB (Chapter 3). I then used [^{11}C] DASB to assess 5-HTT binding in two patient groups, free from antidepressant medication; a) acutely depressed patients and b) recovered patients (Chapter 4 & 5). An advantage of studying recovered depressed patients is that any changes seen in the 5-HTT are unlikely to be attributable to epiphenomena of acute depressive illness or its treatment. To answer the question of whether 5-HTTLPR polymorphisms influence the brain expression of the 5-HTT, I studied 5-HTT binding using [^{11}C]DASB in a large group of healthy volunteers genotyped for the triallelic promoter polymorphism of the 5HTT (Chapter 6). For all the above PET studies, I used a full metabolite corrected arterial input function & graphical analysis to quantify regional activity to measure 5-HTT binding potential. Finally, I investigated the influence of the 5-HTTLPR polymorphisms on brain Gray Matter (GM) volumes in healthy controls using MRI based structural analyses (Chapter 7).

2 GENERAL METHODS

2.1 APPROVAL FOR STUDIES

All the studies were approved by the Research Ethics Committee at Hammersmith Hospital, London. The PET studies were also approved by the Administration of Radioactive Substances Advisory Committee (ARSAC), United Kingdom. ARSAC was set up to supervise studies which involve administration of radioactive substances for medical or research purposes. All clinical studies of radioactive substances must follow the Ionising Radiations Regulations 1999 and ARSAC determines whether the radiation exposure that the trial subjects are to receive is within acceptable limits. Human tissue act guidelines (2004) were followed for collection, storage and disposal of tissue samples (blood, saliva and cheek swab). The studies in the thesis were sponsored by the UK Medical Research Council. Clinical researcher indemnity was provided by Imperial College School of Medicine.

2.2 PARTICIPANTS

2.2.1 Recruitment

Healthy volunteers were recruited by advertisement in national and local newspapers in London, Oxford and other surrounding areas. In addition, volunteers from a research database who previously participated in research studies and expressed interest in future studies were also contacted.

The volunteers who approached were first given a study information sheet. Those who were still interested in taking part had an initial screening interview

which was performed over the telephone. If they were still interested and seemed potentially suitable, they attended the MRC Cyclotron Unit for a face-to-face interview. Informed written consent was obtained by one of the clinical investigators involved in the studies after a verbal explanation and presentation of the written information sheet. The subjects were given as much time as they needed to decide whether or not to take part. Participants were paid a small honorarium for their time commitment and the travel expenses incurred.

Depressed patient were recruited by advertisements placed in newspapers, magazines, websites and in local general practitioners' clinics. In addition, patients referred by clinical colleagues were also recruited.

2.2.2 Study participant screening interview

Subjects were diagnostically assessed by a clinical psychiatrist using the Structured Clinical Interview for DSM-IV (SCID-1) disorders criteria (First et al., 1996). The SCID is a semi-structured diagnostic interview designed to be administered by a clinician or trained mental health professional. The SCID-1 was originally designed to aid accurately diagnose psychiatric disorders based on Diagnostic and Statistical Manual (DSM-IV) of the American Psychiatric Association (1994). Since its introduction the SCID has been widely and reliably used for diagnostic evaluation, research, and the training of mental-health professionals (Skre et al., 1991; Williams et al., 1992).

2.2.3 Inclusion criteria for controls

The healthy control volunteers included in the studies were male subjects, aged between 25−65 years, in good physical health and capable of giving informed consent.

The Hammersmith Research Ethics Committee reviewed the study and requested preclinical data with DASB effect on pregnancy and teratogenicity. However at the time of the ethics application these data were not available. We therefore agreed with the ethics committee to recruit only male participants.

2.2.4 Exclusion criteria for controls

1. Contraindication to PET scanning
2. Current or past history of major psychiatric disorder
3. Present or recent (previous 3 months) use of psychotropic medication
4. Current significant illicit substance/alcohol misuse
5. Current significant general medical morbidity
6. Significant previous radiation exposure
7. MRI contraindications (in particular metal implants are an absolute contraindication)

2.2.5 Inclusion criteria for recovered depressed patients

Subjects were rated to be recovered from depression based on the following

four criteria (Frank et al., 1991):

1. Self-reported euthymia following the last episode of major depression
2. Clinician rated euthymia
3. Absence of criteria for a major depressive episode as determined by SCID and
4. Hamilton Depression Rating Scale (HAM-D) (Hamilton 1960) score of less than 7

Patients included had at least one episode of major depression based on clinical interview and Structured Clinical Interview for DSM-IV Disorders criteria for major depressive disorder as described in Introduction chapter. In addition, included patients met all four criteria for recovery in addition to being euthymic and medication free for more than three months.

2.2.6 Inclusion criteria for depressed patients

Depressed patients were currently depressed based on clinical interview and Structured Clinical Interview for DSM-IV Disorders criteria for major depressive disorder. In addition, secondary co-morbid psychiatric conditions which commonly present in depression such as generalized anxiety disorder, panic disorder, dysthymia and past history of substance use were allowed. The inclusion of depressed patients with related co-morbid illnesses was permitted to improve the study recruitment. In addition, depression is associated with high co-morbidity and inclusion of co-morbid illnesses improves the generalisability of study findings to the typical population seen in the psychiatry clinic.

2.2.7 Exclusion criteria for acute and recovered depressed patients

The general exclusion criteria for both patient groups were similar to the one adopted for healthy subjects. In addition, acute depressed patients were excluded if they had taken psychotropic medication within the 3 months prior to the scan. However occasional use of benzodiazepines for agitation or sedation in depressed patients was accepted. Patients with serious suicidal ideation or plans were also excluded for practical reasons as they required a high degree of psychiatric supervision and it was not thought justified to delay antidepressant treatment.

2.3 PSYCHOLOGICAL QUESTIONNAIRES

Subjects who meet the study criteria for inclusion were then given several validated psychological questionnaires. They were as follows;

1) The Hamilton Rating Scale for Depression (HRSD-17) is a clinician rated 17 item rating scale to assess the severity of depression symptoms (Hamilton, 1960). The scale is based on the clinician's interview with the patient and has questions that probe symptoms such as depressed mood, guilt feelings, suicide, sleep disturbance, anxiety levels and weight loss. Each of the symptom scale ranges either from 0-2 (more categorical) or 0-4 (dimensional) on a severity scale. The maximum score on HRSD-17 is 50, while scores less than 7 are regarded as showing no degree of clinical depression and indicating

recovery.

2) The Beck Depression Inventory (BDI) is a self-rated depression questionnaire (Beck et al., 1961). This rating scale consists of 21 multiple choice questions, each question with four possible responses, with maximum score up to 63. Both HRSD and the BDI are widely used scales for depression symptoms.

3) The Dysfunctional Attitude Scale (DAS) is a self-report scale designed to measure the intensity of dysfunctional attitudes (Nelson et al., 1992; Weissman and Beck, 1978). This scale was based on Beck's cognitive theory of depression which states that individual with maladaptive thinking patterns are vulnerable to stressful life events and depression. The DAS-A consists of 40 items and each item consists of a statement and a 7- point Likert scale (7 = fully agree; 1 = fully disagree). The total score ranges from 40–280.

2.4 POSITRON EMISSION TOMOGRAPHY (PET) IMAGING - BACKGROUND AND PRINCIPLE

Positron Emission Tomography is a three-dimensional imaging technique based on nuclear medicine principles to study biological, pharmacological and physiological function in vivo. PET imaging involves at least three steps: first, the preparation of radiotracer by chemically incorporating a radionuclide into a molecule targeting either a specific site of action (receptor or enzyme) or a normal biochemical process (glucose consumption); second, the administration

of radiotracer to the subject and subsequent imaging of the radiotracer activity by the PET scanner; third, the quantification of PET data into a clinically useful outcome measure by using mathematical modelling and computation. Therefore the success of the PET imaging directly depends on scanner quality, suitability of radiotracer and validity of image analysis.

2.4.1 The fundamentals of PET Physics

Radionuclides used in the PET are produced in the particle accelerator (Cyclotron) by bombarding a stable atom with high energy charged particles (Spinks et al., 2000). The commonly used radionuclides in PET are carbon ^{11}, nitrogen ^{13}, oxygen ^{15} and fluoride ^{18}. All these radionuclides are unstable and have short half-lives. In addition, each of the radionuclides has generally more protons than neutrons. This 'excess' positive charge is released during a process of radioactive decay called beta decay, emitting a positively charged electron or positron, a neutron and a neutrino. A positron is also called an 'antiparticle of electron' with exactly opposite charge. Positrons do not last long in the 'matter' because the emitted positron quickly encounters an electron after travelling up to a few millimetres. This encounter annihilates both particles and in the process, energy is converted into two gamma ray photons of about 511 keV (resting mass of electron and positron) (Figure 2-1). The released photons travel in opposite directions at about 180 degrees (Badawi, 1998).

Figure 2-1: Positron emission and annihilation

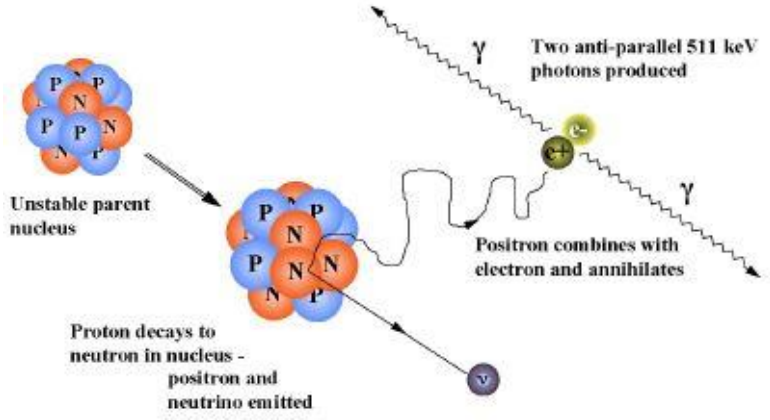


Image Source

http://depts.washington.edu/nucmed/IRL/pet_intro/intro_src/section2.html

2.4.2 PET Camera

The PET camera has a ring of detectors which are connected to a computer system (Turner and Jones, 2003). The participant is placed within the field of view on (FOV) of the detectors. Each detector has a scintillator and Photo Multiplier Tubes (PMT) which detect the released photons after the positron annihilation (Figure 2-2). The annihilation photons strike the scintillator which absorbs its energy and re-emits the absorbed energy in the form of a small flash of light, typically in the visible range. This flash of light is then amplified by PMT and recorded by an electronic circuit which feedbacks to computers for reconstruction. There are different scintillator crystal materials commercially available such as NaI (sodium iodide), CsI (caesium iodide), KI (potassium iodide), GSO (gadolinium orthosilicate), LSO (Lutetium orthosilicate) etc (Spinks et al., 2000).

2.4.3 Coincidence detection

The annihilation gamma ray photons are detected by a pair of opposite PET detectors (Spinks et al., 2000). It is therefore possible to localise their source along the line of coincidence joined by the opposite detectors. This line is also called a Line of Response (LOR). To calculate the exact location of the annihilation event, the detector relies on the time window of coincident detection of the pair of photons travelling nearly 180 degrees opposite to each other. The photons that are incident on the opposite detectors after the annihilation event within the specific time window are considered as 'True coincidence'. The photons that do not reach the detector within the time window are ignored. The PET scanner has high temporal resolution to resolve the timing of event and thus has a high signal to noise ratios.

2.4.4 Sources of error in PET data acquisition

The quality of the PET scan depends upon the ability of the PET camera to record the 'true' coincidence event. The common sources of error that can occur during PET data acquisition are Random coincidence, Scatter coincidence and Attenuation effect (Fig 3) (Badawi, 1998). Random coincidence can occur when two photons arising from different annihilation events are incident on detectors within the same time window. This can lead to false location of an event and produces image artefact. Scatter coincidences can also occur when the pair of photons emitted after the annihilation event are scattered by losing their way due to loss of energy; this is caused by so called

"Compton scattering" or "Compton effect". Compton scattering occurs when high energy photon collide with a stationary electron and thereby lose kinetic energy. The scatter coincidence affects the image contrast and quality due to signal loss. Attenuation of signal can also occur due to differences in the thickness of the surrounding tissue. This produces image artefacts due to signal loss and additional noise. To reduce the effect of activity outside the direct field of view in brain scans, the tomograph is equipped with annular side shielding (Spinks et al., 1998). A transmission scan before the radiotracer administration using a point or rotating rod source is carried out for subsequent attenuation correction. CT or MRI images also aid attenuation correction. The sources of errors described above can be corrected using several pre-processing steps and image reconstruction.

2.4.5 PET Image Reconstruction

The raw data from PET scans are the thousands of coincidence events along the straight line of response. These events are also called as count rate. The count rates are acquired throughout the scan over contiguous time intervals of varying length ranging from 5 seconds to 20 minutes known as Frames. The 3D dynamic emission scan is usually acquired in list mode. After the data acquisition different frames of varying length are generated. The length of frames depends on the count rate statistics. Thus the count rates generated are finally reconstructed into three-dimensional images by computation post processing. The most commonly used PET reconstructions technique is Filtered Back Projection (FBP). The aim of the reconstruction process is to

retrieve the radiotracer spatial signal from the count rate data projected from the scanned object. The FBP method sends the projection data back to the image source ('back projection') to acquire the spatial origin of original signal. However simple projection may be inaccurate due to noise. It is possible to reduce the noise by using a filter. The FBP gives accurate quantification but produces low resolution and strike artefacts. Iterative Reconstruction (IR) is another method provides high resolution; however it has issues such as slow and non-uniform convergence and produces noisy images with sparse dark and white spots. Finally the quantification of reconstructed images gives the distribution of the radiotracer in the tissue.

Figure 2-2– Coincidence event in a PET camera

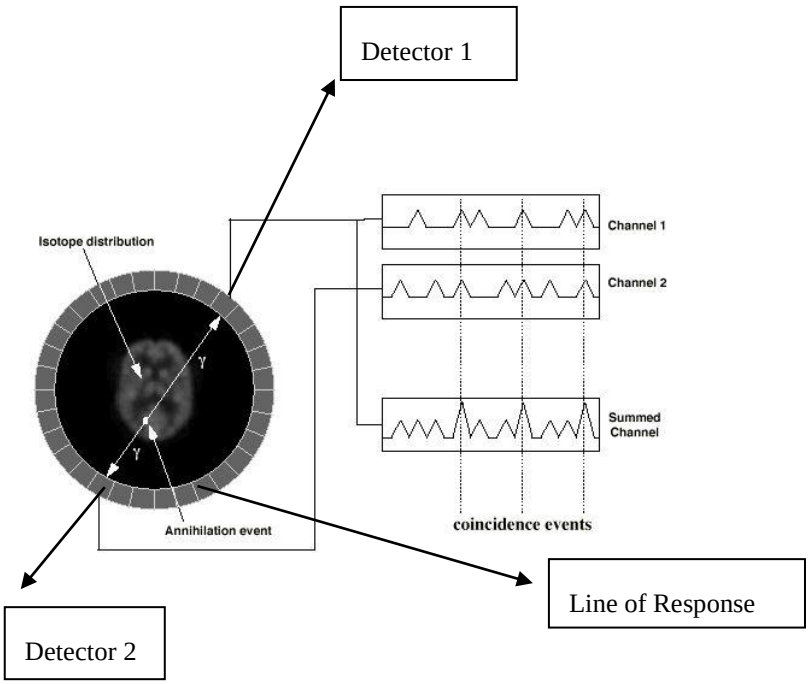


Figure 2-3 – Sources of error in PET acquisition

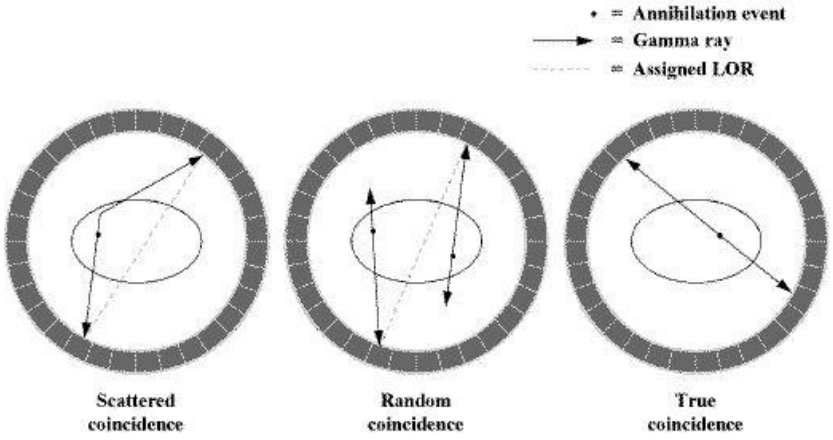


Image Source

http://depts.washington.edu/nucmed/IRL/pet_intro/intro_src/section2.html#2.5

2.5 PRINCIPLES OF RADIOTRACER

PET, when combined with a suitable radiotracer, can be a very powerful tool to study a protein target such as receptors, transporters, enzymes etc. The preparation of a suitable radiotracer for a brain target is a complex scientific process similar to drug development. To study a specific target in brain, a PET radiotracer must have a range of ideal characteristics (Pike, 2009). They are as follows;

- High selectivity and affinity for the target to obtain images with high signal to noise ratio.
- Reversible binding within the scan time to facilitate quantitative modelling
- Moderate to high lipophilic properties to penetrate the Blood Brain

Barrier (BBB) for high brain uptake; should not, however, be excessively lipophilic thereby causing non-specific binding to fat or other tissue in brain.

- No metabolites with radioactivity that can enter the BBB
- Should not alter the functional activity of the target
- Safe to administer and have acceptable radioactivity dose to permit imaging of clinical population.

While PET is a highly sensitive technique to study in-vivo biological systems, it lacks chemical resolution. The tissue activity recorded during the PET scan can be due to the radiotracer bound to the target; to non-specific binding to other targets; or due to radiotracer metabolites. The successful radiotracer has high specific to non-specific binding ratio and no detectable metabolites with radioactivity in tissue. When administered intravenously, the radiotracer rapidly undergoes metabolism by blood and tissue enzymes, so that only a fraction of parent radiotracer compound is left to enter brain. It should be possible to measure free fraction of radiotracer in plasma because this is helpful for accurate quantification of tissue uptake.

2.5.1 Radiotracer for 5-HTT

The neuronal serotonin transporter (5-HTT) plays an important role in regulating 5-HT release in the brain and is a primary site of action of many commonly used antidepressants such as SSRIs. Several PET radiotracers have been

developed for human imaging such as [^{11}C]citalopram, [^{11}C]cyanoimipramine, [^{11}C]fluoxetine, [^{11}C]sertraline, [^{11}C]dapoxetine, [^{11}C]DAPA, [^{11}C]AFM, [^{11}C]ADAM, [^{11}C]McN5652 and [^{11}C]DASB (Huang et al., 2002).

The first successful PET ligand used in clinical studies was [^{11}C]McN5652. Although [^{11}C]McN5652 has high in vitro affinity for 5-HTT (Ki value 0.4 nmol/L), it has several key limitations (Parsey et al., 2000) and has been superseded by [^{11}C]DASB (Frankle et al., 2004; Szabo et al., 2002). [^{11}C]McN5652 has low specific to non-specific binding ration which limits its use in that it can measure 5-HTT binding reliably only in richly innervated 5-HT regions such as midbrain and thalamus. In addition, it is difficult to reliably measure the plasma free fraction f_P of [^{11}C]McN5652 and as a result Binding Potential (BP_F) (see 3.3.4 Compartment model) which is a measure of f_P ($BP_P = f_P * B_{avail} / K_D$). f_P is the plasma free fraction and the concentration of tracer available for transport into tissue. It is difficult to interpret conditions that show differences in brain distribution volumes if f_P is not measurable (Ikoma et al., 2002).

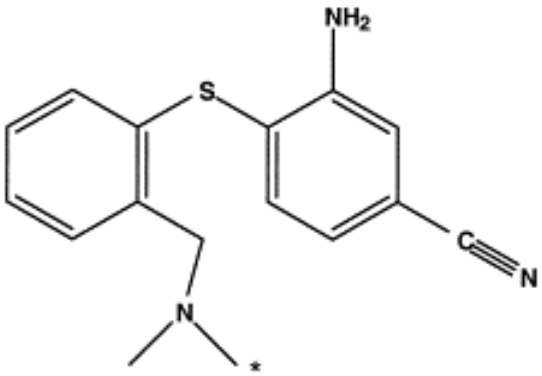
In a non human primate study of five PET ligands, [^{11}C]DASB, when compared with [^{11}C]DAPA, [^{11}C]AFM, [^{11}C]ADAM and [^{11}C]McN5652, has less affinity for 5-HTT and is less lipophilic (Huang et al., 2002). [^{11}C]DASB had higher plasma free fraction, rapid peak brain uptake and washout which produced good contrast among regions with moderate and low 5-HTT binding such as hippocampus and temporal cortex. Only [^{11}C]AFM had higher signal to noise ratio than [^{11}C]DASB in low 5-HTT regions such as limbic regions and

neocortex. In addition, [^{11}C]DASB required minimal scan time and has lower non-specific binding than all the tracers studied (Huang et al., 2002).

2.5.2 [^{11}C]DASB Synthesis

[^{11}C]DASB (*N*,*N*-dimethyl-2-(2-amino-4-cyanophenylthio)benzylamine) belongs to a class of compounds namely, diarylthioester that was developed as a putative radiotracer for 5-HTT in vivo imaging. It is synthesised from ^{11}C-iodomethane and the corresponding N-normethyl precursor (Houle et al., 2000; Wilson et al., 2000).

Figure 2-4: Chemical structure of [^{11}C]DASB {[^{11}C]N,N-dimethyl-2-(2-amino-4-cynophenylthio)benzylamine}



2.5.3 In-vitro and In-vivo Characteristics

DASB has higher affinity for cloned human 5-HTT and low affinity for other monoamine transporters. The selectivity for 5-HTT compared with the noradrenaline and dopamine transporters is more than 1000 fold in in-vitro

studies (Wilson et al., 2002; Wilson et al., 2000). Where Ki is the binding affinity of the inhibitor to the target receptor, the Ki value of DASB to 5-HT, noradrenaline and dopamine transporters is 1.1, 1350, and 1420 nmol/L respectively (Wilson et al., 2002)

2.5.4 Bio-distribution and Dosimetry

The whole body biodistribution and dosimetry studies in humans show that the calculated effective dose is of [^{11}C] DASB is 7 Sv/MBq, or 26 mrem/mCi which is equivalent to 3.8 mSv if the injected dose was 550 MBq (the commonly used injected [^{11}C]DASB dose) (Lu et al., 2004). The highest uptake of [^{11}C]DASB was in lungs which is upto 50 % of injected dose. However about 50% of [^{11}C]DASB lung uptake was washed out within 10 mins after the injection, thereby reducing the overall radiation burden. These results suggest that [^{11}C]DASB has relatively low radiation burden and it is safe to use in human studies.

2.5.5 [^{11}C]DASB Brain distribution

The brain distribution of the [^{11}C]DASB confirmed the pattern of 5-HTT sites with high binding in midbrain, hypothalamus and thalamus; moderate binding in striatum, hippocampus and amygdala; low binding in cortical areas and negligible binding in cerebellum. The hypothalamus to cerebellum as an index of specific to non-specific binding ratio was 7.9 at 60 mins after injection in rats (Wilson et al., 2000) and in humans (Ginovart et al., 2001). The pre-

administration of 'COLD' DASB i.e., without radioactivity, blocked specific binding, confirming the high specificity of DASB (Wilson et al., 2000). In addition, the levels of radioactive [^{11}C]DASB metabolites in rat brain were negligible (Wilson et al., 2000). In human PET studies, the [^{11}C]DASB distribution pattern was similar to preclinical studies (Ginovart et al., 2001). [^{11}C]DASB activity peaked in cerebellum and cortical regions early and later in the other moderate to high 5-HTT regions. The average ratio of thalamus to cerebellar activity at 90 mins is about 3 (Frankle et al., 2004). The results indicate that [^{11}C]DASB is a suitable radiotracer for imaging the brain 5HTT in human participants In human post mortem studies there was very low binding of the 5-HTT in cerebellar grey putamen and cortical regions to cerebellum 5-HTT is 27 and 5 respectively (Kish et al., 2005). This suggests that cerebellar grey matter can be used as a reference region in PET studies using [^{11}C]DASB.

2.6 PET DATA ANALYSIS

2.6.1 Basic tracer pharmacokinetics

The aim of a PET neuroreceptor study is to quantify receptor density or its functional activity by studying radiotracer distribution (Innis et al., 2007). PET receptor imaging can be viewed as an extension of autoradiography or ex-vivo radio-labelling techniques used in preclinical studies. Consider a simple in-vitro pharmacological experiment in which solutions of tracer and receptors are freely mixed, where [L] is the free concentration of ligand, [R] the concentration of receptors, and [LR] the concentration of receptor-ligand complexes. The

binding of radioligand to the tissue receptor is a dynamic process in which there is a continuous binding of ligand L to receptor R and dissociation of bound receptor-ligand (RL) complex. It can be assumed that there exists a time point t, equilibrium state when the net exchange between two states is zero (equation is shown below).

$$\text{Ligand [L]} + \text{Receptor [R]} \underset{K_{OFF}}{\overset{K_{ON}}{\rightleftharpoons}} \text{Bound [L+R]}$$

[L] – concentration of unbound or free ligand

[L+R] – concentration of bound ligand

The K_{ON} is the molecular association rate constant and K_{OFF} is molecular dissociation rate constant.

Based on the law of mass action, at equilibrium, K_D or dissociation constant can be derived.

$$[L][R]/[LR] = K_{OFF}/K_{ON} = K_D,$$

K_D is the reciprocal of the ligand affinity. i.e., affinity of ligand = 1/ K_D. If the K_D of the ligand is high, then affinity will be low and vice versa. When the above concept is applied to ligand binding studies, the receptor density and affinity can be derived by measuring the ratio of specific bound to free ligand from this equation (ratio of Bound/Free ligand at equilibrium);

$$B = B_{MAX}\, F/ K_D + F \text{ (based on Michaelis Menton equation) ---------- eq (1)}$$

Where B_{MAX} – total number of receptors

F – Free tracer or unbound tracer and

B – Bound tracer

However, at tracer doses, the F is very low, such that $F << K_D$. By substituting this into the eq 1, Binding potential can be derived,

$B/F = B_{MAX} / K_D$ or $B_{MAX} \times$ affinity

2.6.2 PET quantification

In PET neuroreceptor imaging, radiotracer activity in the arterial or venous blood (input function) and in brain tissue (output response function) are sequentially measured over time after the administration of the selective radiotracer into the blood stream. If the arterial blood sampling is not available, the input function can also be indirectly inferred from a reference region without target receptors (Laruelle et al., 2002). In a simple region of interest model, a target brain region is identified and a time-activity of tracer for that region is estimated from the images (Figure 2.9 (6)). Regional tracer concentration provides the quantification estimates of receptor density. Therefore the PET data represent tracer concentration (Bq/ml) per unit tissue. In PET studies, the radiotracer is administered at tracer doses and thereby occupy a negligible (<5% to 10%) percentage of target sites. The use of tracer doses will give specific binding of target sites, without significantly affecting the total number of

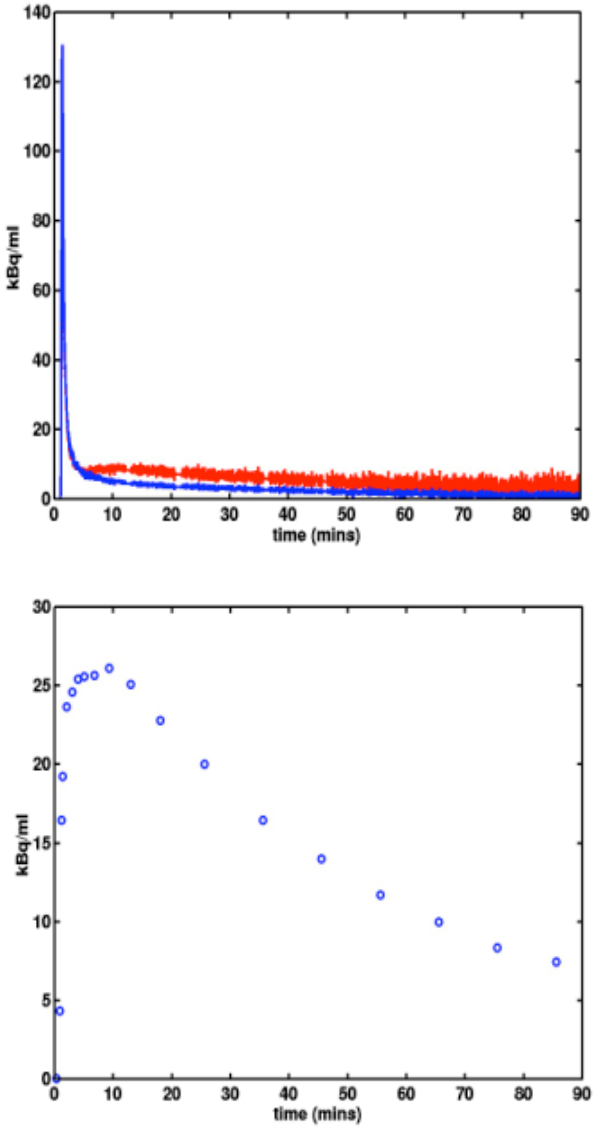
available receptors.

A simple ratio measurement of count rates in target brain region over a region devoid of receptors may produce inaccurate results as the activity recorded by PET will be due to some combination of activity from specific or non-specific binding or free tracer concentration. In addition, the tissue activity is influenced by a number of factors such as blood flow, permeability of blood brain barrier, concentration of competing endogenous ligands and peripheral clearance. Several mathematical model based methods have been proposed attempting to infer the relationship between the blood input function and PET image.

The following discussion about PET modelling is limited to 'Reversible' tracers. As described above in 2.6.1 Basic PET pharmacokinetics, the ligand binding to target is a dynamic process. During the equilibrium state, the rate of uptake and washout of tracers in target region is zero. Reversible tracers, such as [^{11}C]DASB which binds to 5-HTT, are tracers that reach equilibrium rapidly, and therefore enable short scan duration (60-90 min). Irreversible tracers are characterized by a longer equilibration or accumulation time.

Figure 2.4a & 2.4b: Blood and tissue time-activity curve respectively

(Source – lecture slide from Vincent Cunningham, Neuroreceptor mapping PET Pharmacokinetics course 2008, Pittsburg, USA)



2.6.3 Compartmental modelling

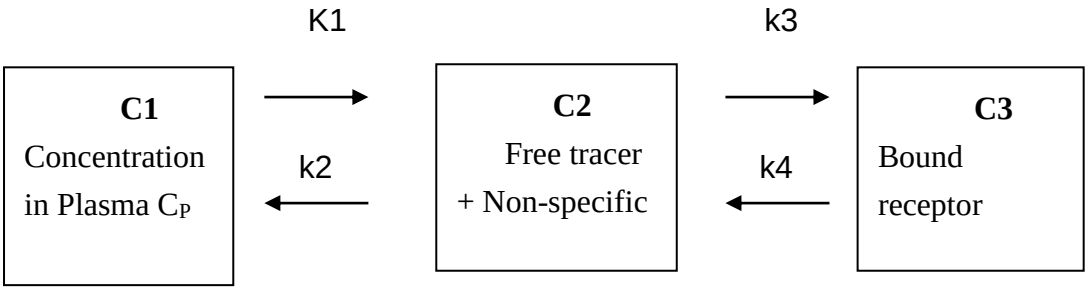
A presupposed theoretical model based on the understanding of the biological fate of tracer in the body is initially needed to make sense of the acquired

imaging data. Tracer kinetics based on in-vitro and preclinical in-vivo data are required to build the model. The intention is to fit the acquired PET data to the model to derive quantitative PET parameters. The compartment model is the most widely used approach. The concept of compartments is a mathematical notion to explain tracer kinetics in the tissue. A compartment is a physiological or biochemical 'space' representing a separate tracer pool (Laruelle et al., 2002). The tracer pool is assumed to be homogenous within the compartments. In a brain receptor PET study in a region of specific binding, at least four possible compartments can be described; Plasma compartment C1, brain tissue in which the tracer is free (C2), specifically bound (C3) and non-specifically bound (C4). Tracer movement between the four compartments and the rates of exchange can be derived from the six fractional rate constants expressed as K1 to k6 (it is conventional to represent K1 in capital letters and the other constants in small letters, (see (Innis et al., 2007)). K1 represents the rate constant for fraction of tracer concentration moving from plasma to tissue compartment per unit time. The model based approaches attempt to estimate parameters by finding a set of rate constants that produce a model curve which is as close as possible to the measured data (Laruelle et al., 2002). The interaction between the compartments C2 and C3 represents specific binding of receptor and ligand and the K3/K4 ratio provides the estimate of specific binding of tracer. However, it may be very difficult to implement four compartments due to the high number of parameters, tissue heterogeneity or tracer behaviour.

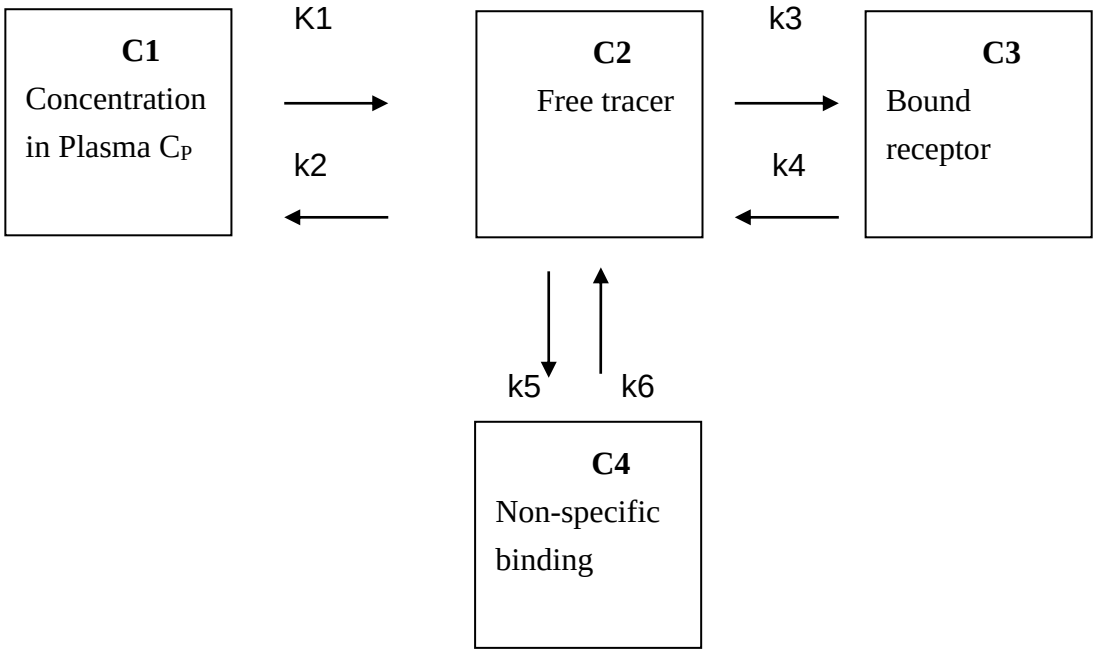
Figure 2-5: PET Compartment model

C1, C2, C3 and C4 represent compartments of plasma, free tracer, specifically bound tracer and non-specifically bound tracer respectively

Three compartment or two tissue compartment model



Four compartment or three tissue compartment model



K1 - rate constant for influx of tracer

k2 - rate constant for efflux of tracer from tissue

k3 - rate constant for transfer of tracer from free to specific binding

k4 - rate constant for transfer of tracer from specific to free tracer

k5 - rate constant for transfer of tracer from free to non-specific binding

k6 - rate constant for transfer of tracer from non-specific to free tracer

The four or three tissue compartment model requires measurement of plasma blood measurement of tracer concentration (both unmetabolised or parent tracer and metabolite fractions) and free fraction of tracer not bound to proteins (Gunn et al., 2001). This requires continuous and discrete arterial blood sampling during PET acquisition. Sometimes it may be difficult to acquire such data due to practical difficulties such as lack of blood monitoring facilities or the patient may be unwilling. By reducing the number of compartments, it is possible to simplify the parameters and the statistical variability (Laruelle et al., 2002). In most situations the kinetics between the free tracer pool C2 and non-specific binding C4 is fast, kinetically indistinguishable and therefore it is possible to ignore C4 in most PET neuroreceptor studies (three or two tissue compartment model). In addition, the two tissue compartment model can be further simplified into single tissue compartment if concentration in C2 and C3 equilibrate rapidly. It is possible to measure BP without arterial blood sampling if there is a reference region which is devoid of any specific binding. However the assumption is that the concentrations of free and non-specifically bound tracer are the same across brain regions.

The disadvantages of compartmental models are mainly that in many situations tracer kinetics are not well understood and kinetic compartments are sometimes not identifiable from the PET data. Therefore applying a presupposed model may not fit the PET data very well (Laruelle et al., 2002). It is therefore important to inspect and then derive the kinetic constants based on the acquired PET data.

2.6.3.1 Binding Potential and Affinity

Mintun et al (1984), proposed 'binding potential' as a key measure for PET neuroreceptor imaging, based on in vitro radioligand binding The concept explains the linear role of two parameters (receptor density and radioligand affinity) to determine the amount of radioligand uptake in brain. Binding potential (BP) can be viewed as the product of B_{MAX} and affinity.

It is possible to separate the two variables B_{MAX} and affinity and get quantitative estimates of the number of binding sites or their affinity. This can be achieved by occupying the binding site with varying concentration of unlabelled ligand or drug (Mintun et al., 1984). However this approach would not be appropriate in in-vivo studies involving human subjects because it involves exposure to high radioactivity and high ligand or drug concentration which may produce unwanted side effects. The BP represents the regional receptor density if K_D can be assumed to be constant in the experimental conditions or the different patient populations.

Applying the kinetic compartment model, BP can be derived from constants k3/k4 which is equal to B_{MAX}/K_D at equilibrium when the net rate of transfer between two compartments is zero. The binding potential derived from different models refers to ratio of concentration of specific binding in reference to other concentrations at equilibrium state. The nomenclature for using different notations has been redefined by international group of PET experts in modelling (Innis et al., 2007). The notation used below will be applied throughout this thesis. They are as follows;

BP_F refers to the ratio at equilibrium of the concentration of specifically bound radioligand in tissue to the concentration of free radioligand in tissue, which is assumed to equal the free concentration in plasma, if the ligand passes the blood– brain barrier only by diffusion.

BP_P refers to the ratio at equilibrium of specifically bound radioligand to that of total parent radioligand in plasma (i.e., free plus protein bound, excluding radioactive metabolites).

BP_{ND} refers to the ratio at equilibrium of specifically bound radioligand to that of nondisplaceable radioligand in tissue. BP_{ND} is the typical measurement from reference tissue methods, as it compares the concentration of radioligand in receptor-rich to receptor-free regions.

2.6.3.2 Volume of Distribution

Based upon clinical pharmacology, volume of distribution is another useful concept in PET. V_T is the distribution volume of total tracer uptake in tissue relative to total concentration of tracer in plasma. V_{ND} is the distribution volume of free and non-specific compartment relative to total concentration of ligand in plasma, $V_{ND} = V_F + V_{NS}$ where V_F and V_{NS} = volume of distribution of free tracer and non-specific binding respectively (Innis et al., 2007).

Using this principle, the relationship between the V_T and different BP parameters can be derived. Because specific binding equals V_T/V_{ND}, substituting this in BP_{ND} calculation provides,

$BP_{ND} = f_{ND}\ Bavail/K_D = k3/k4 = (V_T / V_{ND}) - 1$

$BP_F = Bavail/K_D = = K1k3/f_P\ k2k4 = (V_T - V_{ND})/f_P$

$BP_P = = f_P\ Bavail/K_D = K1k3/k2k4 = V_T - V_{ND}$

Where V_T and V_{ND} are volume of distribution of specific, and free and non-specific compartment relative to total concentration of ligand in plasma respectively

f_P is the plasma free fraction of ligand

f_{ND} is the free fraction of non-displaceable compartment

K1, k2, k3 and k4 are compartmental rate constants

Note that the units of BP_F and BP_P are $mL.cm^{-3}$ while BP_{ND} is unitless (Innis et al., 2007).

2.6.4 Methods of data analysis

There are a number of different analytical approaches to fitting data such as kinetic, graphical, reference tissue, spectral and equilibrium methods (Laruelle et al., 2002).

2.6.4.1 Kinetic Modelling

This is a model-based approach to estimate parameters by fitting the data to the model by minimizing the residual sum of squares over parameter space (Laruelle et al., 2002). This approach gives individual estimates for the parameters K1, k2, k3, and k4. Kinetic modelling provides accurate and unbiased method to estimate volume of distribution V_T. However this approach requires the accurate plasma measurements and unambiguous identification of brain compartments.

2.6.4.2 Graphical analysis (Logan et al., 1990)

This approach refers to the transformation of multiple time measurements of plasma and tissue uptake data into a linear plot, the slope of which provides the V_T and can be related to the number of available tracer binding sites. The advantages of this approach are that it allows easy comparisons among experiments and no prior model assumptions are needed. In addition, when a suitable reference region is available, plasma measurements of tracer are not required. The disadvantages of this method are that the statistical noise in the PET data may result in an underestimation bias of VT estimate (Slifstein and

Laruelle, 2000). However correction procedures are now available (Parsey et al., 2003).

2.6.4.3 Reference tissue models

Simplified Reference Tissue Model (SRTM) (Lammertsma and Hume, 1996) and Multilinear Reference Tissue Model (MRTM) (Ichise and Ballinger, 1996) – the reference region approach uses a brain region which is devoid of specific binding as reference for indirect input function. There are, however, several assumptions; that the exchange rates between specific and non-specific binding compartments are fast enough to be combined as single tissue and the non-specific binding in the reference region is similar to the target region. The model provides three parameters; K1, R1 and k2. K1 is the delivery of tracer from plasma to tissue, k2 is the delivery of tracer to the reference region without specific binding and R1 is the delivery of tracer to target relative to reference tissue. The drawbacks of these methods are the relative high bias and noise in the data underestimation of BP values.

2.6.4.4 Spectral analysis (Cunningham and Jones, 1993)

Spectral analysis assumes that the observed PET data can be described by sets of exponentials as an impulse response function and employs non-negative least squares fitting to estimate exponential basis functions. Spectral analysis also supplies information on the number of tissue compartments and its kinetics. The macroparameter V_T estimates can be directly calculated.

Spectral analysis can be easily implemented on the computer to obtain parametric images. However, this method may produce positive bias in the V_T estimates at the voxel level that is characterised by a lower signal-to-noise ratio than the tissue TACs (Cunningham et al., 1998).

2.6.4.5 Equilibrium method (Abi-Dargham et al., 1994; Carson et al., 1993)

This method is a modification of kinetic method. By administering the radiotracer as a bolus followed by a continuous infusion, it may be possible to obtain the equilibration of tracer, so that the rates of uptake and washout are zero. Then the binding potential can be estimated as the ratio of specific bound activity to free tracer within brain. The advantages of this approach are that it eliminates the variability due to blood flow changes and provides a linear measure related to receptor density. However, on the downside, long infusion time and blood sampling are required.

2.7 TEST RETEST RELIABILITY OF [^{11}C]DASB

[^{11}C]DASB quantification has been studied using a number of different modelling methods. The reported test-retest reliability is generally high and has been comparable between different methods (Frankle et al., 2006; Ginovart et al., 2001; Ichise et al., 2003; Ogden et al., 2007). However there are some differences between the methods. Ginovart et al (2003) found that a one tissue compartment model (1TC) fitted the data better than a two tissue model (2TC). They also reported lower V_T estimates (about 10-15%) using the graphical

method compared with the kinetic method (Ginovart et al., 2001). Frankle et al (2006) reported good reliability in BP and V_T measures between kinetic and graphical models, although the variability was higher in low compared with high 5-HTT regions in all methods. Finally, Ogden et al (2007) reported that likelihood estimation of graphical analysis of the Logan method was preferable for ROI analysis, providing better reproducibility and reliability. Overall, these studies indicate that the choice of modelling methods depends upon the nature of the experimental situation.

2.8 THE LIMITATIONS OF PET IMAGING

The limitations of PET imaging are mainly its relatively poor temporal and chemical resolution. However with the use of a selective and well-defined radiotracer it is possible to address chemical resolution issues. In addition, by combining PET with other brain imaging modalities such as Magnetoencepalography (MEG) and Functional Magnetic Resonance Imaging (FMRI) and preclinical experiments it is possible to overcome the temporality issue. However, the advancement of PET research depends upon the production of novel radiotracers which requires a strong chemistry and physics expertise and considerable ongoing investment. The other limitations are that participants are exposed to radioactivity in PET which limits its use in certain population like pregnant woman or very young people. In addition, PET is not available universally due to the need for a Cyclotron as well as considerable technical expertise which together lead to substantial investment and running costs.

2.9 MRI AND BRAIN MORPHOLOGY

Magnetic Resonance Imaging (MRI) has become a powerful tool in medical practice and research due to its non-invasive approach and the unmatched anatomical detail that it captures. MRI combined with new methods of processing and analysis has transformed the field of structural and functional brain imaging. MRI allows the study of changes in brain volume or size in greater detail than previous imaging techniques such as computerised tomography.

With MRI, the most commonly used methods to study brain structural changes broadly fall into two categories, manually defined region of interest (ROI) and global brain analysis without a priori regions of interest such as Voxel-Based Morphometry (VBM), Deformation Based Morphometry (DBM) and Tensor Based Morphometry (TBM). These methods have been well detailed in a recent computational neuroanatomy review (Ashburner, 2009). DBM and TBM use computational methods to identify global differences in brain structures (relative positions or local shape) of individual brain by mapping to a standard reference. In contrast, VBM is used to study the differences in local concentrations of various tissue types (gray or white) on a voxel-by-voxel basis. Because ROI and VBM analysis are employed in this thesis I will briefly discuss them further below.

2.9.1 Region of Interest (ROI) Analysis

In ROI models, the structures examined must be defined in advance and so this approach is driven by *a priori* hypotheses. The main advantage of the ROI approach is high reliability for well defined brain regions such as hippocampus, amygdala or ventricles. However, manually tracing the MRI regions is operator dependent and therefore reliant on the skills of the researcher. It can be time consuming and prone to some random error and bias. However the bias can be minimised by blinding the researcher who defines and measures the ROI and also by improving the inter-rater reliability. In addition, the ROI approach may neglect other brain regions which may be equally or more important to the aetiology of the disorder under study. Also some ROIs are more difficult to hand trace reliably; these include certain regions which have been implicated in the neurobiology of mood disorders and schizophrenia (e.g. anterior cingulate (ACC)/medial prefrontal Cortex (mPFC)). The availability of automated atlases has significantly improved the reliability of structural analysis of several brain regions (Hammers et al., 2002).

2.9.2 Voxel-Based Morphometry

Voxel-Based Morphometry (VBM) involves a voxel-wise comparison of the local concentration of tissue (gray or white matter) between two or more groups of subjects (Ashburner and Friston 2000). VBM is an objective, fully automated deterministic technique which allows the investigator to look for changes in volume in any part of the brain by applying statistics to the whole brain and

examining significant changes at a voxel level, corrected for the number of comparisons (Ashburner and Friston, 2000; Good et al., 2001b). In contrast to ROI studies, this technique allows analyses at whole brain level and is largely operator independent (Ashburner and Friston, 2000). There is good evidence that VBM has detected all of the well-replicated brain changes reported by hand tracing/ROI, and at the same time has identified reductions in areas that would be more difficult to hand trace reliably (e.g. ACC/mPFC). Voxel-Based Morphometry (VBM) provides an alternative approach and is complementary to ROI methods (Bergouignan et al., 2009; Giuliani et al., 2005; Testa et al., 2004).

2.9.3 VBM Methodology

Voxel-based morphometry of MRI data involves the following steps: template creation, registration, segmentation, normalisation modulation and smoothing (Figure 2-6). There are at least two ways of performing VBM analysis; standard or optimised VBM (Mechelli et al., 2005). In standard VBM, the Individual MRI images are first registered manually to ensure that all scans are in the same orientation as the stored template. This is usually aligned to a common Anterior Commissure (AC) – Posterior Commissure (PC) line. Next, a study-specific brain template of the groups to be compared is created. The individual images are spatially normalized to the same stereotactic space using a template. This normalisation is necessary to allow different brains to be compared, the aim being to minimise the gross differences in anatomy and structure, whilst preserving the local differences. The images are then segmented to separate

the three tissue classes, gray matter, white matter and cerebro-spinal fluid. Smoothing must be carried out next to improve the signal-to-noise ratio and also crucially to increase the statistical power. Finally statistical analysis can be applied to localise significant differences between two or more groups of brains. In optimised VBM, normalisation is performed on segmented MRI to avoid potential source of errors of attributing volumetric differences to local tissue differences (Figure 2-6).

Figure 2-6: Overview of Voxel-Based Morphometry pre-processing
(Source – John Ashburner, Functional Imaging laboratory, London)

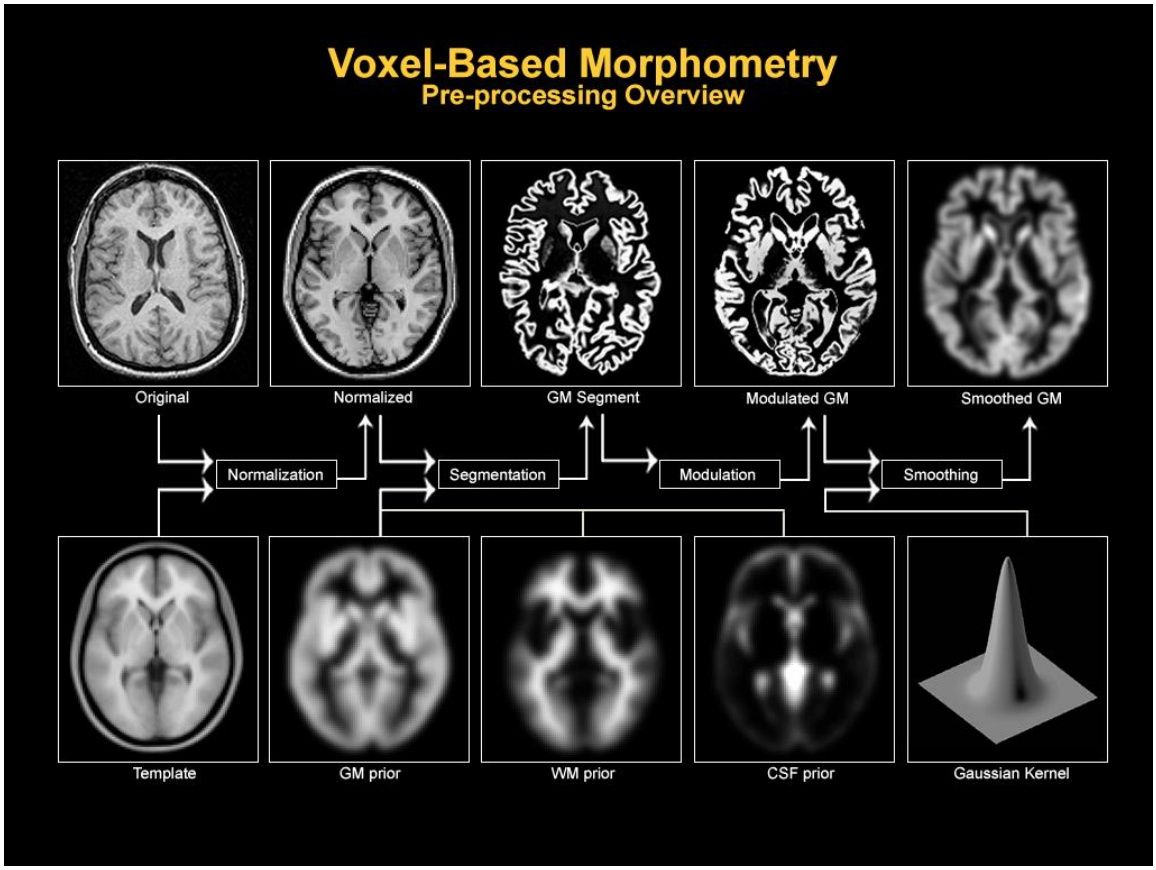
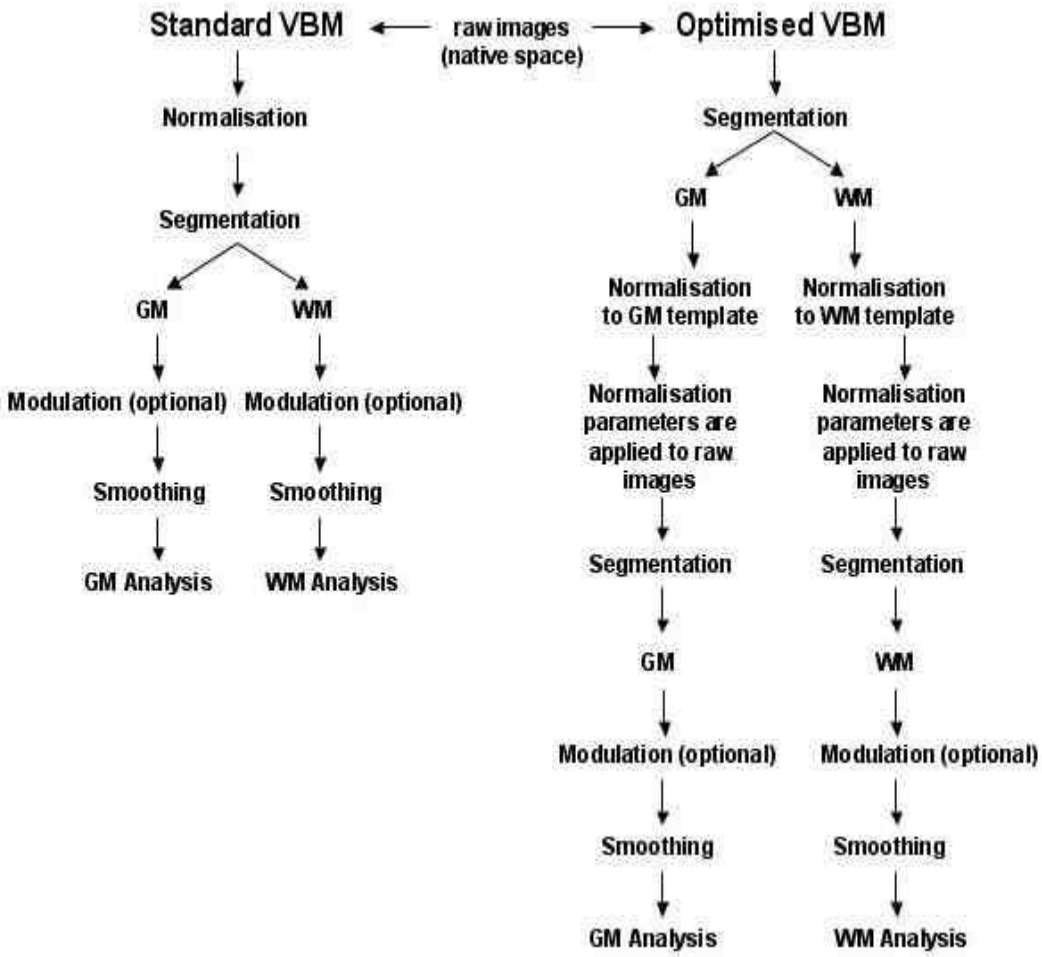


Figure 2-7: Flow chart of standard and optimised Voxel-based morphometry (VBM)

(Source (Mechelli et al., 2005))



2.9.4 VBM Limitations

The results of VBM are very sensitive to the quality of MRI registration, normalisation, segmentation and smoothing steps. If there was any error in these steps, the VBM may attribute false difference to local tissue changes. This potential source of error can be avoided by careful pre-processing of MRI

images. VBM is based on mass univariate statistical approach. For changes that occur non-linearly in different parts of brain, a multivariate approach will be needed (Mechelli et al., 2005). Furthermore the exact nature of gray matter changes observed with VBM is not well understood. For instance, whether the changes in grey matter represents the changes in neuronal numbers, size or shape or more to do with the grey matter thickness or folding can only be addressed using other techniques than MRI such as histology.

While VBM can be sensitive, operator independent and unbiased, ROI technique is useful for studying *a priori* identified regions which are reliably anatomically defined. For instance, for smaller regions such as amygdala and hippocampus, the inter-rater reliability of ROI approach is very high in majority of studies. Therefore the ROI and VBM technique can be complimentary to each other and by combining the two techniques it is possible to study subtle changes in brain structures both well defined and difficult to trace regions.

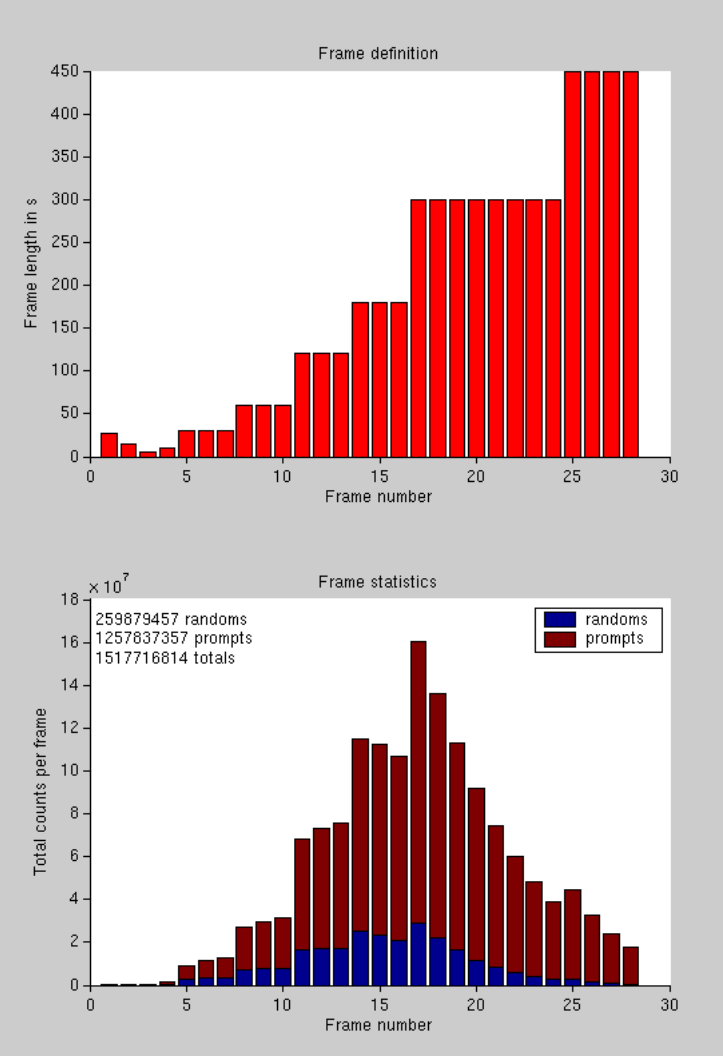
2.10 EXPERIMENTAL PROCEDURE FOR PARTICIPANTS UNDERGOING PET SCANS WITH [^{11}C]DASB

2.10.1 PET scan Acquisition

All PET studies were performed at the MRC Cyclotron unit, Hammersmith Hospital, London. Subjects arrived at least two hours prior to the PET scan and had a cannula placed in the radial artery and a venous cannula inserted in the contralateral antecubital vein.

All PET scans were performed on the high-sensitivity Siemens/CTI scanner ECAT EXACT3D with an axial field of view of 23.4 cm and 95 reconstructed transaxial image planes (Spinks et al., 2000). To reduce the effect of activity outside the direct field of view in brain scans, the tomograph was equipped with annular side shielding (Spinks et al., 1998). A 5-minute transmission scan using a ^{137}Cs point source was carried out prior to each study for subsequent attenuation correction (Xu et al., 1994) and scatter correction (Watson et al., 1996). The 90-minute 3D dynamic emission scan was acquired in list mode. In the post acquisition frame rebinning, 28 time frames of increasing length were generated (30 s background frame prior to the injection, then 1 15s-frame, 1 5s-frame, 1 10s-frame, 3 30s-frames, 3 60s-frames, 3 120s-frames, 3 180s-frames, 8 300s-frames and 4 450s-frames). The spatial resolution of the images reconstructed using the reprojection algorithm (Kinahan and Rogers, 1989) with the ramp and Colsher filters set to Nyquist frequency is close to isotropic: 5.1 mm full width at half maximum (FWHM) transaxially and 5.9 mm FWHM axially averaged over a radius of 10 cm from the centre of the field of view (Spinks et al., 2000).

Figure 2-8: [^{11}C]DASB scan with frame information and total count rate per frame from a healthy participant



2.10.2 DASB synthesis

The radiotracer [^{11}C]DASB was synthesized as previously described (Wilson et al., 2000) by reaction of [^{11}C]methyliodide with the desmethyl precursor. The standard DASB and the precursor desmethyl DASB were obtained from Target Molecules Ltd., Southampton (UK).

2.10.3 [^{11}C]DASB injection

[^{11}C]DASB was injected by hand into an antecubital vein as a smooth bolus over 30 seconds. The injected radioactivity dose was between 366.0 MBq and 566.5 MBq (mean: 519.4 MBq, SD: 33.8 MBq). The radiochemical purity of the injected [^{11}C]DASB was high and ranged from 95 % to 100 % with a mean of 97.5 % and a SD of 1.3 %. The injected mass of cold DASB varied between 0.1 µg and 13.7 µg with a mean value of 3.1 µg and a SD of 2.2 µg. The specific activity was on average 73982.0 MBq·µmol^{-1} with a SD of 88933.3 MBq·µmol^{-1}.

2.10.4 Arterial Input Function

Arterial whole blood activity was monitored continuously for the first 28 min of the scan with a bismuth germanate coincidence detector (Ranicar et al., 1991). For the initial 10 min during which the peak of radioactivity in the blood occurs and fine temporal sampling of the signal is required, the blood flow rate through the detector system was set to 5 ml/min. Thereafter the blood pump rate was reduced to 2.5 ml/min. Ten discrete arterial blood samples were taken at 3, 9, 15, 21, 28, 35, 42, 50, 70 and 90 min into heparinised syringes. The activity concentration of the whole blood and the plasma were measured.

Eight plasma samples per scan (at 3, 9, 15, 21, 35, 50, 70 and 90 min) were analysed for metabolites using a semi-automated system with on-line solid-

phase extraction (SPE) followed by reverse-phase chromatography with on-line radioactivity and UV detectors and integration system (Luthra et al., 1993). The plasma samples were loaded onto the SPE column and eluted with di-ammonium hydrogen phosphate (0.01 M) and further analysed using reverse-phase column (Bondapak C_{18} column, 30 cm x 0.78 cm internal diameter) eluted with a mixture of ammonium formate (10 mM) and methanol [35:65 v/v] at a flow rate of 3 ml/min. The eluate was monitored for UV absorbance at 254 nm and radioactivity and subsequent data captured on a PC based integrator. The amount of [^{11}C]DASB and its radioactive metabolites at a given time point was calculated from the decay-corrected integrated radiochromatogram and the levels of radioactivity in the SPE eluate and expressed as a percentage of total plasma samples injected.

2.10.5 MRI scans and Regions of Interest (ROI) Definition

All volunteers had a structural T1 MRI scan at the Robert Steiner MRI unit at the Hammersmith Hospital, London, UK. The MRI scan were performed on either 0.5T (0.5 Apollo system, Marconi Medical Systems, Cleveland, Ohio) or 1.5T (1.5 Eclipse system, Marconi Medical Systems, Cleveland, Ohio) MR scanners [TR=30s, TE=3s, flip angle=30, NSA=1, voxel dimensions 0.98 mm x1.6 mm x1.6 mm, acquisition time=13 mins] or 3T (3T Intera Philips Medical Systems) MR scanners [TR=9.6s, TE=4.6s, flip angle=8, NSA=1, voxel dimensions 0 94 mm x 0.94 mm x 1.2 mm]. The scans were inspected by an independent clinical radiologist and found to be normal. Due to the upgrade of the hospital imaging facilities we had to use different scanners.

Magnetic resonance images (MRI) were resliced to a voxel size of 1 mm x 1 mm x 1 mm, centered on anterior commissure (AC) and aligned to the AC-PC line. MR images were co-registered to the individual's summated PET images using SPM2 (Functional Imaging Laboratory London, UK) which adopts a rigid body transformation using normalised mutual information method. Regions of interest (ROI) were defined on the co-registered MRI with the help of a probabilistic brain atlas template (Hammers et al., 2003; Hammers et al., 2002). The standard MNI T_1 template (available in the SPM2) was normalised to the co-registered individual MRI and the deformation parameters were applied to the probabilistic atlas. This normalised brain atlas was resliced to PET space and segmented to obtain data from grey matter only.

The following ROIs were chosen for the analysis.

- 5-HTT moderate to rich regions: brainstem and thalamus
- Regions with moderate 5-HTT density: hippocampus, amygdala, putamen and caudate
- A region with low 5-HTT density: frontal cortex
- A region with very low concentration of 5-HTT: cerebellum.

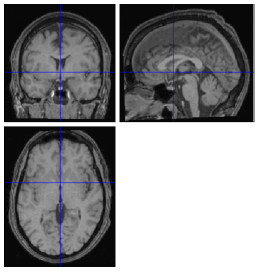
We obtained data from cerebellar grey matter up to 5 to 8 slices carefully avoiding spill over from occipital cortex or venous sinuses by placing the volume of interest well within the cerebellar cortex area leaving a margin of several millimeters around to the outer borders of the cerebellum as defined in

Hammers et al. (2003), page 240 (Hammers et al., 2003). Cerebellar grey matter was used as a reference region because of the reported negligible density of 5- HTT in the cerebellum (Kish et al., 2005).

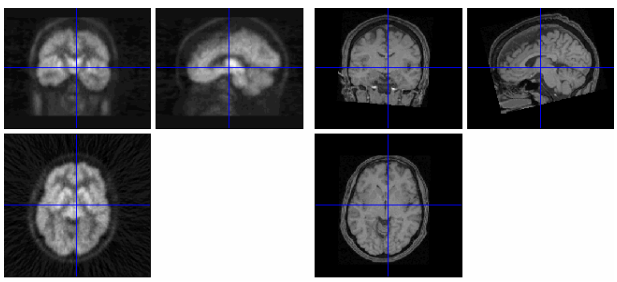
The dynamic PET scans were then sampled by applying the individual ROI object maps to create regional tissue TACs. The PET data were not corrected for head motion. Based on visual inspection of the tissue time-activity curves, all PET scans were free of any head motion to the extent that would be detectable this way.

Figure 2-9: [11C]DASB Image analysis flow chart

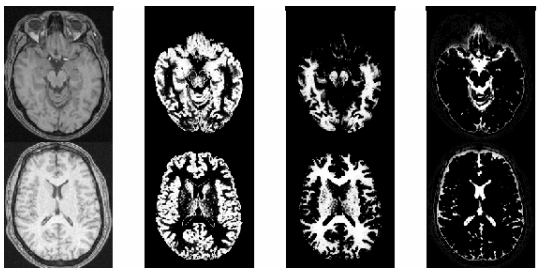
1) Realignment of MRI image to Anterior Commissure (AC) to Posterior Commissure (PC)



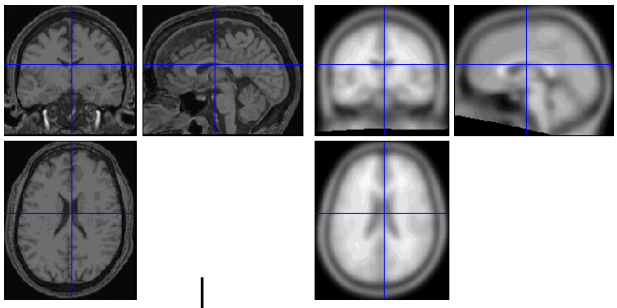
2) Coregistration of MRI to native PET space



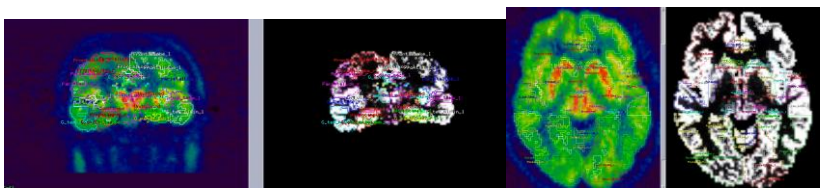
3) Segmentation of MRI into three different tissue classes grey matter, white matter and cerebrospinal fluid

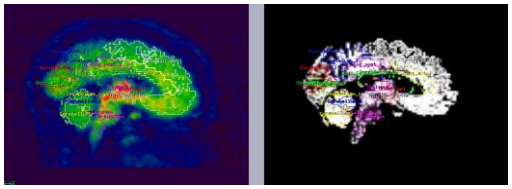


4) Use the segmented MRI for normalization with MRI template derived Montreal MNI 152

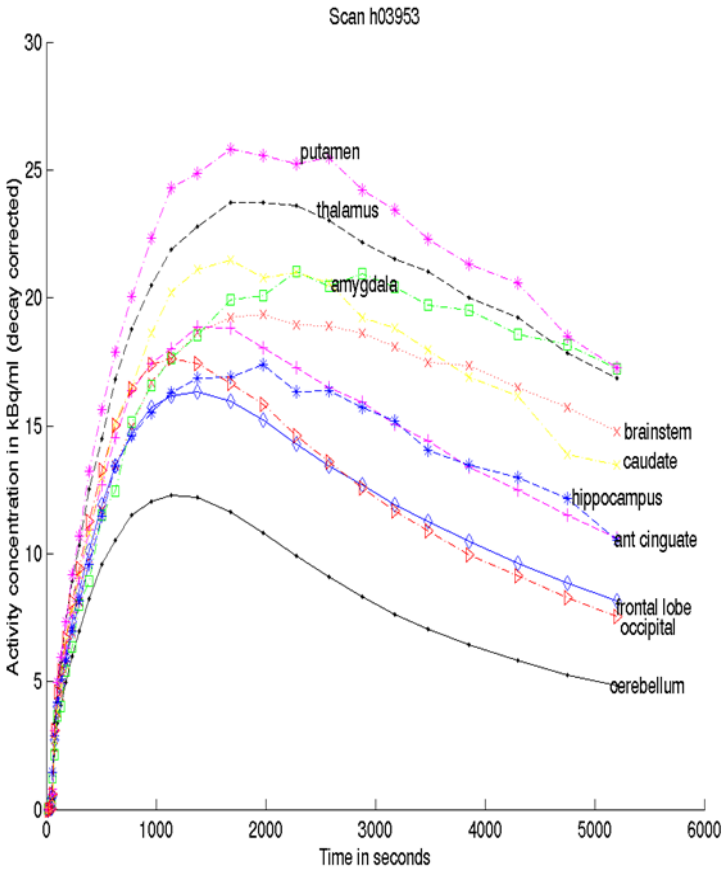


5) Region of Interest (ROI) drawn using automated probabilistic atlas, grey matter ROI only used





6) The dynamic PET scans were then sampled by applying the individual ROI object maps to create regional tissue Time activity curve (TAC).



2.10.6 Generation of the Plasma Input Function

For the generation of the plasma input functions, the time course of the plasma-

to-blood ratio, obtained from the first five discrete arterial samples at 3, 9, 15, 21 and 28 min scan time, was first fitted to a sigmoidal. Then the measurement of the arterial whole blood activity obtained from the continuous detector system (Ranicar et al., 1991) was multiplied with that ratio to obtain a total plasma activity curve for the first 28 min of the scan. This curve was then combined with the discrete plasma activity concentration measurements at 35, 42, 50, 70 and 90 min to an input function describing the total plasma activity concentration for the entire scan.

The input function of the activity concentration due to unmetabolised [^{11}C]DASB in plasma was then created by multiplying the total plasma activity input function with the function obtained from the fit of the model for the parent fraction in plasma to the eight measurements of the parent compound during the scan. Finally, the time delay of the arrival of the radioactivity bolus at the peripheral sampling site relative to the brain was determined (Hinz and Turkheimer, 2006).

All calculations were performed using Matlab® (The MathWorks, Inc., Natick, MA, USA) on Sun Ultra™ 10 workstations (Sun Microsystems, Inc., Santa Clara, CA, USA).

Figure 2-10: Fraction of unmetabolised parent [^{11}C]DASB compound in arterial plasma over time.

Black dotted line represents the predicted mean, red dotted line represent actual data from a healthy participant and yellow shade represents the standard

deviation from the predicted mean

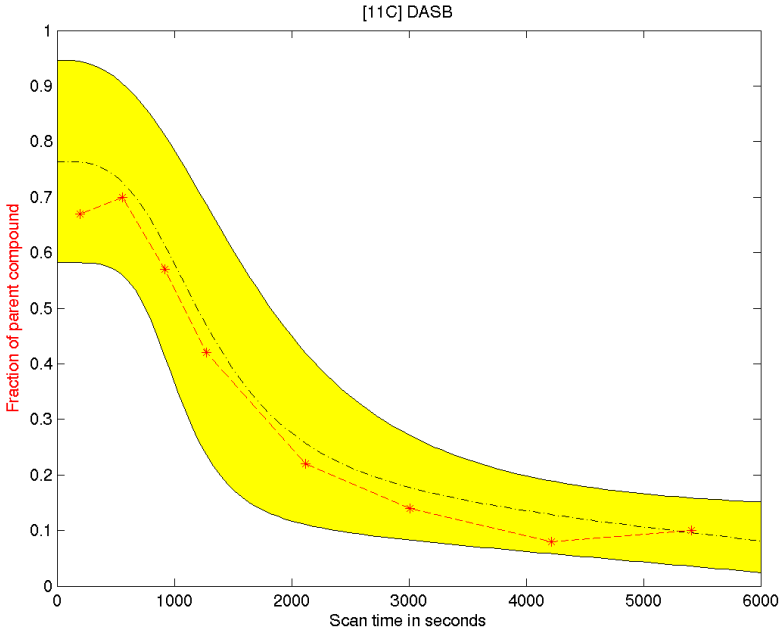
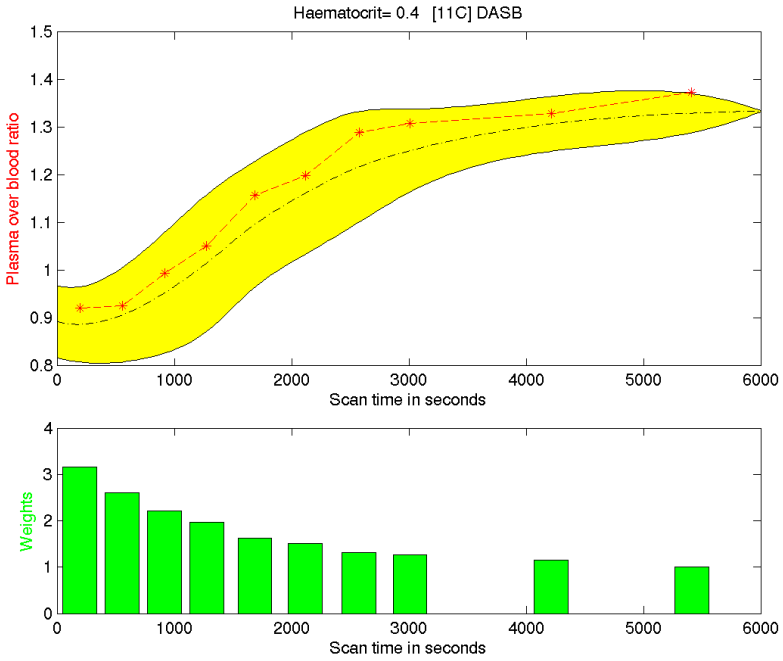


Figure 2.11: Ratio of plasma activity concentration over whole blood activity over the scan duration from a healthy participant



2.10.7 Quantification of the Ligand Binding in Tissue

For the quantitation of the [^{11}C]DASB binding in brain tissue, different previously used approaches were considered (Frankle et al., 2006; Ginovart et al., 2001; Ogden et al., 2007), with the aim of expressing the radioligand binding in tissue relative to the radioligand concentration in the arterial plasma in order to be able to assess the properties of the reference region.

Estimates of compartmental model parameters were obtained from weighted fits of the regional Time Activity Curve (TACs). The regional TACs were initially fitted to the reversible two-tissue compartment, four rate constants model with a free blood volume term without constraints (Gunn et al., 2001; Hinz et al., 2007). However, in several instances, difficulties with the convergence of the minimisation algorithms were encountered, and negative estimates of the rate constant k4 were obtained. Sometimes even the estimates of the rate constant k3 were negative. Similar difficulties in obtaining reliable estimates for the unconstrained two-tissue, four rate constants compartment model were reported by Frankle et al (2006) (Frankle et al., 2006). After a reduction of the model order to an unconstrained reversible one-tissue, two rate constants model with a free blood volume term, the parameter estimation procedures always converged to a solution. However, the quality of the fits, particularly in regions with lower uptake, often deteriorated substantially relative to the fits with the four rate constants model, as indicated by the residual sum of the squared errors. Therefore, the graphical analysis of reversible binding (Logan et

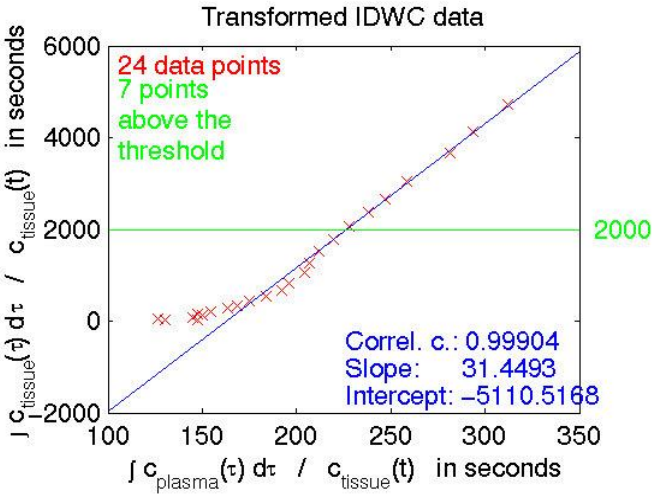
al., 1990) was used to obtain estimates of the total volumes of distribution V_T without explicitly deciding on the model order.

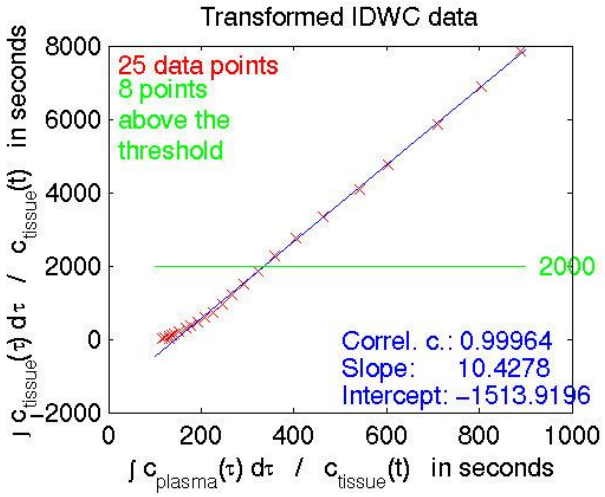
One of the requirements of the graphical analysis is the choice of the threshold time t* from which the portion of the graph is fitted by a straight line whose slope then provides an estimate of V_T (Logan et al., 1990). If this portion of the graph still has a remaining curvature, then the straight line fit is a secant rather than a tangent to the graph and as such provides an underestimation of the gradient of the curve. The threshold was set at 35 min, i.e., the transformed data from frames 20 to 28 were fitted with to a straight line. This value was therefore chosen as the threshold time t* for the data analysis, that is, the transformed data from frames 20 to 28 were fitted to a straight line (Figure 2-12). This threshold provided a trade-off between parameter bias (underestimation of the slope on average 3%) and parameter variance arising from fits based on eight data points or six degrees of freedom. A negative bias of parameter estimates obtained with the Logan plot has been shown by Silfstein and Laruelle (2000); however, previous investigators reported that the Logan analysis estimates obtained from [11C]DASB regional tissue TACs, that is, data sets of good statistical quality in comparison with the voxel level, appeared to be largely unbiased (Frankle et al., 2006; Ginovart et al., 2001).

Figure 2-12: [11C]DASB Logan plot from a healthy participant showing brain stem (Top) and cerebellum (bottom) .

The plot is the integral concentration of the tissue activity of target region over plasma activity. The transformed data from frames 20 to 28 were fitted to a straight line with

slope of the plot provides the regional volume of distribution V_T





The main study outcome was the in vivo binding potential $BP = B_{MAX} / K_D$ as the ratio of the serotonin transporter density B_{MAX} and the radioligand equilibrium dissociation constant K_D (Innis et al., 2007).

The binding potential of the specifically bound radioligand relative to the

nondisplaceable radioligand in tissue $BP_{ND} = f_{ND} \cdot BP = f_{ND} \cdot B_{MAX} / K_D$ with f_{ND} being the fraction of free radioligand in the nondisplaceable tissue compartment was calculated as follows, $BP_{ND} = (V_T - V_{ND}) / V_{ND}$.

Alternatively, The binding potential of the specifically bound radioligand relative to the parent radioligand in plasma $BP_P = f_P \cdot BP = f_P \cdot B_{MAX} / K_D$ with f_P being the fraction of free radioligand in plasma was calculated as follows.

$$BP_P = V_T - V_{ND}$$

Where V_T is the distribution volume of total ligand uptake in tissue relative to total concentration of ligand in plasma and V_{ND} is the distribution volume of nondisplaceable compartment relative to total concentration of ligand in plasma (Innis et al., 2007). V_{ND} is derived from the V_T of the cerebellar reference region. Therefore, the value of BP_P in a particular ROI is given by: V_T (ROI) – V_T (cerebellum).

The BP_{ND} is used as the main outcome measure throughout the thesis. However where there is an observed difference in reference region binding between two groups (cerebellum) V_{ND}, BP_P is used as a main outcome as it is less biased if there is some displaceable binding in reference region. In these situations, data from both BP_P and BP_{ND} are presented.

2.11 STATISTICAL METHODS

Statistical analyses were performed using Statistical Package for Social

Sciences (SPSS Inc., Chicago, Illinois, USA) version 12. All values are expressed as mean (standard deviation). Kolmogorov–Smirnov test was used to test the normality of data. Demographic data were analyzed using independent sample t tests. Differences across conditions were compared using Repeated Measures Analysis Of Variance (RM-ANOVA). Significant effects on the RM-ANOVA were followed up with post-hoc independent t tests. Correlations of parametric data were analysed using Pearson's correlation coefficient and non-parametric data using Spearman’s coefficient. All significance was set at $p<0.05$.

3 EFFECTS OF CITALOPRAM INFUSION ON 5-HTT BINDING

3.1 INTRODUCTION

As described in Chapter 1, underscoring its central position in the regulation of serotonergic neurotransmission, a number of attempts have been made to perform in vivo quantification of 5-HTT binding in humans with either single photon emission computerised tomography or positron emission tomography (PET). The two PET radioligands, which have been most widely used in the last decade, are the ^{11}C-labelled (+) enantiomer of trans-1,2,3,5,6,10b-hexahydro-6-[4-(methylthio)phenyl]-pyrrolo[2,1-a]-isoquinoline or [^{11}C](+)McN5652 (Suehiro et al., 1993) and (N,N-dimethyl-2-(2-amino-4-cyanophenylthio)benzylamine labelled with ^{11}C or [^{11}C]DASB (Houle et al., 2000). Of these two, comparison in animals and humans have shown that [^{11}C]DASB has the advantages of a higher ratio of specific binding to nonspecific binding and of a measurable free fraction in plasma (Frankle et al., 2004; Szabo et al., 2002).

Various tracer kinetic modelling approaches for human [^{11}C]DASB studies making use of a plasma input function or of a reference tissue input function have been compared (Frankle et al., 2006; Ginovart et al., 2001; Ogden et al., 2007). Furthermore, methods for the fast generation of parametric maps using a cerebellar time-activity curve (TAC) as the input function were presented (Ichise et al., 2003; Kim et al., 2006).

In general, the quantification of the specific binding in brain PET studies is based on two assumptions regarding the use of a reference region

(Cunningham and Lammertsma, 1995b). First, the reference region should effectively be devoid of specific binding. Second, the free and nonspecific binding of the radioligand should be uniform across the entire brain such that the binding estimate in the reference region can be used as a measure of the free and nonspecific binding in the other parts of the brain. However, in studies of PET radioligand binding to the 5-HTT, a growing amount of evidence suggests that these assumptions may not be fully met. Five examples may serve here as an illustration of these findings.

(1) Szabo et al (2002) observed changes of [^{11}C](+) McN5652 binding and of [^{11}C]DASB binding in the cerebellum of baboons after lesioning serotonin terminals with MDMA (methylenedioxymethamphetamine) or after treatment with the SSRI, paroxetine.

(2) Ikoma et al (2002) developed a dual scan paradigm based on administration of both stereo-isomers of [^{11}C]McN5652, the nonspecifically binding [^{11}C](-)McN5652, and the 5-HTT selective [^{11}C](+)McN5652 (Suehiro et al., 1993), to obtain estimates of the regionally variable free and nonspecific binding of [^{11}C](+)McN5652. The authors reported that the distribution of nonspecific binding of [^{11}C](+)McN5652 may not be uniform in the brain.

(3) Kish et al (2005) found in postmortem brain of normal adult subjects that the concentration of 5HTT binding sites in cerebellar cortex and white matter was approximately 20% of the concentration in cerebral cortex or 5% of the concentration in striatum.

(4) Parsey et al (2006c) reported a 33% reduction of the [^{11}C]DASB

distribution volume in cerebellar grey matter after daily oral sertraline treatment in healthy volunteers.

(5) The changes of radioligand binding to the 5-HTT in the cerebellum observed by, for example, Kent et al., 2002; Parsey et al., 2006c, and Szabo et al., 2002, were all greater than what would be expected from in vitro measurements of the 5-HTT density (Kish et al., 2005; Kretzschmar et al., 2003).

Citalopram is a commonly used antidepressant drug and is one of the most selective serotonin reuptake inhibitors (Hyttel, 1982). Although citalopram infusion has been used as a neuropharmacologic probe of serotonergic function (Lotrich et al., 2005), there are only two functional imaging studies with PET after parenteral citalopram both of which describe local changes in cerebral glucose metabolism (Geday et al., 2005; Smith et al., 2002). However, brain 5-HTT occupancy measured with PET after repeated oral citalopram administration has been measured (Meyer et al., 2001; Meyer et al., 2004b). The authors reported about 80% occupancy of striatal 5-HTT receptors during treatment with clinical doses of citalopram (20-40mg).

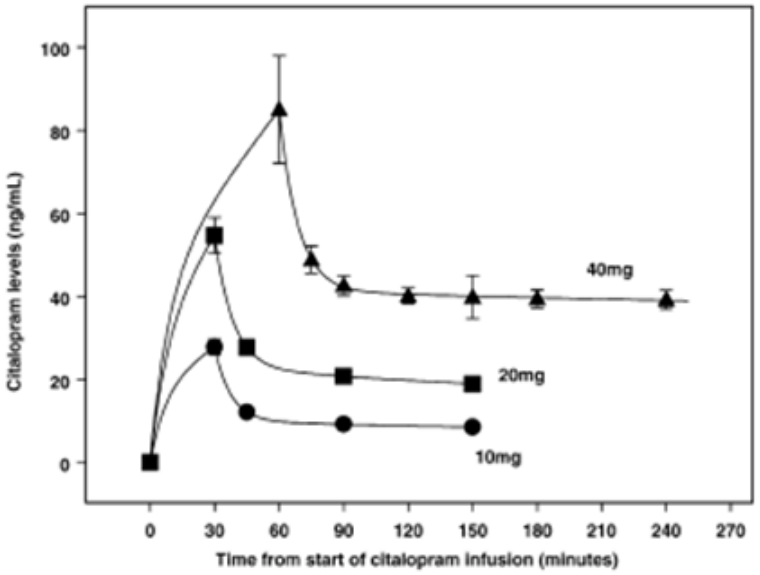
In the present study, I aimed to assess the effects of a single bolus infusion of 10 mg of citalopram on the kinetics of [^{11}C]DASB in plasma and on in vivo 5-HTT specific binding in the brain. The secondary aim is to compare the results with those previously published after oral citalopram administration.

3.2 MATERIALS AND METHODS

3.2.1 Subjects and Medication

Four healthy male control subjects (aged 49, 37, 57, and 42 years) gave written informed consent to be included in the study. Subjects were randomised to receive either a slow intravenous infusion of citalopram 10mg or placebo over 30 mins. The [^{11}C]DASB was injected about 15 mins after the completion of citalopram infusion. The dose and timing of the injection were based on previous studies showing robust and sustained effects of this dose of citalopram on anterior pituitary hormones - a putative marker of serotonergic system integrity (Attenburrow et al., 2001; Bhagwagar et al., 2002a). As published by Lotrich et al (2005) (Figure 3.1), this schedule leads in healthy control subjects to a fairly stable citalopram plasma concentration of about 10 ng/mL between 45 and 150 mins after the start of the infusion with little between-subject variability (Lotrich et al., 2005). Subjects were studied at least a week apart for both experiments, mean interval 9±3.4 days. The details of subject screening and recruitment was described in the Methods chapter. Subjects arrived at least 2 h before the PET scan and had a cannula placed in the radial artery and a venous cannula placed in the contralateral antecubital vein. All PET studies were performed in the late morning or early afternoon within a time window of approximately 3 h.

Figure 3-1: Mean plasma citalopram concentrations (±SEM) following 10 mg, 20 mg and 40 mg infusions (Lotrich et al 2005)



3.2.2 Positron Emission Tomography Scan Acquisition

The details of PET scan acquisition is detailed in the Methods chapter. All PET scans were performed on the high-sensitivity Siemens/CTI scanner ECAT EXACT3D with an axial field of view of 23.4 cm and 95 reconstructed transaxial image planes (Spinks et al., 2000). Positron emission tomography data were not corrected for head motion. On the basis of visual inspection of the tissue TACs, it was ensured that all PET scans were free of detectable head motion.

The radiotracer [^{11}C]DASB was synthesised as previously described (Wilson et al., 2000) by reaction of [^{11}C]methyl-iodide with the desmethyl precursor. The standard DASB and the precursor desmethyl DASB were obtained from Target Molecules Ltd (Southampton, UK). [^{11}C]DASB was injected by hand into an

antecubital vein as a smooth bolus for more than 30 secs. The injected radioactivity dose was between 487 and 547 MBq (mean: 523 MBq, s.d: 24 MBq). The radiochemical purity of the injected [^{11}C]DASB was high and ranged from 97% to 100% with a mean of 98% and an s.d. of 1.2%. The injected mass of cold DASB varied between 1.07 and 7.05 mg with a mean value of 2.4 mg and an s.d. of 1.9 mg. The specific activity was on average 81.0 GBq μmol^{-1} with an s.d. of 30.6 GBq μmol^{-1}.

Arterial whole blood activity monitoring and measurement as described in Chapter 2 occurred continuously for the first 28 mins of the scan with bismuth germanate coincidence detector (Ranicar et al., 1991). For the initial 10 mins during which the peak of radioactivity in the blood occurs and fine temporal sampling of the signal is required, the blood flow rate through the detector system was set to 5 mL/mins. Thereafter, the blood pump rate was reduced to 2.5 mL/mins. Ten discrete arterial blood samples were taken at 3, 9, 15, 21, 28, 35, 42, 50, 70, and 90 mins into heparinised syringes. The activity concentration of the whole blood and the plasma were measured. Eight plasma samples per scan (at 3, 9, 15, 21, 35, 50, 70, and 90 mins) were analysed for metabolites using a semiautomated system with online solid-phase extraction followed by reverse-phase chromatography with online radioactivity and UV detectors and integration system (Luthra et al., 1993). The amount of [^{11}C]DASB and its radioactive metabolites at a given time point was calculated from the decay-corrected integrated radiochromatogram and the levels of radioactivity in the solid-phase extraction eluate and expressed as a percentage

of total plasma samples injected.

3.2.3 MRI Scans and Definition of Regions of Interest

All volunteers had a structural T1 magnetic resonance (MR) scan performed on either 0.5 or 1.5 T MRI Scanners (GE Signa scanner; GE Medical Systems, Milwaukee, WI, USA). The definitions of region of interest (ROI) procedures are covered in Chapter 2. Only gray matter of ROIs was sampled. The following seven ROIs were chosen for the analysis based upon previous literature (Meyer et al., 2004a). They were brainstem, thalamus, amygdala, putamen, caudate and hippocampus. Cerebellum, which reportedly has a low concentration of 5-HTT was employed as a reference region (Kish et al., 2005). We obtained data from posterior cerebellar grey matter up to 5 to 8 slices carefully avoiding spill over from occipital cortex or venous sinuses by placing the volume of interest well within the cerebellar cortex area, leaving a margin of several millimeters around to the outer borders of the cerebellum as defined in Hammers et al (2003), page 240. The dynamic PET scans were then sampled by applying the individual ROI object maps to create regional tissue time-activity curves (TACs).

3.2.3.2 Generation of the Plasma Input Function

For the generation of the plasma input functions, the time course of the plasma-to-blood ratio, obtained from the first five discrete arterial samples at 3, 9, 15, 21, and 28 mins scan time, was first fitted to a sigmoidal curve. Then, the

measurement of the arterial whole blood activity obtained from the continuous detector system (Ranicar et al., 1991) was multiplied with that ratio to obtain a total plasma activity curve for the first 28 mins of the scan. This curve was then combined with the discrete plasma activity concentration measurements at 35, 42, 50, 70, and 90 mins to an input function describing the total plasma activity concentration for the entire scan. The input function of the activity concentration due to unmetabolised [^{11}C]DASB in plasma was then created by multiplying the total plasma activity input function with the function obtained from the fit of the model for the parent fraction in plasma to the eight measurements of the parent compound during the scan. Finally, the time delay of the arrival of the radioactivity bolus at the peripheral sampling site relative to the brain was determined (Hinz and Turkheimer, 2006). All calculations were performed using Matlab (The MathWorks Inc., Natick, MA, USA) on Sun UltraTM 10 workstations (Sun Microsystems Inc., Santa Clara, CA, USA).

3.2.3.3 Quantification of the Ligand Binding in Tissue

For the quantitation of the [^{11}C]DASB binding in brain tissue, a number of different previously used approaches were considered (Frankle et al., 2006; Ginovart et al., 2001; Ogden et al., 2007), with the aim of expressing the radioligand binding in tissue relative to the radioligand concentration in the arterial plasma so that the properties of the reference region could be assessed. Estimates of compartmental model parameters were obtained from weighted fits of the regional TACs. Details of this procedure were described in a previous study (Hinz et al., 2007). As a second method, the graphical analysis

of reversible radioligand binding using the plasma input function (Logan et al., 1990) was applied to obtain regional estimates of the total volume of distribution V_T from the slope of the linear part of the plot. Finally, spectral analysis (Cunningham and Jones, 1993) was used to create parametric images of V_T. The functional basis was set up with 100 functions logarithmically spaced between 0.0007 and 0.1/secs.

As described in the methods chapter 2, the binding potential was calculated as follows;

The binding potential of the specifically bound radioligand relative to the nondisplaceable binding BP_{ND} was calculated indirectly

$$BP_{ND} = V_T^{\text{target region}}/V_T^{\text{cerebellum}} - 1 \quad \text{---------- (1)}$$

and the binding potential of the specifically bound radioligand relative to the parent radioligand in plasma BP_P was also calculated indirectly

$$BP_P = V_T^{\text{target region}} - V_T^{\text{cerebellum}} \quad \text{---------- (2)}$$

The occupancy was expressed as the percentage reduction of the binding potential between baseline and blocked condition

$$Occ = (1 - BP^{\text{blocked}}/BP^{\text{baseline}}) \times 100\% \quad \text{---------- (3)}$$

where Occ_P was used to indicate occupancy derived from BP_P and Occ_{ND} was used to indicate that the occupancy was calculated from BP_{ND}.

3.3 RESULTS

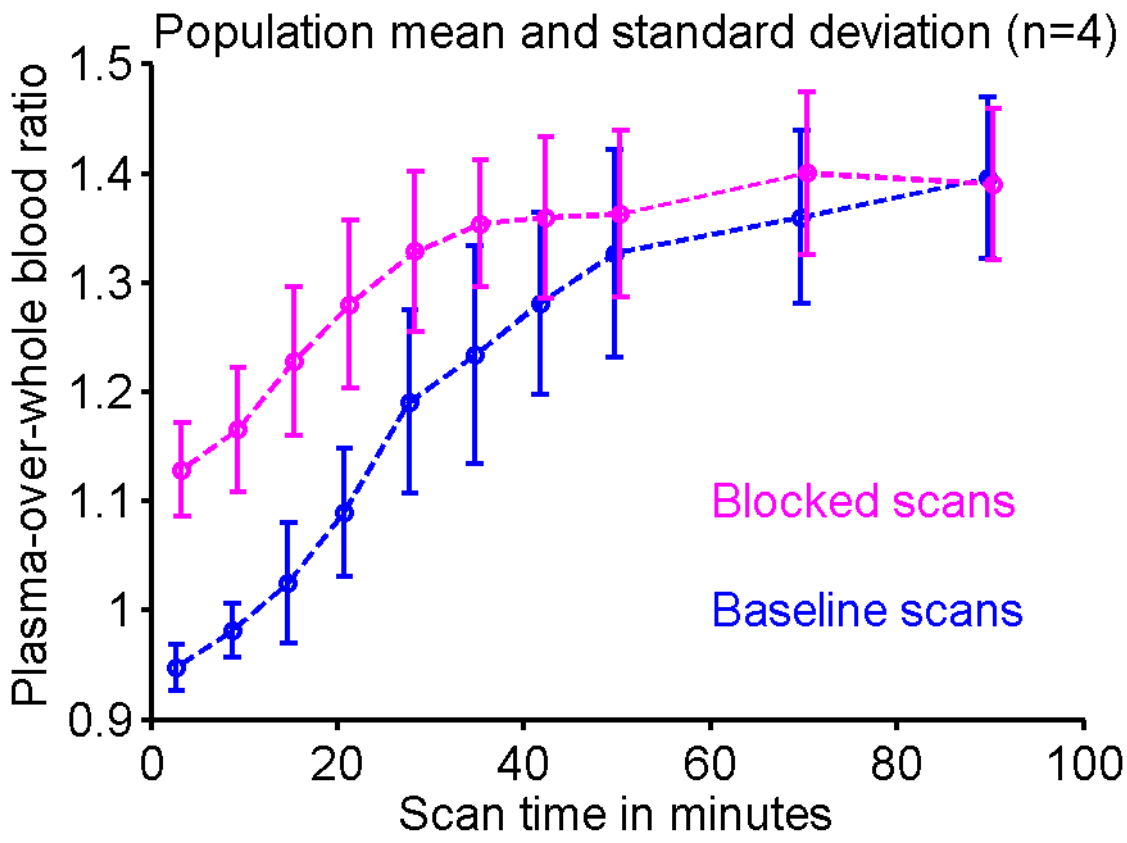
3.3.1 Input Function

In Figure 3-2, the observed time courses of the ratio of plasma activity

concentration over whole blood activity concentration are plotted for the two different scanning conditions. Under baseline condition after placebo infusion, the plasma-over-whole blood activity concentration ratio (POB ratio) was less than one, which means that the radioactivity concentration in whole blood was higher than in plasma. Owing to similarities in the properties of the membranes of red blood cells with the properties of the blood-brain barrier (BBB), the higher concentration of a lipophilic radiotracer such as [^{11}C]DASB, which is thought to cross the BBB by passive diffusion, in the red cell fraction than in the plasma fraction can be expected. During the time course of the PET scans, the POB ratios continually increased. This is consistent with the fact that the radiolabelled metabolites of [^{11C}C]DASB were reported to be more polar than the parent compound [^{11}C]DASB (Wilson et al., 2000) and as such are expected to preferentially accumulate in the plasma fraction rather than the red cell fraction.

Figure 3-2: Ratio of plasma activity concentration over whole blood activity concentration after placebo infusion (blue circles) or citalopram infusion (purple circles).

The mean values with their standard deviations are given for each of the 10 discrete arterial blood samples

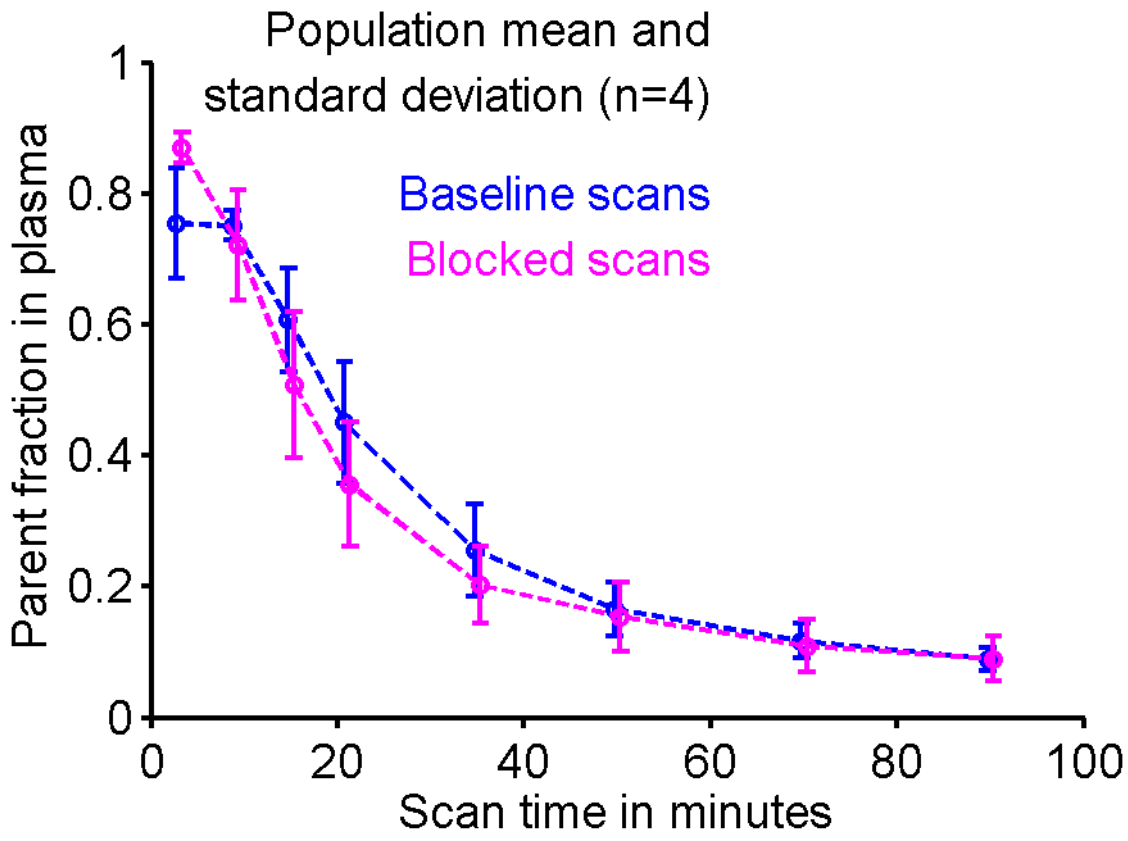


In the initial phase of the scans performed after citalopram infusion, the POB ratios were significantly higher than under baseline condition. As the scans progressed, this difference became gradually smaller, such that at the end of the scans at 90 mins, the POB ratios were no different between baseline and blocked condition. The initially higher POB ratio is likely because of citalopram blocking the 5-HTT binding sites on the platelets, which are part of the red cell

fraction when the blood samples are centrifuged. As a consequence, the concentration of [^{11}C]DASB in plasma is higher than in the red cell fraction. Because more and more radioactivity in the blood is represented by radiolabelled metabolites than by the unmetabolised [^{11}C]DASB and because the citalopram concentration in blood is also going down, the partition of the radioactivity between plasma and the red cell fraction approaches that observed after placebo infusion.

Figure 3-3: Fraction of unmetabolised parent compound in arterial plasma after placebo infusion (blue circles) or citalopram infusion (purple circles).

The plotted bars represent mean values and standard deviations from the four scans under each condition (baseline scans marked by blue circles and blocked scans marked by purple circles)



When a tracer is administered as a bolus, the initial injected compound is the original or parent tracer compound, which is metabolised over time. In Figure 3-3, the time course of radioactivity of the unmetabolised parent compound [^{11}C]DASB in plasma, is depicted for the two conditions. Despite the fact that the radiochemical purity of the injected dose was at least 97%, the parent fraction measured in the 3-mins sample was well below 90% (after citalopram infusion) or below 80% (after placebo infusion). A similar low parent fraction of the first arterial sample, followed by a higher parent fraction in the second samples has been reported by Parsey et al., 2006c. Dynamic acquisitions of the activity distributions in humans, baboons, and rhesus monkeys have shown that for the first 5 mins or so more than 50% of the total injected [^{11}C]DASB activity is concentrated in the lungs (Belanger et al., 2004; Lu et al., 2004; Tipre et al., 2004). As the lungs have been described as an organ of high metabolic activity and with a high concentration of serotonin reuptake sites, the intravenous infusion of citalopram before the [^{11}C]DASB administration and the subsequent blockade of the 5-HTT binding sites in the periphery by citalopram are consistent with the observed increase of the parent fraction at the onset of the PET scan. As the scan progressed, the differences between the measured parent fractions under baseline and blocked condition are no longer significant (Figure 3-3). As with the POB ratio, at the end of the PET scan at 90 mins, there is no difference between the two conditions in the parent fraction. The statistical uncertainty of the late parent fraction measurements was in the order of 5% to 10% as the entire late scan time chromatograms had only a few thousand counts acquired over an HPLC run time of 12 mins, and the parent

fraction peak then represented about 10% of the total plasma radioactivity.

To be able to account for this qualitative difference in the measured time course of the parent fraction, two different mathematical functions were used. The first model function is a sigmoidal

$$\text{Parent}(t) = c - (p_1 + p_2 x)/(p_3/x)^{p4} + 1 \quad \text{---------- (4)}$$

where x = t/3600 secs is the normalised time, p1 > 0, p2 > 0, p3 > 0, and p4 > 0 are the four free parameters of the model, and c is a fixed parameter of the model equal to the value of the function at t = 0. This function is strongly monotonic decreasing and, therefore, cannot have a local maximum. It was used to fit the parent fraction measurements of all four PET scans after citalopram infusion and of two scans (subjects 1 and 4) after placebo infusion, because in these six cases the measured values were monotonically decreasing.

For the measurements of the parent fraction in plasma obtained in subjects 2 and 3 after placebo infusion where the measured parent fractions at 9 mins were greater than those at 3 mins, the following model function with five free parameters was used to allow for a local maximum

$$\text{Parent}(t) = q_1 e^{+(q_2 t - q_3 t2)} + q_4 - q_5 t \quad \text{---------- (5)}$$

with all qi > 0 (i = 1y5). This lack of monotony under baseline condition is reflected in Figure 3-3 by the standard deviation of the second time point (9 mins) being much smaller than the standard deviation of the first time point (3

mins).

The overall impact of the citalopram infusion on the [^{11}C]DASB arterial plasma input functions is expressed as the AUC (area under the curve) for all four subjects in Table 3-1. After 5 mins, the AUC after citalopram infusion was by a factor of two to three more than after placebo infusion. This relative increase of the bioavailability of [^{11}C]DASB after SSRI administration continued throughout the scan, although to a lesser extent such that at 90 mins, the AUCs were, on average, 24% increased in comparison with the placebo scans.

Table 3-1: Area under the curve (AUC) in Bq/cm3/mins per MBq injected of the activity concentration (corrected for radioactive decay) due to parent compound [^{11}C]DASB in plasma.

	Subject 1		Subject 2		Subject 3		Subject 4	
scan time	placebo	citalopram	placebo	citalopram	placebo	citalopram	placebo	citalopram
5 min	49.7	103.0	30.6	89.1	28.2	122.4	44.6	98.2
30 min	158.1	196.2	151.7	207.7	165.8	259.8	140.3	194.6
90 min	225.7	250.4	245.9	295.5	272.2	353.9	196.3	247.5

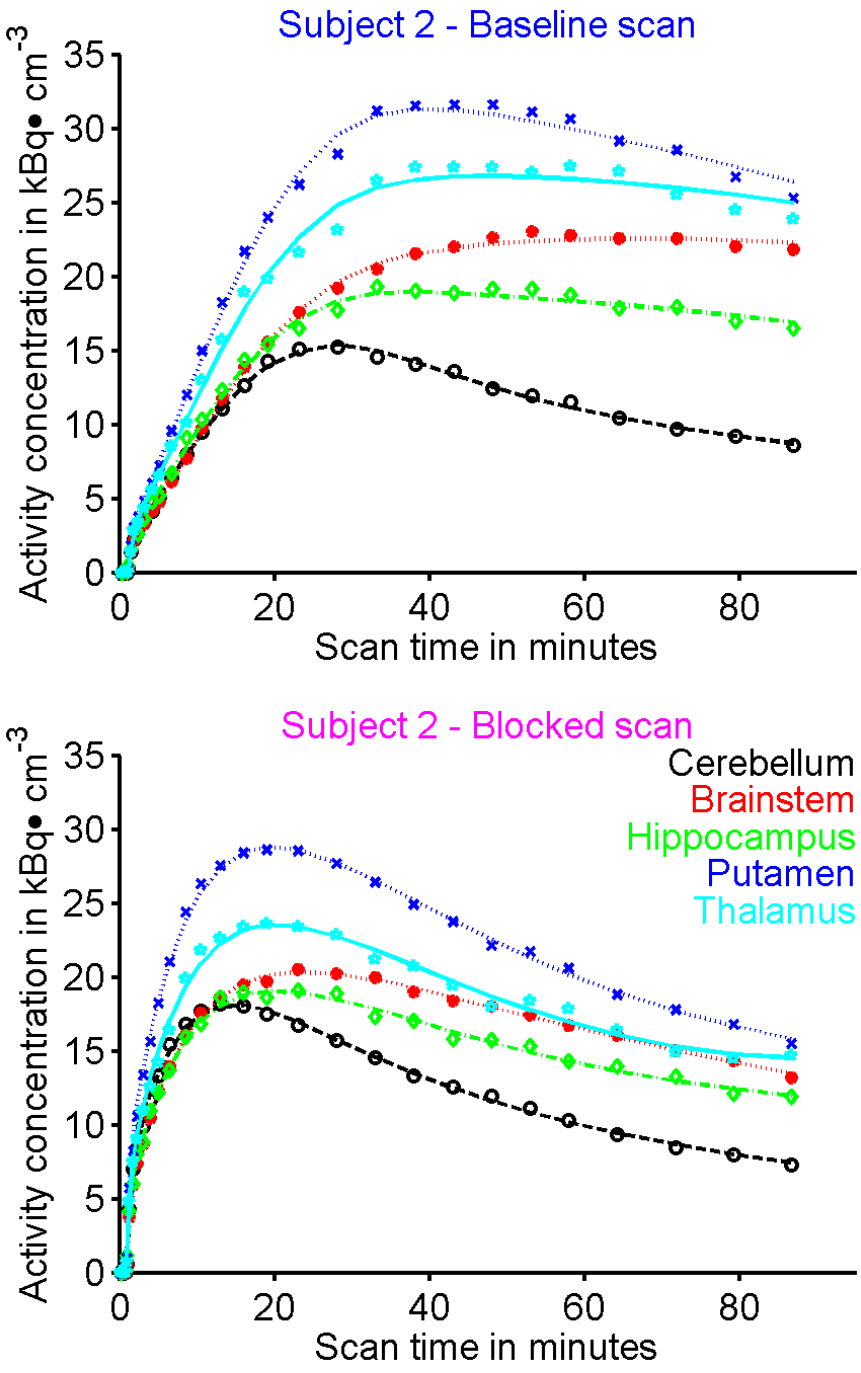
3.3.2 Tissue Response

In correspondence with the known distribution of the 5-HTT in human brain and as previously reported (Houle et al., 2000), high uptake of [^{11}C]DASB was observed in thalamus, midbrain, and hypothalamus, moderate uptake in hippocampus and basal ganglia, and relatively low uptake in the cerebellum.

Figure 3-4 shows tissue TACs from five selected regions of one subject after placebo infusion and after citalopram infusion, respectively. Under baseline condition and consistent with the observations by (Frankle et al., 2004), the local maxima of the TACs occurred, dependent on the speed of the regional kinetics, between 20 and 60 mins. After citalopram infusion, the peak times of the regional TACs were reached earlier (between 10 and 30 mins); thus, the kinetics was accelerated in comparison with the baseline condition. The peak activity concentration in the cerebellum was as a consequence of the increased availability of [^{11}C]DASB in plasma higher after citalopram infusion than it was after placebo infusion (Figure 3-4).

Figure 3-4 Five selected regional tissue TACs from one subject after placebo infusion (A) and after citalopram infusion (B), respectively.

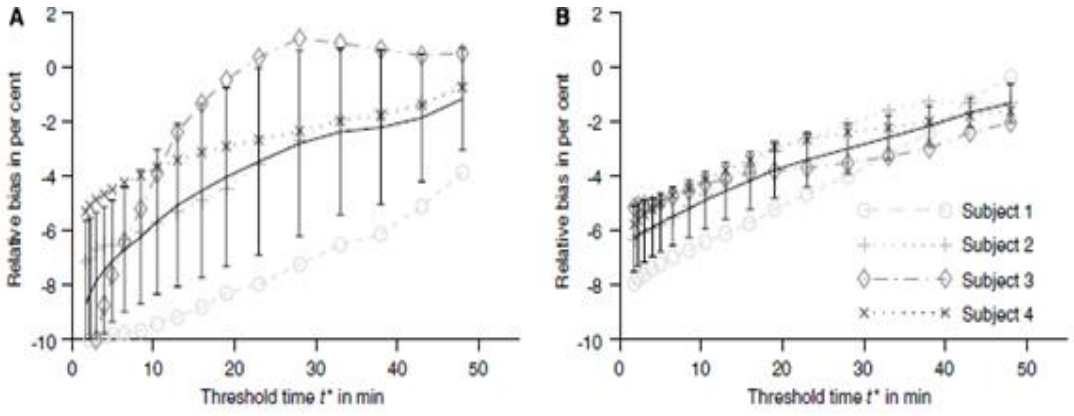
The lines represent the fits through the measured data points as obtained with the two-tissue compartment model.



The regional TACs were initially fitted to the reversible two-tissue compartment, four rate constants model with a free blood volume term without constraints, details of the procedure were described previously (Hinz et al., 2007). However, there were several problems emerged when the two tissue kinetic model was used. They were poor convergence of the minimisation algorithms, negative estimates of the rate constant k4, on some instances negative k3 and the poor quality of fits in some regions with lower uptake. Therefore the Logan graphical analysis of reversible binding (Logan et al., 1990) was used to obtain estimates of the total volumes of distribution V_T without explicitly deciding on the model order. One of the requirements of the graphical analysis is the choice of the threshold time t* from which the portion of the graph is fitted by a straight line whose slope then provides an estimate of V_T (Logan et al., 1990). If this portion of the graph still has a remaining curvature, then the straight line fit is a secant rather than a tangent to the graph and as such provides an underestimation of the gradient of the curve. This effect is illustrated in Figure 3-5 showing the relative underestimations of the slope as a function of the choice of the threshold time t*.

Figure 3-5: Relative bias of the estimated slope from the Logan plot analysis as a function of the threshold time t*.

The bars in the black represent the mean values and standard deviations across the four subjects under baseline condition (**A**) and after citalopram infusion



Theoretically, two data points would be sufficient for a straight line. However, such fits with zero degrees of freedom would provide only parameter estimates, which are extremely sensitive to the noise in these two measurements which is a particular problem when these two points are obtained from the low count data of the last two frames of a 90-mins PET scan with an ^{11}C-labelled compound. To calculate the relative bias of the estimated slope, the 'true' value of the Logan plot slope needs to be known, which means this value has, at the same time, to be an unbiased and low variance estimate of the slope. For the purpose of the calculations presented in Figure 3-4, the 'true' Logan plot slope was obtained from the mean value of the slopes estimated from the last four, five, and six frames of the dynamic study, that is, fits with two, three, and four degrees of freedom as the model function has the two free parameters slope

and intercept. This 'true' slope value corresponds to a 0% relative bias in Figure 3-5.

The underestimate of the slope is less severe under the blocked condition (Figure 3-5B) than under the baseline condition (Figure 3-5A). As the tracer kinetics in blood and tissue were faster after citalopram infusion, the steady-state conditions required to achieve linearity of the Logan plot (Logan et al., 1990) were approached faster than after placebo infusion. In Figure 3-5, the citalopram infusion also appears to have resulted in a reduction of the between-subject variability. The mean rate of change of the slope estimate with increasing threshold time t* plateaus off after about 35 mins in Figure 3-5A. This value was therefore chosen as the threshold time t* for the data analysis, that is, the transformed data from frames 20 to 28 were fitted to a straight line. This threshold provided a trade-off between parameter bias (underestimation of the slope on average 3%) and parameter variance arising from fits based on eight data points or six degrees of freedom. As the citalopram infusion led to the described faster kinetics in tissue and for consistency of the methods, the same t*-value was used for all subjects and regions, and for both conditions.

The results from all four subjects are given in Table 3-2. A negative bias of parameter estimates obtained with the Logan plot has been shown by Slifstein and Laruelle (2000); however, previous investigators reported that the Logan analysis estimates obtained from [^{11}C]DASB regional tissue TACs, that is, data sets of good statistical quality in comparison with the voxel level, appeared to be largely unbiased (Ginovart et al, 2001; Frankle et al, 2006).

The reduction of the cerebellar VT from the baseline to the blocked condition was 19%±13% for the four subjects. A paired two-tailed t-test did not reject the null hypothesis that there was no significant difference of the cerebellar VT between the baseline and blocked scans ($P > 0.067$). This, however, indicates a trend towards significance.

The intrasubject variability of the occupancy Occ_{ND} calculated from BP_{ND} between the six regions listed in Table 3-2 was highest in subject 4 with 10% or less for the others. Two parametric images of the total volume of distribution V_T after placebo infusion and citalopram infusion are shown in Figure 3-6. Visual inspection reveals that the V_T in the citalopram scan is lower in all regions of the brain including the cerebellum compared with the baseline scan performed after placebo infusion. The parameter estimates obtained from sampling the parametric maps generated with spectral analysis are given for all four subjects in Table 3-3. Individual V_T estimates are higher than those obtained from the regional analyses of tissue TACs with the Logan plot. This may be because of a negative bias in the estimates obtained from the Logan analysis (Slifstein and Laruelle, 2000), a positive bias in the V_T estimates obtained with spectral analysis at the voxel level that is characterised by a lower signal-to-noise ratio than the tissue TACs (Cunningham et al., 1998) or a combination of these two factors. In either case, the reduction of the cerebellar V_T in the parametric maps from the baseline to the blocked condition was 24%±11% for the four subjects. A paired two-tailed t-test rejected the null hypothesis that there was no

significant difference of the cerebellar V_T between the baseline and blocked scans ($P < 0.041$). Therefore, the changes of the cerebellar V_T in the parametric maps were statistically significant.

The mean occupancy Occ_{ND} calculated from BP_{ND} across all subjects was 59%. When BP_P was used to calculate the occupancy Occ_P, then a mean occupancy was 69%. The mean occupancy findings are in agreement with those obtained from the Logan analysis. Regardless of the kinetic model used, the occupancies calculated from BP_P are always equal to or greater than the occupancies calculated from BP_{ND}.

Table 3-2: Parameter estimates from the graphical analysis of reversible binding regional tissue time-activity curves

	Subject 1					*Subject 2*					*Subject 3*					*Subject 4*				
	Placebo		*Citalopram*			*Placebo*		*Citalopram*			*Placebo*		*Citalopram*			*Placebo*		*Citalopram*		
Volume of interest name	V_T	BP_{ND} BP_P	V_T	BP_{ND} BP_P	Occ_{ND} Occ_P	V_T	BP_{ND} BP_P	V_T	BP_{ND} BP_P	Occ_{ND} Occ_P	V_T	BP_{ND} BP_P	V_T	BP_{ND} BP_P	Occ_{ND} Occ_P	V_T	BP_{ND} BP_P	V_T	BP_{ND} BP_P	Occ_{ND} Occ_P
Cerebellum	9.2		9.2			9.9		7.9			12.7		9.6			9.3		6.4		
Amygdala	26.3	1.85	15.3	0.66	65	30.6	2.08	13.5	0.70	66	41.5	2.27	14.7	0.54	76	29.5	2.17	11.9	0.85	61
		17.1		6.1	65		20.6		5.6	73		28.8		5.1	82		20.2		5.4	73
Brainstem	26.9	1.92	15.3	0.66	66	30.1	2.03	13.3	0.68	66	34.5	1.71	14.4	0.50	71	25.4	1.74	11.3	0.75	57
		17.7		6.1	66		20.1		5.4	73		21.8		4.8	78		16.1		4.8	70
Caudate	23.7	1.57	13.5	0.46	71	23.4	1.35	12.9	0.62	54	31.7	1.49	14.5	0.51	66	22.5	1.42	9.9	0.54	62
		14.5		4.2	71		13.5		4.9	63		19.0		4.9	74		13.2		3.5	74
Hippocampus	17.0	0.84	12.1	0.31	64	19.6	0.97	11.7	0.48	51	26.5	1.08	13.7	0.44	60	17.4	0.87	10.0	0.57	35
		7.8		2.8	63		9.7		3.8	61		13.8		4.2	70		8.1		3.6	55
Putamen	29.1	2.15	16.2	0.75	65	29.5	1.97	15.7	0.99	50	34.6	1.72	16.3	0.71	59	28.5	2.06	13.4	1.09	47
		19.8		7.0	65		19.5		7.8	60		21.8		6.8	69		19.2		7.0	64
Thalamus	28.7	2.11	14.4	0.55	74	28.6	1.88	13.9	0.75	60	30.5	1.40	15.6	0.63	55	28.4	2.06	12.6	0.96	54
		19.5		5.1	74		18.7		6.0	68		17.8		6.0	66		19.1		6.1	68
Mean ± s.d.					67 ± 4					58 ± 7					64 ± 8					52 ± 10
					67 ± 4					66 ± 6					73 ± 6					67 ± 7

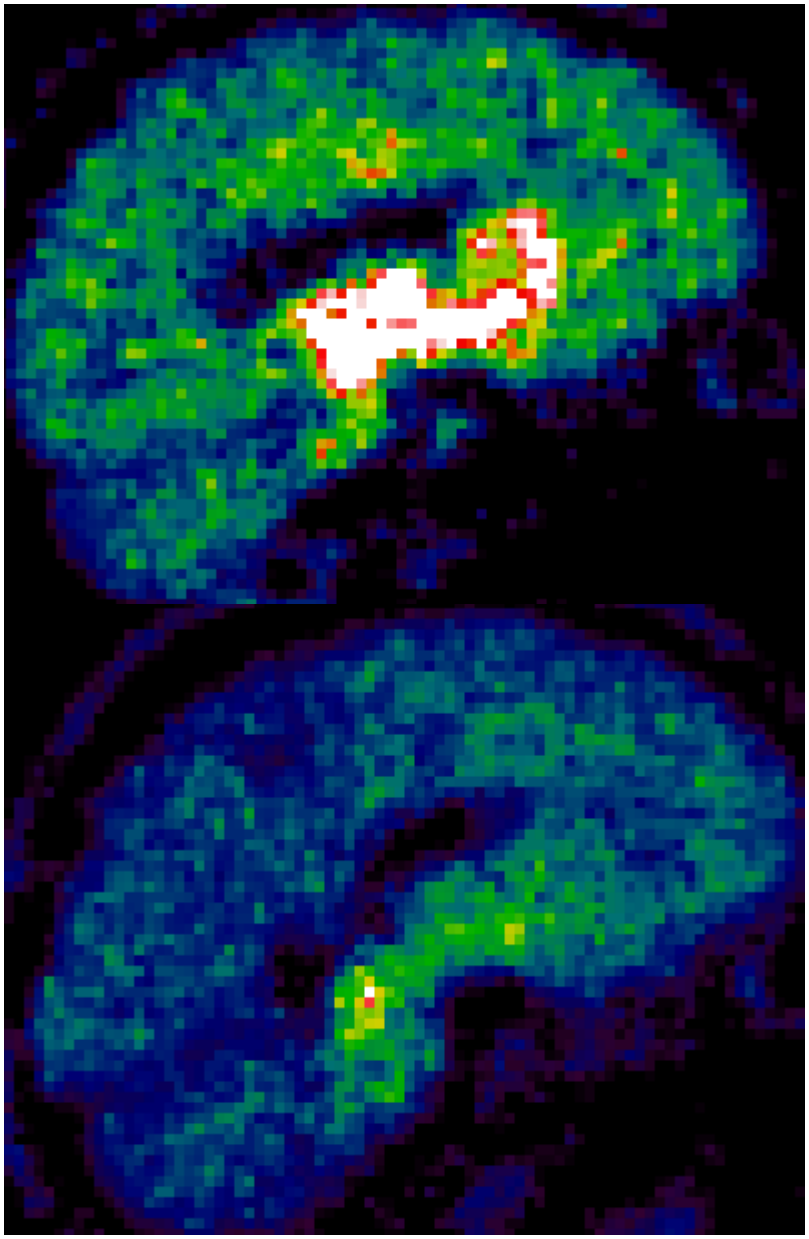
The total volumes of distribution V_T and the binding potentials relative to parent in plasma concentration BP_P are given in units of mL plasma per mL extravascular tissue, the binding potentials of the nondisplaceable uptake BP_{ND} are unitless, and the occupancies Occ_{ND} and Occ_P are expressed in %.

Table 3-3 Parameter estimated from sampling of parametric maps of V_T generated with spectral analysis

	Subject 1					Subject 2					Subject 3					Subject 4				
	Placebo		Citalopram			Placebo		Citalopram			Placebo		Citalopram			Placebo		Citalopram		
Volume of interest name	V_T	BP_{ND} / BP_P	V_T	BP_{ND} / BP_P	Occ_{ND} / Occ_P	V_T	BP_{ND} / BP_P	V_T	BP_{ND} / BP_P	Occ_{ND} / Occ_P	V_T	BP_{ND} / BP_P	V_T	BP_{ND} / BP_P	Occ_{ND} / Occ_P	V_T	BP_{ND} / BP_P	V_T	BP_{ND} / BP_P	Occ_{ND} / Occ_P
Cerebellum	11.8		10.8			13.5		10.3			17.1		11.5			11.7		8.4		
Amygdala	10.4	1.58	18.4	0.71	55	32.0	1.36	16.4	0.59	57	37.3	1.18	18.5	0.61	48	33.8	1.88	13.0	0.80	58
	18.6		7.6		59	16.5		6.1		67	20.2		7.0		65	22.0		6.7		70
Brainstem	10.3	1.57	18.1	0.68	57	31.6	1.33	16.0	0.54	59	35.0	1.04	17.3	0.51	51	29.5	1.51	13.8	0.66	57
	18.5		7.3		60	18.0		5.6		69	17.6		5.8		67	17.7		5.5		69
Caudate	10.4	1.58	15.1	0.40	73	30.1	1.22	14.7	0.43	65	39.5	1.30	17.3	0.51	61	27.6	1.35	11.7	0.40	70
	18.6		4.3		77	16.5		4.4		73	22.4		5.8		74	15.8		3.3		79
Hippocampus	21.9	0.86	14.1	0.30	65	23.6	0.74	13.6	0.33	55	31.1	0.62	16.8	0.46	43	21.3	0.81	11.9	0.43	48
	10.2		3.3		68	10.1		3.4		66	14.0		5.3		62	9.5		3.6		63
Putamen	16.1	2.06	18.2	0.69	67	37.1	1.74	10.1	0.75	57	43.1	1.51	19.0	0.65	57	34.5	1.94	13.5	0.85	56
	24.3		7.4		70	23.5		7.7		67	28.9		7.5		71	22.7		7.1		69
Thalamus	15.6	2.03	16.5	0.53	74	35.3	1.61	15.9	0.54	66	38.5	1.25	18.5	0.61	51	34.5	1.94	14.5	0.73	62
	24.0		5.7		76	21.8		5.6		74	21.4		7.0		67	22.8		6.1		73
Mean ± s.d.					65 ± 8					60 ± 5					52 ± 6					58±8
					68 ± 8					69 ± 4					68 ± 4					70±5

The total volumes of distribution V_T and the binding potentials relative to parent in plasma concentration BP_P are given in units of mL plasma per mL extravascular tissue, the binding potentials of the nondisplaceable uptake BP_{ND} are unitless, and the occupancies Occ_{ND} and Occ_P are expressed in %.

Figure 3-6 Oblique slice through parametric images of the total volume of distribution V_T from the same subject as in Figure 3-4 generated with spectral analysis after placebo infusion (A) and after citalopram infusion (B)



3.4 DISCUSSION

A single intravenous infusion of 10 mg citalopram 45 mins before administering an intravenous [^{11}C]DASB bolus led to a substantial increase of the concentration of [^{11}C]DASB in arterial plasma compared with a similar paradigm that employed a saline placebo infusion before the [^{11}C]DASB PET scan. This appears to be a consequence of the blockade of the peripheral 5-HTT binding sites by citalopram, for instance, in the lungs, the organ that was shown to have the highest uptake of [^{11}C]DASB in the early phase of the PET scan (Belanger et al., 2004; Lu et al., 2004; Tipre et al., 2004).

As a consequence of these quite dramatic changes to the time course of the [^{11}C]DASB concentration in the plasma, the kinetics of the [^{11}C]DASB binding in brain tissue was also affected in the sense that the peak activity of the regional TACs occurred earlier during the scanning period than in baseline condition. The total volumes of distribution V_T were lower in the blocked scans in all brain regions examined including the cerebellar grey matter, the region with the lowest 5-HTT concentration. The mean reduction of the cerebellar V_T was 19% (graphical analysis of reversible binding performed on the regional tissue TACs) and 24% (as obtained from the parametric images of V_T generated with spectral analysis) for the four subjects in our cohort. There was, however, one subject in whom the cerebellar V_T remained unchanged when the graphical analysis of reversible binding of the TAC was performed (Table 3-2, subject 1). The reductions of the cerebellar V_T of this investigation are in line with previous reports by Parsey et al (Parsey et al., 2006c) who found in a [^{11}C]DASB study a

33% occupancy in cerebellar grey matter of subjects 4-6 days after 25 mg to 100mg of daily sertraline treatment or by Kent et al (Kent et al., 2002) who reported from a [^{11}C]McN5652 study of five subjects with social phobia a reduction of the cerebellar V_T of 23%±12% after paroxetine treatment. However, these reductions appear to be higher than expected from a blockade of the specific binding of the radioligand in the cerebellum given that the specific binding of [3H]citalopram in auto-radiographic studies of porcine brain has been reported as only 2.3 pmol/g tissue in the cerebellum, in comparison with 26 pmol/g tissue in the amygdaloid area (Kretzschmar et al., 2003). From postmortem immunoreactivity studies of human brain and amygdala-to-cerebellar cortex 5-HTT ratio of 35 has been reported (Kish et al., 2005).

Several authors (Kent et al., 2002; Szabo et al., 2002) therefore suggested that the experimental paradigms employed in the 5-HTT imaging studies with PET such as MDMA lesioning or SSRI administration may have affected what is generally termed as 'nondisplaceable binding.' However, the underlying nature of these effects is unclear. Rochat et al (1999) reported that the citalopram transport across the BBB is mediated by a carrier mechanism (Rochat et al., 1999). If [^{11}C]DASB competed with citalopram for the same BBB transport mechanism, then the entry of [^{11}C]DASB into the brain might be reduced in the presence of citalopram.

Despite these changes of the V_T in the cerebellum, I obtained indirect estimates of the binding potentials BP_{ND} and BP_P from which regional occupancy

estimates Occ_{ND} and Occ_P were calculated (Tables 3-2 and 3-3). As previously demonstrated, the BP_{ND} derived occupancy estimates (Occ_{ND}) underestimate the true occupancy in a target region if the total volume of distribution V_T from a reference region with displaceable binding is used as a measure of the volume of distribution of the nondisplaceable binding V_{ND} in the target region (Asselin et al., 2007). In contrast, the BP_P derived occupancy estimates Occ_P are always equal to or greater than the BP_{ND}-derived occupancies (Occ_{ND}). Both methods of calculating occupancy gave the same result for subject 1 in Table 3-2, because there was no change in the cerebellar V_T, which indicates that in this case the assumption of no displaceable binding in the reference region was not violated. The observation that the mean BP_{ND} derived occupancy in our study is about 10% smaller than the mean BP_P derived occupancy corresponds with a mean BP_{ND} $^{\text{reference region (blocked)}}$ of 0.11. Nevertheless, the occupancy estimates obtained were fairly homogeneous across the 5-HTT rich regions considered with Occ_P showing much less between-subject variability than Occ_{ND}. Because it was not possible to obtain reliable measurements of the [^{11}C]DASB free fraction in plasma f_P in this study, the possibility of changes of f_P between the baseline and blocked condition could not be eliminated. Conversely, the comparability of BP_{ND} between the two conditions requires that the free fraction of the nondisplaceable compartment f_{ND} has not changed. Therefore, using BP_P as the outcome parameter has the advantage over the use of BP_{ND} in that BP_P can provide occupancy estimates, which are not biased in the presence of specific binding in the reference region provided that there are no differential occupancies across regions (Cunningham et al., 2010). The mathematical

expression for the BP_P-derived occupancy calculation that followed from equations (2) and (3)

$$Occ_P = (V_T^{baseline} - V_T^{blocked)} / (V_T^{baseline} - V_{ND}) \quad \times 100\%$$

is identical with the equation provided by Lassen et al (1995) (equation 11) for the calculation of occupancy in studies without a receptor free reference region (Lassen et al., 1995).

In agreement with previous reports (Frankle et al., 2004; Frankle et al., 2006), ROIs with low 5-HTT density (e.g., cortical areas) could not be reliably quantified with [^{11}C]DASB (data not shown). Furthermore, the same two reports described difficulties in obtaining 'good' fits of the regional tissue TACs with reversible compartmental models (with either one tissue compartment/two rate constants or two tissue compartments/four rate constants) as indicated by a nonrandom distribution of the residuals (Frankle et al., 2004). Similar problems were also encountered in this study.

As both [^{11}C]DASB and citalopram bind specifically to the SERT, the increased bioavailability of [^{11}C]DASB after citalopram infusion is a direct result of the blocking of the SERT binding sites in the periphery. However, [^{11}C]DASB and citalopram are different chemical entities following different metabolic pathways and as such the presence of the SSRI citalopram does not necessarily result into changes of the rates of the [^{11}C]DASB biotransformation. Thus, apart from the initial blockade of the first pass interaction of [^{11}C]DASB in the lungs, there

is currently no hypothesis about different rates of metabolism or different parent fractions of [^{11}C]DASB after citalopram administration.

A possible reason may be the violation of the assumption that the rate constants of the compartmental models are constant over time. The experimental paradigm of infusing citalopram 45 mins before commencing the PET scan probably results in kinetic parameters changing with time. This is consistent with the observation that the rate constants k3 and k4 of the two-tissue compartment, four rate constants model, appear most frequently to suffer from identifiability problems. These are the constants expected to be primarily affected by the action of the SSRI at the binding sites. In contrast, the graphical analysis of reversible binding and spectral analysis provided the macroparameter V_T as outcome measure and, therefore, appeared to be less sensitive to the violation of the requirement of time constancy of an underlying microparameter. A full discussion of the system identifiability properties after changes of the specific binding of the radioligand has been provided by Endres and Carson (1998) (Endres and Carson, 1998). However, the parametric images of V_T generated with spectral analysis may be positively biased in comparison with the results obtained from an analysis of regional tissue TACs.

The differences between the V_T obtained from regional analysis (Table 3-2) and the V_T obtained from sampling parametric maps (Table 3-3) are in line with those differences previously reported from an investigation into balancing bias, reliability, and noise properties of spectral analysis-generated parametric maps

from studies with [^{11}C]diprenorphine, which is a nonsubtype selective opiate receptor ligand with slow kinetics in tissue (Hammers et al., 2007). Owing to its relatively slow kinetics in tissue—for instance Frankle et al (2004)determined a minimal scanning time of 95 mins required to derive time-invariant distribution volumes in all regions - a parametric image of the value of the impulse response function (IRF) at a late time point may be a measure of [^{11}C]DASB binding more robust to noise-induced bias than the parametric image of V_T (Cunningham et al., 1998). Such a recommendation to use IRF images instead of V_T images to facilitate the comparison between studies or subjects in different physiological or pharmacological conditions has previously been made for the generation of parametric images of [^{11}C]diprenorphine binding with spectral analysis (Tadokoro et al., 1998). However, this option was not investigated here, because I was interested in quantifying the changes of regional [^{11}C]DASB binding with a parameter that is established across the discipline and can be obtained with many of the widely used analysis methods. Therefore, the distribution volume V_T and not the late scan time value of the IRF was used.

The past years have seen continued efforts to develop radioligands that would enable quantification of the binding to the 5-HTT in brain regions with low 5-HTT density, which cannot be reliably assessed with [^{11}C](+)McN5652 or [^{11}C]DASB. As for other neuroreceptor systems, for instance the dopaminergic system where the quantification of the binding to extrastriatal D_2/D_3 receptors was enabled by the introduction of high-affinity radioligands such as [^{11}C]FLB

457 (Asselin et al., 2007), current efforts appear to be directed towards an increase of the affinity of putative radioligands for the 5-HTT. However, the abundance of the 5-HTT in many parts of the body outside the brain may prevent the success of these efforts to achieve reliable quantification of 5-HTT binding in low 5-HTT brain areas with high-affinity radioligands if they are not combined with measures to reduce, at the same time, the binding of the radioligands to peripheral 5-HTT sites (Malizia et al., 1997).

In summary, the mean 5-HTT occupancy of acute intravenous citalopram (10mg) in the cohort of four subjects was estimated at about 60% when calculated from binding potential estimates of the nondisplaceable binding BP_{ND} and at 69% when calculated from binding potential estimates of the specifically bound radioligand relative to the parent radioligand in plasma BP_P. Lotrich et al (2005) reported a mean plasma citalopram concentration of circa 10 ng/mL between 45 and 150 mins after an infusion of 10 mg citalopram in healthy control subjects (Lotrich et al., 2005). Meyer et al (2004) (Figure 1) measured a striatal 5-HTT occupancy of about 50% for a plasma citalopram concentration of 10 ng/mL in subjects who had received daily oral doses of citalopram for 4 weeks (Meyer et al., 2004b). The same authors reported occupancy of 80% across five SSRIs (including citalopram) at minimum therapeutic doses. In conclusion, our data suggest that a 10-mg citalopram infusion in healthy control subjects results in an acute 5-HTT occupancy of 60% to 70%, which is below the 80% occupancy reported from minimum therapeutic doses of SSRIs, including oral citalopram during repeated treatment.

Furthermore, the citalopram induced cerebellar displacement suggests there is no ideal reference region for in vivo 5-HTT studies; cerebellar gray matter seems to be the best available choice (Kish et al., 2005; Parsey et al., 2006c). This is important, particularly if there are any changes in nonspecific binding in the disease process, because interpretation of the estimated change of 5-HTT may require continued measurement of arterial input functions (Ikoma et al., 2002; Parsey et al., 2006c).

4 5-HTT BINDING IN MAJOR DEPRESSION

4.1 INTRODUCTION

The serotonin transporter (5-HTT) plays a key role in regulating brain serotonin neurotransmission. As discussed in the Introduction, it is the primary site of action of commonly used antidepressants such a selective serotonin reuptake inhibitors (SSRIs). The 5-HTT has been a key target of interest in the studies of pathophysiology in depressive disorders and was often studied in peripheral models such as the blood platelet (Ellis and Salmond 1994). By using Positron and Single Photon Emission Tomography (PET and SPET) and selective 5-HTT radioligands it is now possible to image the 5-HTT directly in the living human brain.

The SPET radioligand most commonly used to study depressed patients has been [^{123}I]β-CIT, a cocaine derivative that binds with high affinity to both 5-HTT and dopamine transporters (Laruelle et al., 1993b). Apart from lack of selectivity, accurate quantification of [^{123}I]-βCIT SPET is made difficult by relatively low image resolution and the derivation of binding parameters from tissue ratios rather than kinetic analysis. On balance, in single photon emission computerized tomography (SPECT) using [^{123}I]-βCIT or the newer agent [^{123}I]-ADAM, depressed patients appear to have decreased binding potential (BP) of the 5-HTT in midbrain and brain stem (Joensuu et al., 2007; Lehto et al., 2006; Malison et al., 1998; Newberg et al., 2005; Staley et al., 2006; Willeit et al., 2000). However, some authors found increased 5-HTT BP in both regions in adolescents (Dahlstrom et al., 2000) or found no difference between adult

depressed participants and controls (Herold et al., 2006; Ruhe et al., 2009).

A number of PET ligands are also now available to image the 5-HTT, in particular [^{11}C](+)McN5652 and [^{11}C]DASB (Szabo et al., 1995; Wilson et al., 2002). Both these radiotracers are highly selective for the 5-HTT; however, [^{11}C]DASB has advantages in terms of a higher ratio of specific binding to nonspecific binding and a measurable free fraction in plasma (Frankle et al., 2004; Szabo et al., 2002). Once again the data in acute depressive states are somewhat contradictory. Parsey and colleagues (2006b), using [^{11}C] McN5652 with positron emission tomography (PET), found that unmedicated patients with major depression had lower 5-HTT BP in amygdala and mid-brain than healthy controls However, two smaller studies employing the same ligand found increased 5-HTT binding in thalamus and cingulate cortex and no change in mid-brain in depressed patients (Ichimiya et al., 2002; Reivich et al., 2004).

Using [^{11}C] DASB and PET to measure the 5-HTT, Meyer et al (2004a) found no differences in 5-HTT BP in unmedicated Major Depressive Disorder (MDD) patients relative to healthy controls. However, Cannon et al (2007) also using [^{11}C] DASB in MDD patients, found increased BP in thalamus, striatum and insula. Reimold et al (2008) found decreased binding in brainstem and thalamus in depressed patients which significantly correlated with anxiety symptoms.

The reasons for these inconsistent findings are unclear and may be due to a number of different factors, including patient characteristics and effects of

previous antidepressant drug treatment. Another potential confound relates to SPET and PET methodology, in particular the use of a reference region that itself contains displaceable 5-HTT binding and may therefore differ in 5-HTT binding between patient and control group. The latter problem can be resolved only by the use of a quantitative approach using arterial input modeling (Innis et al., 2007).

In this study, I used [^{11}C] DASB and fully quantitative arterial input model to assess 5-HTT binding in a group of unmedicated acutely depressed patients.

4.2 METHODS AND MATERIALS

4.2.1 Participants

The study was approved by the Research Ethics Committee at Hammersmith Hospital, London, and the Administration of Radioactive Substances Advisory Committee, UK. All participants gave written informed consent for the study. I recruited 12 men (mean ± SD age 42.1 ± 11.6 years) who were currently depressed based on clinical interview and Structured Clinical Interview for DSM-IV Disorders criteria for major depressive disorder (MDD). Except for one participant who used nitrazepam occasionally, the depressed patients were free of antidepressant and other psychotropic medication for a mean duration of 41 months (range 4-240 months); four patients had never received any antidepressant medication. Overall the mean duration of the current depressive episode was 12.4 months (range 4-20 months). Eight patients had a family

history of mood disorder. Six of the depressed patients had co-morbid illnesses; four had dysthymia, one had a past history of panic disorder, two had current generalized anxiety disorder symptoms, and one subject had a history of alcohol dependence (in remission for 18 years).

I recruited healthy controls with no current or past psychiatric history or history of substance misuse a) by randomly selecting 15 healthy men (mean age 42.4 ± 11.4 years) from our age-matched [^{11}C]DASB healthy volunteer database; and b) 9 healthy men from advertisement via public newspaper and posters. All the patients and controls were scanned during the same period. The details of participant characteristics are shown in Table 1. Patients and healthy subjects with any major medical or neurological (current or past) illness were excluded from the investigation. All subjects were administered the Hamilton Rating Scale for Depression (17 item; HAM-D), Beck Depression Inventory (BDI) and the Dysfunctional Attitude Scale (DAS). All participants completed a dysfunctional attitude scale (DAS) because a previous study showed that DAS scores correlated positively with regional 5-HTT BP in acutely depressed patients (Meyer et al., 2004a). We restricted our study to male subjects only because of a lack of toxicology data (effect of [^{11}C]DASB on pregnancy and on fetus) for [^{11}C]DASB in females at the time of ethics committee approval for the study.

4.2.2 PET scanning

PET scans were carried out as described in the Methods chapter. Briefly, all

participants underwent a 90 min dynamic 3D emission scan in list mode on the ECAT EXACT3D tomograph.

The metabolite-corrected arterial plasma input functions for each scan were derived from continuous on-line whole blood activity monitoring and 10 discrete blood samples, in eight of which the fraction of the unchanged parent compound in plasma was determined. The plasma free fraction (f_P) was determined by mixing 1ml cell free plasma (collected before DASB injection) with radiotracer. A known aliquot of 10-20 µl was then transferred into ultrafilteration unit (Microcon YM-30 (Millipore), centrifuged at room temperature for 15 mins at 14000 rpm, activities from the plasma and ultrafiltrate were then counted (corrected for non-specific binding). The f_P was estimated from the ratio of activity in the ultrafiltrate to total activity (Frankle et al., 2004). Note, however, that due to accidental loss of some of the blood samples the plasma free fraction was only determined in a subgroup of 7 controls and 6 patients, respectively.

The radiotracer [^{11}C]DASB was injected, into an antecubital vein, as a smooth bolus over 30 seconds. There was no significant difference between the participants groups in the amount of radioactivity, in the specific activity, the amount of cold ligand injected or the free fraction in plasma (Table 4-1).

4.2.3 MR scans and definition of volumes of interest

All volunteers had a structural T1 MRI scan performed on either 0.5T (0.5

Apollo system, Marconi Medical Systems, Cleveland, Ohio) or 1.5T (1.5 Eclipse system, Marconi Medical Systems, Cleveland, Ohio) MR scanners [TR=30s, TE=3s, flip angle=30, NSA=1, voxel dimensions 0.98 mm x1.6 mm x1.6 mm, acquisition time=13 mins] or 3T (3T Intera Philips Medical Systems) MR scanners [TR=9.6s, TE=4.6s, flip angle=8, NSA=1, voxel dimensions 0.94 mm x 0.94 mm x 1.2 mm]. The scans were inspected by an independent clinical radiologist and found to be normal.

The regions of Interest (ROI) analysis has been described in Methods chapter. I studied nine regions of interest, namely, amygdala, anterior cingulate cortex (ACC), brain stem, caudate, frontal cortex, hippocampus, insula, putamen and thalamus. The brain stem regional definition included midbrain, pons and medulla oblongata. Cerebellar gray matter was used as a reference region because of the reported negligible density of 5-HTT in the cerebellum (Kish et al., 2005). We obtained data from cerebellar gray matter up to 5 to 8 slices carefully avoiding spill over from occipital cortex by placing the volume of interest well within the cerebellar cortex area leaving a margin of several millimeters around to the outer borders of the cerebellum as defined in (Hammers et al., 2003).

4.2.4 Quantification of DASB binding

For the quantitation of the [^{11}C]DASB binding in brain tissue relative to the radioligand concentration in arterial plasma, we used graphical analysis together with the metabolite-corrected plasma input function (Logan et al.,

1990) to obtain regional estimates of the total volume of distribution V_T from the slope of the linear part of the plot. As described in Methods chapter, parameters such as the threshold for the graphical analysis t^*= 35 min were set as previously optimised for [^{11}C]DASB.

The main study outcome was the in vivo binding potential $BP = B_{MAX} / K_D$ as the ratio of the serotonin transporter density B_{MAX} and the radioligand equilibrium dissociation constant K_D (Innis et al., 2007). The binding potential of the specifically bound radioligand relative to the parent radioligand in plasma $BP_P = f_P \cdot BP = f_P \cdot B_{avail} / K_D$ with f_P being the fraction of free radioligand in plasma was calculated as follows;

$$BP_P = V_T - V_{ND}$$

Where V_T is the distribution volume of total ligand uptake in tissue relative to total concentration of ligand in plasma and V_{ND} is the distribution volume of nondisplaceable compartment relative to total concentration of ligand in plasma (Innis et al., 2007). V_{ND} is derived from the V_T of the cerebellar reference region. Therefore, the value of BP_P in a particular ROI is given by: V_T (ROI) – V_T (cerebellum).

Alternatively, the binding potential of the specifically bound radioligand relative to the nondisplaceable radioligand in tissue $BP_{ND} = f_{ND} \cdot BP = f_{ND} \cdot B_{avail} / K_D$ with f_{ND} being the fraction of free radioligand in the nondisplaceable tissue compartment was calculated as follows.

$$BP_{ND} = (V_T - V_{ND}) / V_{ND}$$

4.3 STATISTICAL ANALYSIS

Statistical analyses were performed using Statistical Package for Social Sciences (SPSS Inc., Chicago, Illinois, USA) version 12. Demographic data were analyzed using independent sample t tests. I tested the hypothesis that regional 5-HTT receptor binding potential would be reduced in acutely depressed patients compared with healthy control subjects using a repeated measures ANOVA with "group"" (acute depressed vs controls) as a between subjects factor, and "region" (nine ROIs as described above) as a within-subjects factor, with Huynh-Feldt correction. Significant effects on the repeated measures ANOVA were followed up with post-hoc independent t tests. Correlations (duration of symptoms, BDI and HAM-D vs ROI BP_P) were analysed using Pearson's correlation coefficient 'r' and non-parametric rank order data (age of onset and no of episodes vs ROI BP_P) using Spearman's correlation coefficient 'ρ' . The significance was set at $p<0.05$.

4.4 RESULTS

The clinical characteristics of the depressed patients are shown in Table 4-1. Age did not differ between the groups ($t= 0.43$; $df= 34$; $p= 0.7$) nor the free fraction in plasma (independent t test $p= 0.48$). There was significant positive correlation of age on BP_P values in healthy controls in five out of nine regions using Pearson's r (all $p < 0.05$; amygdala, caudate, frontal cortex, insula and putamen); in patients, age positively correlated only with amygdala BP_P. However, none of these correlations survived multiple comparison tests. There

were no significant age correlations with the ROIs in controls and patients. Age was used as a covariate in the further analysis.

Table 4-1: Clinical characteristics of the participants and Radiochemical parameters

CLINICAL CHARACTERISTICS	**Healthy Controls (n=24)**	**Acute depressed (n=12)**
Age (years; mean ± SD)	41.9 ± 11.4	43.8 ± 13.6
HDRS	0.4 ± 0.8	20.3 ± 5.3
BDI	2.3 ± 3	33.3 ± 10.3
DAS	105.4 (23.8)	170.3 (31)
Mean age at onset of depression (range)	-	33.6 (26-62)
Mean number of episodes (range)	-	2.2 (1-4)
Mean months duration of current episode (range)	-	12.4 (4-24)
Mean months medication free since last episode (range)	-	41 (4-240)
Medication naïve (n)	-	4
Melancholic depression (n)	-	2
Suicide attempts (n)	-	2
Family history of depression (n)	-	8
PET PARAMETERS		
Injected Radioactivity (MBq)	537.3 ± 20.2	529 ± 35.9
Specific activity (MBq/µmol)	57852 ± 39560	49129 ± 19681
Injected stable 'COLD' ligand (µg)	3.7 ± 2.2	3.8± 2
Plasma free fraction f_P (unitless)	0.043 ± 0.01 (n=7)	0.05 ± 0.02 (n=6)

The cerebellar total volume of distribution V_T (cerebellar V_T) was significantly less in acute depressed patients than controls (9.1 ± 1.9 ml.cm-3 vs 10.5 ± 1.6 ml.cm-3; t= 2.34; df= 34; p= 0.03). The repeated measures ANOVA of the BP_P data showed a significant effect of group (F=16.79; df = 1, 33; p < 0.001); there were also significant main effects of region (F=5.27; *df* = 8, 264; *p* < 0.001) and a significant region by group interaction (F = 8.04; df = 8, 264; p < 0.001). There was a significant effect of age (F = 6.74; df = 1, 33; p = 0.01) and a significant region by age interaction (F = 3.55; df = 8, 264; p < 0.01). Post-hoc independent t-tests (uncorrected) showed that BP_P of the 5-HTT in acute depressed patients were significantly less than the controls in six of the nine ROIs (brainstem, thalamus, caudate, putamen, ACC and frontal cortex, (Figure 4-1 and Table 4-2). The analysis of the BP_{ND} data in acute depressed showed more restricted changes with significantly reduced 5-HTT BP_{ND} in brain stem and thalamus and there was also a trend level decrease in caudate (Table 4-2).

In the acutely depressed patients there was a significant negative correlation between BDI score and BP_P in frontal cortex (pearson $r_{uncorrected}$=-0.65; p=0.02) and trend level significance in caudate (r=-0.55; p=0.06); ACC (r=-0.55; p=0.07) and insula (r=-0.51; p=0.09). There was also a significant negative correlation between DAS score and BP_P in frontal cortex (pearson $r_{uncorrected}$=-0.59; p=0.04), ACC (pearson $r_{uncorrected}$=-0.60; p=0.04) and trend level significance in hippocampus (r=-0.55; p=0.06) and insula (r=-0.55; p=0.06). However there was no significant correlation between HAM-D score and BP_P in any of the

ROIs.

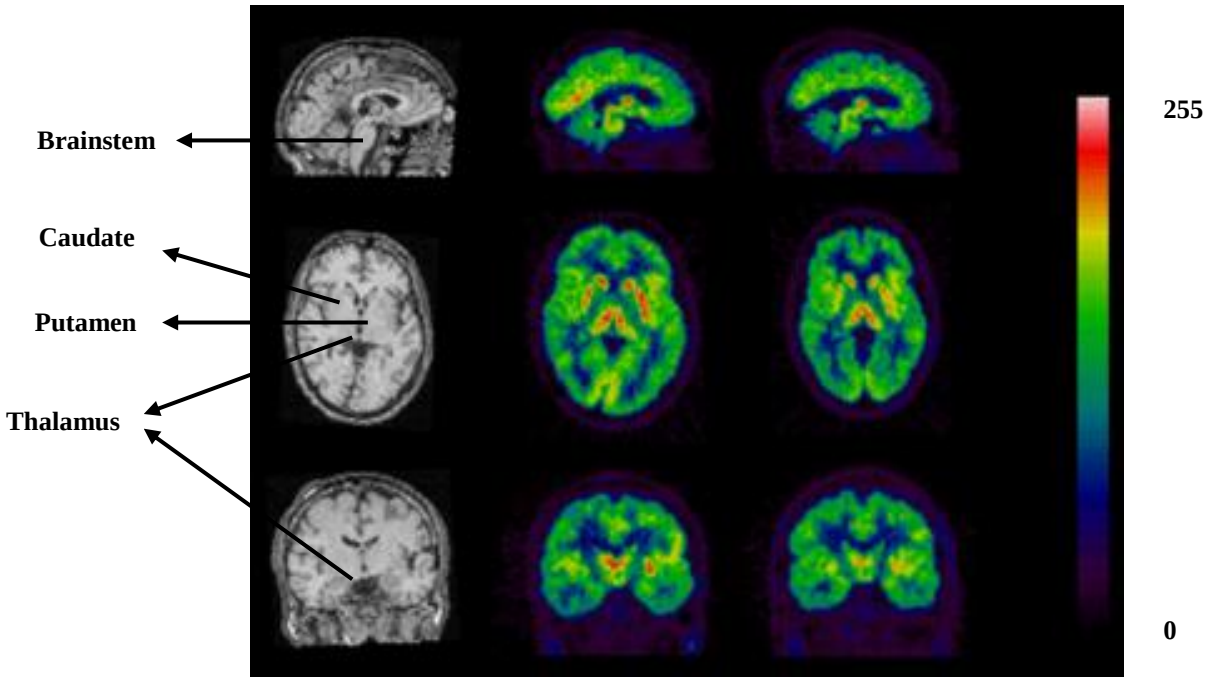
There was a positive correlation between age of onset of illness and BP_P in caudate (Spearman $\rho_{uncorrected}$ =0.57; p=0.05) and frontal cortex ($\rho_{uncorrected}$ =0.57; p=0.05) and trend in putamen (ρ=0.54; p=0.07) (the earlier the age of onset of illness the lower BP_P). There was also a significant negative correlation in the acutely depressed patients between the number of episodes of depression and BP_P in the thalamus ($\rho_{uncorrected}$ = -0.68; p=0.02), and putamen ($\rho_{uncorrected}$ =-0.62; p=0.03). However, none of the reported correlations survived multiple comparison correction. There was no correlation between duration of current episode and BP_P in any of the ROIs (all p>0.1).

Table 4-2: Binding potential (BP_P) (ml.cm-3) and BP_{ND} of [^{11}C]DASB in control subjects and medication-free acute depressed patients.
*p<0.05, ** p<0.01, *** p<0.001, uncorrected for multiple comparison

Regions of Interest (ROI)	**Controls (n=24) BP_P Mean (SD)**	**Patients (n=12) BP_P Mean (SD)**	**P value (independent t-test)**	**Controls (n=24) BP_{ND} Mean (SD)**	**Patients (n=12) BP_{ND} Mean (SD)**	**P value (independent t-test)**
Amygdala	19.3 (4.3)	16.8 (4.9)	0.12	1.84 (0.3)	1.84 (0.3)	0.99
Anterior cingulate cortex	8.0 (1.8)	6.2 (2.5)	0.02*	0.77 (0.2)	0.69 (0.3)	0.31
Brain stem	19.4 (3.1)	13.1 (4.6)	<0.001***	1.87 (0.3)	1.44 (0.4)	<0.0001 ***
Caudate	15.2 (4.2)	9.7 (5.4)	0.002**	1.46 (0.4)	1.12 (0.7)	0.06
Frontal cortex	4.8 (1.0)	3.6 (1.9)	0.02*	0.46 (0.1)	0.40 (0.2)	0.3
Hippocampus	9.6 (2.5)	8.7 (3.3)	0.33	0.92 (0.2)	0.98 (0.4)	0.58
Insula	11.5 (2.9)	9.5 (3.5)	0.08	1.10 (0.3)	1.06 (0.3)	0.67
Putamen	20.6 (4.8)	15.2 (4.3)	0.002**	1.99 (0.5)	1.72 (0.5)	0.11
Thalamus	18.4 (4.2)	11.9 (4.7)	<0.001***	1.77 (0.4)	1.35 (0.6)	0.01*

Figure 4-1: MRI and [^{11}C]DASB summated image from a representative control subject in the left and middle column, respectively and [^{11}C]DASB summated image from an acute depressed (right most column)

Subjects were chosen such that their brain stem and thalamus BPP was closest to the respective group mean. From top row to bottom: sagittal, axial and coronal view, respectively.



4.5 DISCUSSION

My data suggest that unmedicated, acutely depressed patients have statistically significant decreases in binding potential (BP_P) of the 5-HTT in multiple brain regions including brain stem, thalamus, striatum, ACC and frontal cortex. The significant decreases in brain stem and thalamus was also seen if BP_{ND} used as a quantitative measure. While these findings appear relatively clear-cut, it must be acknowledged that imaging studies of the 5-HTT in acute depression

have yielded conflicting results (Cannon et al., 2006; Cannon et al., 2007; Dahlstrom et al., 2000; Herold et al., 2006; Ichimiya et al., 2002; Joensuu et al., 2007; Lehto et al., 2006; Malison et al., 1998; Meyer et al., 2004a; Newberg et al., 2005; Oquendo et al., 2007; Parsey et al., 2006b; Reimold et al., 2008; Reivich et al., 2004; Staley et al., 2006; Willeit et al., 2000). Why this should be the case is not easy to explain. Technical factors may well be involved, particularly the use of different ligands to label the 5-HTT binding site. However, even studies using [^{11}C]DASB, often regarded as the best currently available radiotracer, are quite inconsistent (Cannon et al., 2007; Meyer, 2007; Meyer et al., 2004a; Reimold et al., 2008).

4.5.1 MODELLING METHODS IN LIGAND IMAGING

As noted in the Introduction and Methods chapter, reference tissue modelling methods can be confounded if the reference region itself possesses specific displaceable binding of the radioligand under investigation. The cerebellum is often used as a reference region in studies of the 5-HTT; however, it is now well-established that treatment of subjects with selective serotonin re-uptake inhibitors displaces 5-HTT binding in the cerebellum, suggesting that this brain region does possess displaceable 5-HTT binding (Kent et al., 2002; Parsey et al., 2006c). Indeed my study, like that of Oquendo et al (2007) revealed low 5-HTT binding in cerebellum in depressed participants relative to controls though the patients in the latter study suffered from bipolar illness. In these circumstances it is unlikely that total volume of distribution V_T of [^{11}C]DASB in the cerebellum is an accurate reflection of the volume of distribution of the

nondisplaceable tissue uptake (VD_{ND}) required to obtain valid estimates of in vivo binding potential using a reference tissue model as discussed in chapter 3 and (Innis et al., 2007).

Where there is evidence of displaceable 5-HTT binding in the reference region, the outcome measure BP_P should be more sensitive than the more usually employed BP_{ND} to detect changes in specific binding of the 5-HTT in patient groups (Innis et al., 2007; Oquendo et al., 2007). However, to assess whether the cerebellar V_T in an investigational group is different from controls, and to calculate BP_P, it is necessary to quantify radioligand binding in tissue relative to the concentration of parent radiolabelled compound in the plasma input function. Therefore, investigations using simplified scanning protocols without measurement of the plasma input function cannot assess changes in the cerebellar V_T or obtain BP_P (see Chapter 3; (Innis et al., 2007).

In my study, the decrease in cerebellar V_T in the depressed patients was small relative to the decrease of V_T in most of the ROIs and therefore significant decreases in BP_P in several ROIs were still apparent (though may be underestimated because of the reduction in cerebellar V_T). However, had the decrease of V_T in cerebellum been greater, then reductions in 5-HTT in other brain regions could have been missed. It is possible therefore that the presence of displaceable binding of 5-HTT in the cerebellum, with undetected differences in V_T between patients and controls, may have contributed to the inconsistent findings of imaging studies of the 5-HTT in depression (Oquendo et al., 2007).

In addition, the BP_{ND} analysis revealed significant differences in brain stem and thalamus regions only and in not in other regions. It may be possible that these brain areas are the ones most likely to reveal changes in acute depression, perhaps because the high density of 5-HTT binding sites in this brain area provides a strong imaging signal.

Recently, using [^{11}C]DASB, Praschak-Rieder et al (2008) reported that serotonin transporter binding potential values were significantly higher in healthy subjects when scanned in the fall and winter compared with those in the spring and summer. In my sample, I did the analysis using the same seasonal cut-off period as reported in the Praschak-Rieder et al (2008). I found the BP_P results were still significantly different if a subgroup of patients vs controls scanned in winter and fall were analysed (8 out 9 regions $p<0.05$). Similarly thalamus and brain stem BP_P ($p<0.05$) remained significantly different if the subgroup of patients vs controls scanned in spring and summer were analysed. I also did not find significant effect of seasonality on ROI BP_P in healthy controls. In my data therefore I could not find any effect of seasonal variation on serotonin transporter differences between the two groups.

The current study was restricted to male participants and further work is needed to delineate brain 5-HTT binding with [^{11}C]DASB in acutely depressed and recovered depressed women. Recently, Ruhe et al (2009) reported low BP in midbrain and diencephalon in a subgroup of male depressed subjects using SPET ligand [^{123}I]- βCIT although there was no overall difference between the

patients and controls (Ruhe et al., 2009). However, Staley et al (2006) found lowered diencephalic 5-HTT binding specifically in acutely depressed women making it unlikely that abnormal 5-HTT binding in acute depression is restricted to men.

The number of depressed patients in my study was relatively small, mainly because of my intention to recruit participants who had been medication free for significant periods of time. In addition my patients had been depressed for relatively long periods of time and may therefore have a poor prognosis. While, to some extent, this avoids problems in interpretation of binding data posed by recent antidepressant use, it may mean that my findings are not generalisable to the broad range of depressed patients.

In summary, this study suggests that the use of [^{11}C]DASB in conjunction with arterial input modeling reveals widespread decreases in 5-HTT availability in acutely depressed patients. This indicates decreased 5-HTT binding may be a marker of depression in some patients. Whether this is a state or trait marker will be resolved by follow up imaging studies in the same group of patients or a separate group of patients who have recovered from depression

5 5-HTT BINDING IN RECOVERED DEPRESSED PATIENTS

5.1 INTRODUCTION

As illustrated in Introduction chapter and chapter 4, in vivo imaging studies of the 5-HTT has generally been conducted in patients suffering from acute depression and the results have been somewhat inconsistent perhaps, in part, because of the differing methodologies used.

The results of 5-HTT imaging studies in depression have been summarised in Introduction chapter (Table 1.). The majority of 5-HTT imaging studies have found decreased 5-HTT binding, particularly in thalamus and brain stem, in acutely depressed patients (Joensuu et al., 2007; Lehto et al., 2006; Malison et al., 1998; Newberg et al., 2005; Oquendo et al., 2007; Parsey et al., 2006b; Reimold et al., 2008; Staley et al., 2006; Willeit et al., 2000); however, there are some notable inconsistencies with some groups reporting either increased (Cannon et al., 2006; Cannon et al., 2007; Dahlstrom et al., 2000; Ichimiya et al., 2002) or no change in 5-HTT binding in the same areas (Herold et al., 2006; Meyer et al., 2004a; Reivich et al., 2004).

In a previous PET investigation, I found significant decreases in binding potential (BP) of the 5-HTT in multiple brain regions including brain stem, thalamus, striatum, ACC and frontal cortex in a group of unmedicated acutely depressed patients when compared to healthy controls (chapter 4). In this study I planned to use PET in conjunction with [^{11}C] DASB to study the 5-HTT in recovered depressed patients withdrawn from medication. An advantage of this approach is that any changes seen in the 5HTT are unlikely to be

attributable to epiphenomena of acute depressive illness or its treatment. Low levels of 5-HTT binding in recovered subjects would suggest a persistent deficit in the 5-HTT and perhaps in pre-synaptic 5-HT innervation.

5.2 METHODS

5.2.1 Participants

The study was approved by the Research Ethics Committee at Hammersmith Hospital, London, and the Administration of Radioactive Substances Advisory Committee, UK. All participants gave written informed consent for the study. We recruited 20 healthy men (mean ± SD age 38.9 ± 11.9 years) with no current or past psychiatric history and 24 recovered depressed men (mean age 35.7 ± 9.8 years) who had experienced at least one episode of unipolar major depression in the past (mean number of episodes, 2.4, range 1-5 [87.5% had >2 episodes]). All patients had been euthymic for a mean duration of 31 ± 31 months, (range 3 – 108 months), nine patients had never received any antidepressant medication and the rest were medication free for 23 ± 30 months (range 3 – 120 months). The mean age of onset of first episode of depression in the patient was 24.6 ± 9.3 years (range 16-52 years) and the overall duration of illness was 11.5 ± 7.6 years (range 1-30 years). Four patients had attempted suicide in the past during their depressive episodes, nine patients had had melancholic symptoms during at least one of their episodes and eight patients had a family history of major depressive disorder.

All patients met Structured Clinical Interview for DSM-IV Disorders criteria for major depressive disorder in the past and were fully recovered by the criteria described in the Methods chapter and were medication free for at least three months. Subjects with any serious medical or neurological (current or past) illness, alcohol or illicit substance dependence and other axis I or II disorders were excluded. All subjects were administered the Hamilton Rating Scale for Depression (17 item; HAM-D), Beck Depression Inventory (BDI) and the Dysfunctional Attitude Scale (DAS). We included only male subjects in this study because of a lack of toxicology data for [^{11}C] DASB in females.

5.2.2 PET scanning

PET scans were carried out as described in the Methods chapter on an ECAT EXACT 3D scanner (CTI, Knoxville, TN) with an axial field of view of 23.4 cm and 95 reconstructed transaxial image planes (Spinks et al., 2000).

5.2.3 Radiotracer

The radiotracer [^{11}C]DASB was injected, into an antecubital vein, as a smooth bolus over 30 seconds. The injected radioactivity dose was between 366 MBq and 566.54 MBq (mean: 540.11 MBq, SD: 31 MBq). The radiochemical purity of the injected [^{11}C]DASB was high and ranged from 95 % to 99 % with a mean of 97 % and a SD of 1 %. The injected mass of cold DASB varied between 0.69 µg and 10.5 µg with a mean value of 3.3 µg and a SD of 1.9 µg. The specific activity was on average 61021 MBq·µmol^{-1} with a SD of 34608 MBq·µmol^{-1}.

5.2.4 MR scans and definition of Regions of interest

All volunteers had a structural T1 MRI scan performed on either 0.5T (0.5 Apollo system, Marconi Medical Systems, Cleveland, Ohio) or 1.5T (1.5 Eclipse system, Marconi Medical Systems, Cleveland, Ohio) MR scanners [TR=30s, TE=3s, flip angle=30, NSA=1, voxel dimensions 0.98 mm x1.6 mm x1.6 mm, acquisition time=13 mins] or 3T (3T Intera Philips Medical Systems) MR scanners [TR=9.6s, TE=4.6s, flip angle=8, NSA=1, voxel dimensions 0 94 mm x 0.94 mm x 1.2 mm]. The scans were inspected by an independent clinical radiologist and found to be normal. Eight regions of interest (ROI) (amygdala, anterior cingulate cortex, caudate, frontal cortex, hippocampus, insula, dorsal raphe, and thalamus) were identified as described in the Methods Chapter

MRIs were resliced to a voxel size of 1 mm x 1 mm x 1 mm; centered on Anterior Commissure (AC) and aligned to the AC-PC line. MRIs were co-registered to the individual summated PET images using SPM2, which adopts a rigid body transformation using a normalised mutual information method. Eight regions of interest (ROI) -amygdala, anterior cingulate cortex, caudate, frontal cortex, hippocampus, insula, dorsal raphe, thalamus, and the cerebellum were defined on the co-registered MRI with the help of a probabilistic brain atlas template (Hammers et al., 2002). Cerebellar grey matter was used as a reference region because of the negligible density of 5-HTT in the cerebellum (Kish et al., 2005). The dorsal raphe region was manually defined as a fixed size region (900 mm^3) on the summed PET images of each individual. Dynamic PET scans were sampled by applying the individual ROI object maps.

5.2.5 Input function

The arterial plasma input function was derived from continuous on-line whole blood monitoring (initial 28 minutes) and 10 discrete blood samples, in 8 of which the fraction of unmetabolised parent compound was determined. The full methodology is given in the Methods Chapter

5.2.6 Quantification of DASB binding

To quantify the binding of [^{11}C]DASB in brain tissue, the graphical analysis of reversible radioligand binding using the plasma input function (Logan et al., 1990) was applied to obtain regional estimates of the total volume of distribution V_T from the slope of the linear part of the plot. The threshold was set at 35 min, i.e., the transformed data from frames 20 to 28 were fitted with a straight line.

Using the definition of binding potential *BP* introduced by Mintun et al (Mintun et al., 1984), estimates of binding potential in target regions of interest (with specific binding) was obtained from the estimated V_T in those region and in cerebellum (reference region without specific binding) (Gunn et al., 2001) (see equation below).

$$BP_{ND} = (V_T^{\text{target region}} / V_T^{\text{reference region}}) - 1$$

To also assess [^{11}C]DASB binding on a pixel level, spectral analysis was used to generate parametric maps of V_T (Cunningham et al., 1993; Cunningham and Jones, 1993). A set of 100 basis function logarithmically spaced between β_{min}=

0.0007 s^{-1} and β_{max}= 0.1 s^{-1} was chosen to obtain unbiased estimates of V_T for the specific kinetics of [^{11}C]DASB (chapter 3) (Hinz et al., 2006). Individual V_T images were then normalised to the standard MNI T1 template and average V_T images for the two cohorts were calculated.

5.3 STATISTICAL ANALYSIS

Statistical analyses were performed using Statistical Package for Social Sciences (SPSS Inc., Chicago, Illinois, USA) version 12. Demographic data were analyzed using an independent samples t test. We tested our hypothesis that regional 5-HTT receptor binding potential would be reduced in patients recovered from depression using a repeated measure analysis of variance (ANOVA) with “diagnosis” (patients vs. controls) as a between subjects factor, and “region” (brain region of interest) as a within-subjects factor; a Huynh-Feldt correction was applied as appropriate where the assumption of sphericity was violated. Significant interactions or main effects were explored using post hoc independent two-tailed t tests. Correlations were analysed using Pearson's correlation coefficient and significance was set at $p<0.05$.

5.4 RESULTS

There was no significant difference between recovered depressed patients and controls in either BDI (healthy volunteers, 4.0 ± 7.8 vs. patients, 5.8 ± 5.0; t= 0.88, df=42, p=0.39) or HAM-D ratings (healthy volunteers, 0.4 ± 0.7 vs

patients, 1 ± 1.5; t=1.8, df=42, p=0.075). However, patients scored significantly higher on the DAS (healthy volunteers, 104 ± 27 vs. patients, 128 ± 30; t=2.8, df=42, p=0.008).

There was no significant difference in the specific activity (healthy volunteers, 55788 ± 42361 MBq/µmol vs patients, 65383 ± 26705 MBq/µmol; t=0.9, df=42, p=0.4) or amount of cold ligand injected (healthy volunteers, 3.7 ± 1.8 µg vs patients, 3.1± 2.1 µg; t=1.1, df=42, p=0.3).

The cerebellar total volume of distribution V_T (cerebellar V_T) was not significantly different between patients and controls (10.5 ± 1.6 ml.cm-3 vs 10.5 ± 1.6 ml.cm-3; t= 0.012; df= 46; p= 0.99).

The repeated measures ANOVA of the BP data showed a main effect of region (F=178.9; df=1.3, 53.1; p <0.001) with the highest binding density apparent in dorsal raphe, intermediate levels in thalamus, anterior cingulate and hippocampus and lowest density in the frontal cortex. However, there was no significant main effect of group (F=1.68; df=1, 42; p=0.2) or group by region interaction (F=1.23; df=1.3, 53; p=0.28) (Table 5-1, Figures 5-1 and 5-2). There were also no group differences between healthy controls and patients with previous episodes of melancholia (F=2.1; df=1, 27; p=0.15) or medication naïve patients (F=1.97; df=1, 27; p=0.17) or patients with a positive family history (F=1.2; df=1, 26; p=0.29). Scores on the DAS in the patients did not correlate with BP values in any of the eight ROIs studied (all p values > 0.1). There was

also no significant correlation between BP in any region and the number of episodes of depression or duration of illness or age of onset of depressive episode or duration of euthymia in the patient group (all p values > 0.1)

Table 5-1: Binding potential (BP_{ND}) of [^{11}C] DASB in control subjects and medication-free, euthymic subjects recovered from depression.

Regions of Interest (ROI)	Controls (n=20) Mean (SD)	Patients (n=24) Mean (SD)	P value (unpaired t-test)
Amygdala	1.79 (0.33)	1.79(0.52)	0.97
Anterior Cingulate	0.73 (0.17)	0.73 (0.15)	0.98
Caudate	1.39 (0.43)	1.27 (0.39)	0.325
Frontal cortex	0.44 (0.09)	0.42(0.09)	0.62
Hippocampus	0.9 (0.20)	0.84 (0.26)	0.36
Insula	1.1 (0.25)	1.1(0.21)	0.85
Thalamus	1.75 (0.44)	1.69 (0.46)	0.64
Dorsal raphe	5.1 (1.79)	4.45 (1.79)	0.23

Figure 5-1: Mean [^{11}C] DASB V_T (volume of distribution) images obtained from parametric maps generated with spectral analysis of healthy volunteers (N=20, left) and recovered depressed patients (N=24, right) in the coronal, sagittal and transverse views respectively.

Healthy volunteers **Recovered depressed patients**

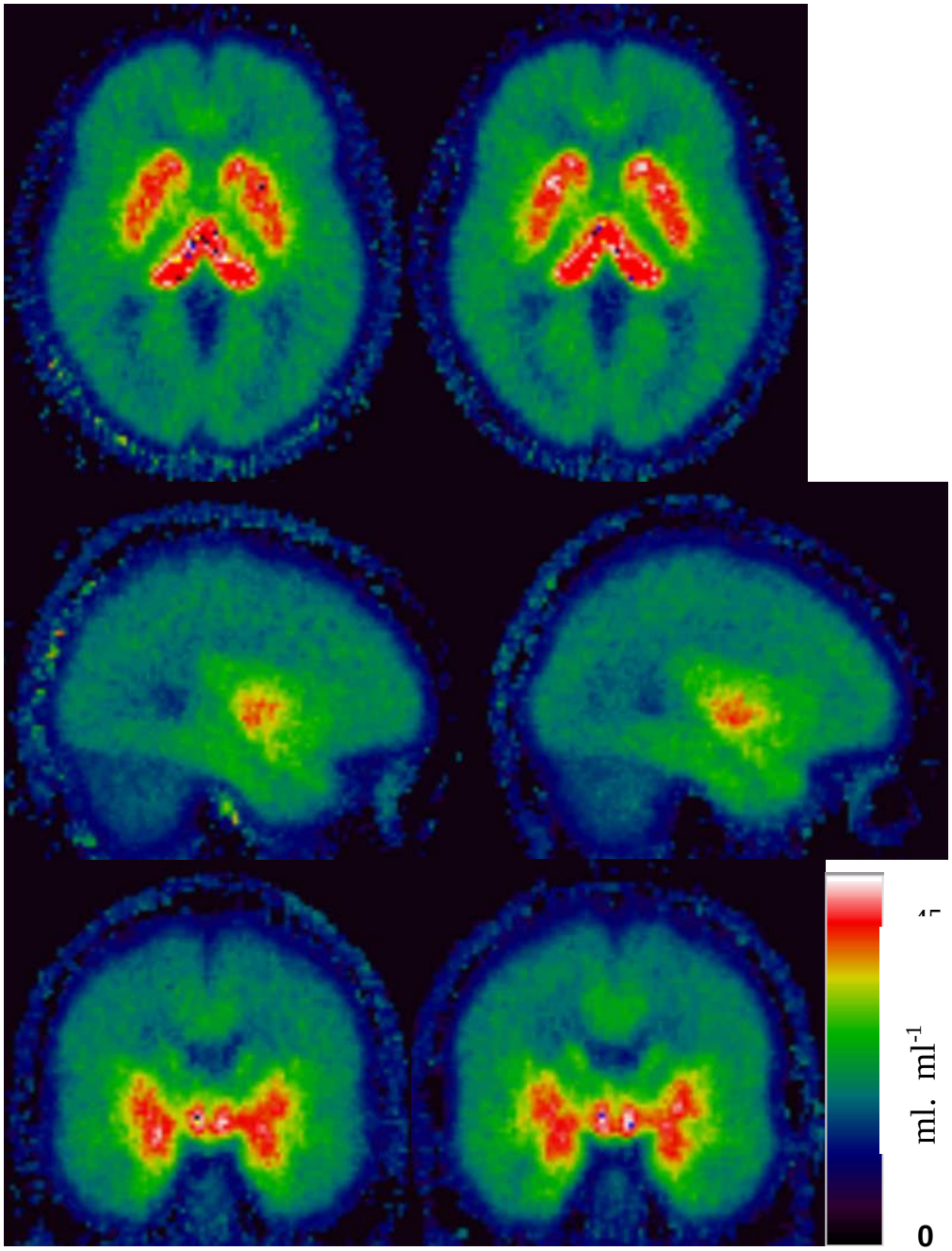
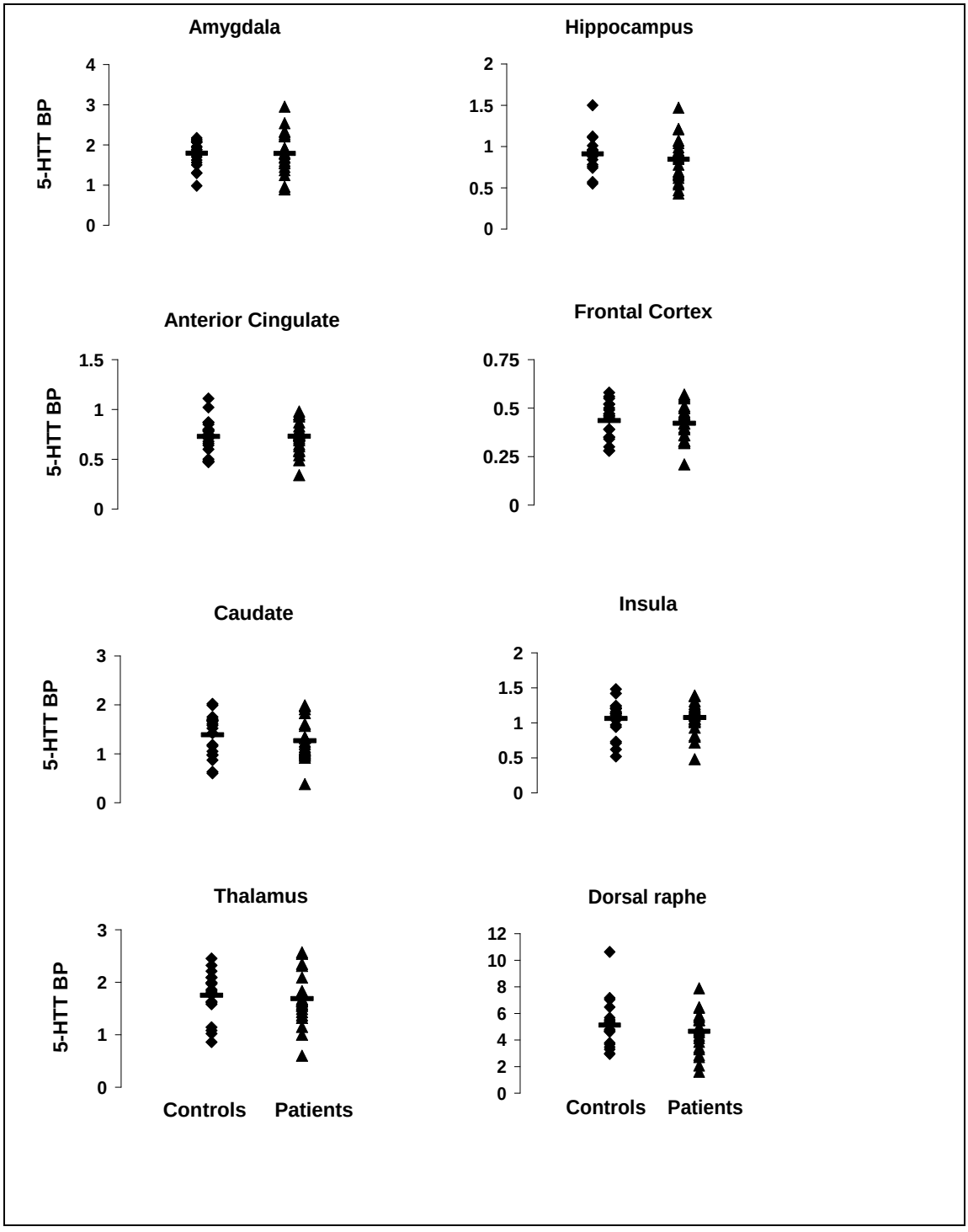


Figure 5-2: Scatter plots of individual BP_{ND} estimates of [^{11}C] DASB in the regions of interest (ROIs).

There are no significant differences between recovered depressed patients and healthy controls (see Table 5-1).



5.5 DISCUSSION

The results of this study indicate that the 5-HTT BP is not altered in a number of pathophysiologically relevant brain regions in male recovered depressed patients. This finding argues against the idea that depressed patients have persistent deficits in the availability of the 5-HTT. In addition, insofar as the 5-HTT provides an index of 5-HT neuronal density (Soucy et al., 1994), the results suggest that the pre-synaptic 5-HT innervation of limbic and cortical areas is unchanged in recovered depressed patients.

As noted in the Introduction chapter the results of ligand imaging studies of the 5-HTT in patients with acute depression have yielded contradictory findings. There are a number of factors that could explain these discrepancies including psychiatric co-morbidity, differences in ligand specificity, previous drug treatment and effects of acute illness (for example weight loss and insomnia). Studying recovered depressed patients avoids some of these potential confounds. In addition, the ligand I used for this study, [^{11}C] DASB, binds with high affinity and selectivity to the 5-HTT and has a number of advantages over other 5-HTT tracers including better specific-to-nonspecific binding (Frankle et al., 2004; Szabo et al., 2002).

A previous study by Meyer et al (2004a) in patients with acute unipolar depression found no difference in [^{11}C] DASB BP between depressed patients and controls. However, in the latter investigation there was a positive

correlation between self-ratings on a scale of dysfunctional attitudes (the DAS) and 5-HTT BP in the depressed patients. This relationship was not seen in the present study despite patients showing significantly higher DAS scores than healthy volunteers. However, because the patients were clinically recovered, their mean DAS scores were lower than those found in the acutely depressed patients in the study of Meyer et al (2004a) where patients with DAS scores of greater than 190 had significantly greater DASB binding than controls. Therefore it is possible that only patients with particularly high levels of dysfunctional attitudes might demonstrate increased 5-HTT binding. However, in my study of acutely depressed patients, there were hints that, if anything, DAS scores correlated negatively with 5-HTT binding potential (chapter 4). A recent study by Cannon et al, also using [^{11}C] DASB, found several interesting changes in 5-HTT in acutely depressed bipolar patients. While increased 5-HTT BP was seen in cingulate cortex and thalamus, 5-HTT binding was lowered in the brainstem at the level of the pontine raphe. No change was seen in the midbrain.

In general, studies with [^{123}I]-βCIT have indicated a lowering of 5-HTT in midbrain and hypothalamus of acutely depressed patients, though here too there are inconsistencies. The most recent study with [^{123}I]-βCIT by Staley and colleagues (2006) again found a decrease in 5-HTT availability in diencephalon in unmedicated depressed patients. However, this reduction was limited to female subjects. Because of lack of availability of suitable toxicity data with [^{11}C] DASB I was not able to include female participants in the present study.

Therefore these negative findings are applicable only to male participants and it is possible that 5-HTT availability might be persistently decreased in recovered female depressed patients. However, Cannon et al (2006) found no clear effect of gender in their study of [^{11}C] DASB in bipolar depressed patients.

Previous studies in acutely depressed patients have used graphical methods of analysis with a reference region approach and simplified reference tissue models. I also found no detectable differences in [^{11}C] DASB BP between recovered depressed patients and healthy volunteers using three further methods of analysis i) graphical analysis of reversible binding using a reference region (cerebellum) input function (Logan et al., 1996); ii) a reversible two tissue compartments, four rate constant compartmental model with free blood volume term; and iii) spectral analysis (data not shown). Mean parametric maps of V_T obtained with spectral analysis shown in Figure 5-1 also illustrate the similarity in BP between recovered depressed patients and controls. In these circumstances the sensitivity of my analysis to detect changes in BP between the two participant groups becomes a critical issue. Power analysis suggests that with this study population I would have been able to detect a change of 15-20 % in the BP estimates in most of the brain regions studied at 80% power and $P < .05$. This suggests that my study was sufficiently powered to detect differences of the order usually reported between acutely depressed patients and controls in ligand imaging studies of the 5-HTT.

5.5.1 Relationship of low 5-HTT binding and clinical symptomatology

Using an identical methodology, I found significant decreases in binding potential (BP) of the 5-HTT in multiple brain regions including brain stem, thalamus, striatum, ACC and frontal cortex in unmedicated *acutely* depressed patients vs healthy controls (chapter 4). However, I found no differences in 5-HTT binding in unmedicated *recovered* depressed participants compared to controls. This suggests that lowered 5-HTT binding might be a state marker of acute depression which remits with clinical recovery. However, this conclusion must remain tentative at present because there were some potentially important clinical differences between the acutely depressed patients in the previous study and the recovered depressed subjects who participated in this investigation.

For example, in comparison to the recovered subjects, the acutely depressed patients had greater levels of psychiatric co-morbidity and higher rates of affected first-degree relatives. It is therefore possible that this particular group of acutely depressed patients might have lowered 5-HTT binding even after recovery. It is also possible that low 5-HTT binding might delineate a group of acutely depressed patients less likely to recover. Indeed, I found in several brain regions that low 5-HTT binding was correlated with greater number of depressive episodes and early age of onset, both factors associated with a poorer long-term prognosis (Gelder et al., 2006). However, caution must be applied to interpretation of the correlational findings because they did not

survive correction for multiple comparisons. Interestingly, a recent prospective study by Miller et al (2008) reported that lower pre-treatment 5-HTT binding was associated with a decreased likelihood of remission during the following year. Meyer (2007) has suggested that low 5-HTT binding in depressed patients may be associated particularly with psychiatric co-morbidity which is also regarded as negative prognostic factor (Gelder et al., 2006).

A number of other possible explanations need to be considered for the observed lack of difference between 5-HTT BP in recovered depressed patients and controls. For example, while the patients had been unmedicated for long periods of time, the long-term effects of previous antidepressant treatment in the human brain are not known. Studies in animals have shown that treatment with different classes of antidepressants can produce adaptive changes in the 5-HTT (Benmansour et al., 1999; Yau et al., 1999), but the duration of these effects after treatment cessation has not been clarified. Conceivably, however, persistent treatment-induced adaptive changes in the 5-HTT might have obscured an underlying pathophysiological abnormality in our subjects. However, consideration of treatment naïve subjects alone did not reveal any trend to a difference in BP.

While my findings appear to exclude an abnormality in 5-HTT availability in recovered depressed patients there is increasing evidence from animal studies that altered 5-HT function early in life can have profound effects on neuronal development and these effects can in turn influence responses to stress and

adversity in adulthood (Sibille and Lewis, 2006). Hence normal levels of the 5-HTT in adult life do not exclude important effects of early changes in the 5-HTT activity on the development of the neural circuitry supporting emotional regulation. Indeed other PET studies in recovered depressed patients have revealed altered availability of cortical post-synaptic 5-HT_{1A} and 5-HT_{2A} receptors. These receptors are often co-localised on cortical neurons where they have opposing physiological roles (Santana et al., 2004). Thus even in the presence of normal levels of the 5-HTT, recovered depressed patients appear to have changes in post-synaptic 5-HT receptor expression (Bhagwagar et al., 2004) which could lead to abnormalities in the excitability of cortical networks. The notion that such changes could be developmental in origin is intriguing and will require appropriate studies in high-risk subjects before the onset of depressive disorder.

Based on my findings in acute and recovered depressed patients, I suggest that decreased 5-HTT binding may be a state marker of depression which resolves with clinical recovery. Follow up imaging studies in the same patients before and after clinical recovery will be required to confirm this possibility.

6 5-HTT POLYMORPHISMS AND [^{11}C] DASB BINDING

6.1 INTRODUCTION

AS noted previously, the neuronal serotonin transporter (5-HTT) plays a critical role in the regulation of serotonin (5-HT) neurotransmission and drugs targeting the 5-HTT such as selective serotonin re-uptake inhibitors (SSRIs) are used extensively in the management of mood and anxiety disorders. The gene encoding the 5-HTT has a number of polymorphic variants and one in the 5-HTT-linked promoter region (5-HTTLPR) is composed of a short (S) and long (L) version which results in differential transcription of the 5-HTT in vitro, with the L form being associated with higher 5-HTT expression levels (Lesch et al., 1996). More recently the 5-HTTLPR has been shown to exist in a triallelic form because the L allele itself has two functional variants (L_A and L_G) with the L_G form exhibiting similar levels of 5-HTT expression in vitro as the S allele (Hu et al., 2006).

It is important to determine whether 5-HTTLPR genotype affects expression of the 5-HTT in the human brain as this would have important implications for the role of individual variation of the 5-HTTLPR in the pathophysiology of emotional disorders and the effects of antidepressant treatment. It is possible to approach this question using positron or single photon emission tomography (PET or SPET) in conjunction with ligands designed to bind specifically to the 5-HTT.

The results to date of these investigations have been inconsistent probably as a consequence of relatively modest sample sizes and ligands of varying specificity for the 5-HTT. Using [^{123}I]-βCIT with SPET in 96 healthy subjects,

van Dyck et al (2004) reported higher 5-HTT binding in brainstem & striatum among carriers of the SS genotype, but this result was not confirmed in two smaller investigations also using [^{123}I]-βCIT (Jacobsen et al., 2000; Willeit et al., 2001). A limitation of studies with [^{123}I]-βCIT is that this ligand has similar affinity for the dopamine transporter and the 5-HTT and it is not possible to image the 5-HTT in cortical brain areas relevant to emotional regulation such as anterior cingulate cortex and limbic structures. However, two more recently developed PET ligands, [^{11}C] McN5652 and [^{11}C] DASB, allow specific quantification of the 5-HTT in these brain areas. Once again the data regarding the effect of 5-HTTLPR genotype are contradictory. Using [^{11}C] McN5652, Parsey et al (2006a) found no effect of the triallelic polymorphism on 5-HTT binding in 42 healthy subjects and 25 acutely depressed patients. However, Praschak-Rieder et al (2007) using [^{11}C] DASB in 43 healthy subjects reported increased 5-HTT in putamen specifically in those with an L_A/L_A genotype. Reimold et al (2007), showed a similar effect in midbrain in 19 healthy volunteers with L_A/L_A genotype.

As a 5-HTT ligand, [^{11}C]DASB compares favourably to [^{11}C](+)McN5652 in terms of the ratio of specific to non-specific binding. In this study I used [^{11}C]DASB in conjunction with PET to assess the role of 5-HTTLPR polymorphisms on the availability of brain 5-HTT to [^{11}C] DASB binding, in a relatively large group of healthy volunteers, using a full metabolite corrected arterial input function & graphical analysis to quantify regional activity.

6.2 MATERIALS AND METHODS

6.2.1 Participants

The study was approved by the Research Ethics Committee at Hammersmith Hospital, London, and the Administration of Radioactive Substances Advisory Committee (ARSAC), UK. All participants gave written informed consent for the study. I recruited 63 healthy European caucasian men (mean ± SD age 38.5 ± 11.1 years) with no current or past psychiatric history or substance misuse problems. Subjects with any serious medical or neurological (current or past) illness, alcohol or illicit substance dependence and other axis I or II disorders were excluded. I included only male subjects in this study because of a lack of toxicology data for [^{11}C] DASB in females.

Each subject had a PET scan with [^{11}C] DASB and a structural MRI scan for drawing accurate regions of interest. I implemented the same methods and procedures for PET and MRI scanning; image analysis; and quantification of [^{11}C]DASB binding potentials as described in the Methods chapter.

The injected radioactivity dose, in this study, was between 432 MBq and 564 MBq (mean: 509 MBq, SD: 26 MBq). The radiochemical purity of the injected [^{11}C]DASB was high and ranged from 95% to 100% with a mean of 98% and a SD of 1%. The injected mass dose varied between 0.1 and 13.7 µg with a mean value of 3.1 µg and a SD of 2.3 µg. The specific activity was high, on average 100966 MBq•µmol-1 with a SD of 197723 MBq•µmol-1.

Seven regions of interest (ROI) -amygdala, caudate, dorsal raphe, anterior cingulate cortex, hippocampus, putamen, thalamus and a reference region - cerebellum were defined on the co-registered MRI with the help of a probabilistic brain atlas template (Hammers et al., 2002). Cerebellar grey matter was used as a reference region because of the negligible density of 5-HTT in the cerebellum (Kish et al., 2005). The dorsal raphe region was manually defined as a fixed size region (900 mm3) on the summed PET images of each individual. Dynamic PET scans were sampled by applying the individual ROI object maps. The regional volumes of distribution were determined using linear graphical analysis with metabolite corrected arterial input function and [^{11}C]DASB binding potentials estimated by using cerebellum as reference region. The full methodology is given in the Methods Chapter.

6.2.2 Genotyping

Blood samples were collected from subjects and DNA was extracted from whole blood using the QIAamp DNA Mini Kit (Qiagen Inc, Canada). The genotyping was carried out at the Dr. James L. Kennedy' lab, Psychiatric Neurogenetics Section, centre for addiction and mental Health, Toronto, Canada. The 5HTTLPR region of SLC6A4 was examined by amplifying with PCR using standard methods. The PCR products were visualized using gel electrophoresis performed in agarose gels prepared with ethidium bromide and 1X TBE (Tris, boric acid, EDTA). The 5HTTLPR and rs25531 were genotyped according to the protocol by Deluca et al., 2005 (De Luca et al., 2005). To control for genotyping errors, a random subsample of 10% of the sample was

re-genotyped. There were no differences between the original and the re-genotyped samples, thus it was assumed that the genotyping error rate was very low.

6.2.3 STATISTICAL ANALYSIS

Statistical analyses were performed using Statistical Package for Social Sciences (SPSS Inc., Chicago, Illinois, USA) version 12. My primary hypothesis was that regional 5-HTT receptor binding potential would be lower in subjects with an SS genotype using the biallelic classification of S and L. I tested this using repeated measures analysis of variance (ANOVA) with "genotype" (LL vs SL vs SS) as a between subjects factor, and "region" (brain region of interest) as a within subjects factor with age as a covariate. I then repeated the analysis, classifying participants on the basis of triallelelic genotyping where L alleles were classified as L_A and L_G. For the purposes of this analysis, L_G & S alleles were combined as S' and L_A was coded as L'. The three genotype groups consisted of S'S' (SS + S L_G + L_GL_G); S'L' (S L_A + L_AL_G); and L'L' (L_AL_A). Age was added as a covariate to all the ANOVAs.

6.3 RESULTS

Bialleleic genotyping of the 5-HTTLPR revealed that of the 63 participants, 10 (16%) were SS, 35 (56%) were SL and 18 (28%) were LL (Table 6-1). The frequencies of the triallelic genotypes are shown in Table 6-2. These frequencies did not differ significantly from the Hardy-Weinberg equilibrium (Chi

squared = 1.054, and p=0.3047).

The binding of [^{11}C] DASB was most concentrated in raphe with moderate densities apparent in several other brain regions including putamen, thalamus, caudate and amygdala. Lesser degrees of binding were detectable in anterior cingulate cortex and hippocampus. The RM ANOVA comparing the binding potential [^{11}C] DASB of all participants using the biallelic classification showed a significant main effect of brain region (F= 25.5; df= 6,354; p= 0.001) but no main effect of genotype (F= 0.61; df= 2, 59; p= 0.55) or region by genotype interaction (F= 0.28; df= 12,354; p= 0.83) (Table 6-1; Figure 6-1). There were no significant main or interactive effects of age (all values >0.5).

I then carried out the same analyses using the triallelic classification. There was no main effect of genotype (F= 0.09; df= 2, 59; p = 0.91), no interaction between genotype and brain region (F= 0.63; df= 6,330; p= 0.48) and no main or interactive effects of age (all p values >0.5) (Table 6-2, Figure 6-1).

Table 6-1: Mean (SD) [^{11}C] DASB binding potential in different brain regions by 5-HTTLPR biallelic genotypes

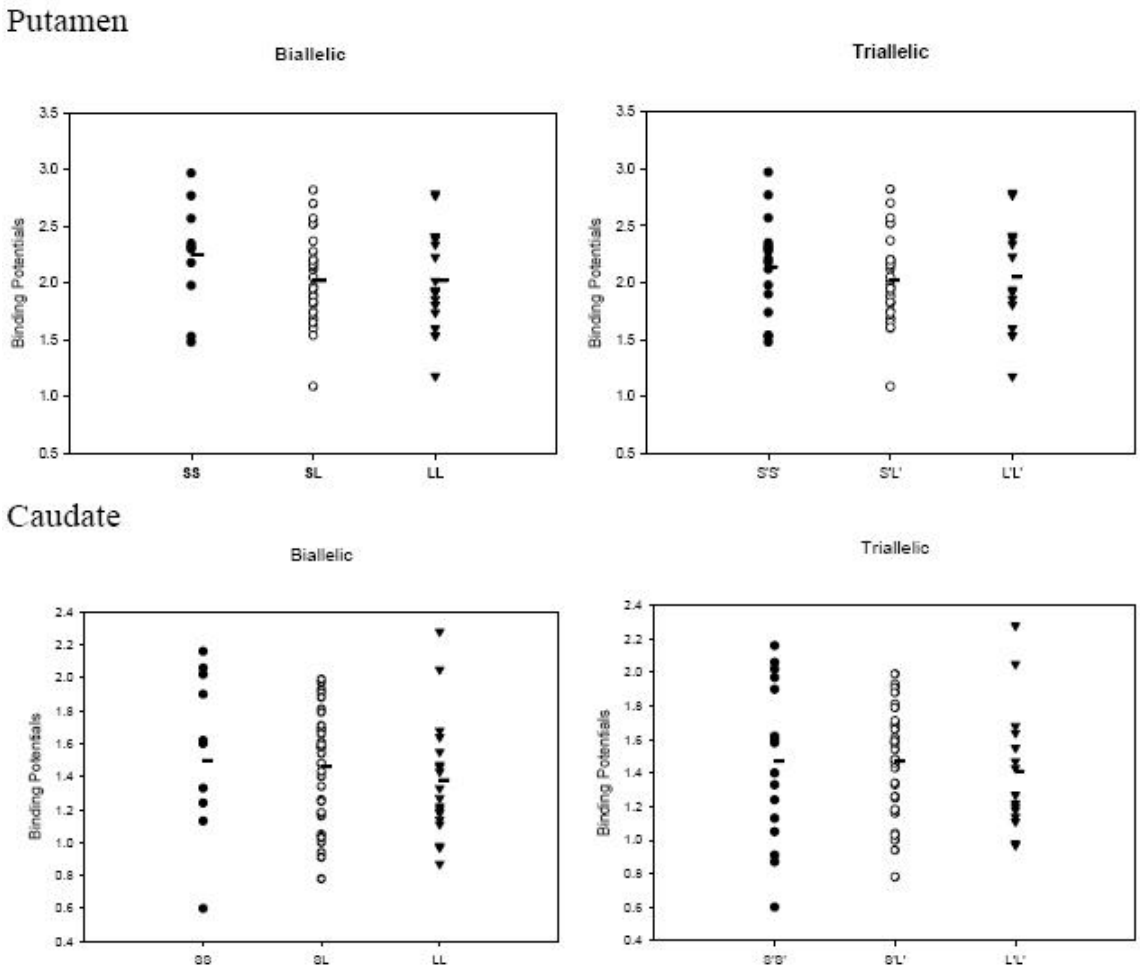
Region	SS (N=10)	SL (N=35)	LL (N=18)	RM ANOVA
Raphe	4.30 (1.16)	4.47 (1.59)	4.55 (1.26)	F=0.61, df 2,59, p=0.55
Amygdala	2.07 (0.44)	1.87 (0.33)	1.70 (0.39)	
Ant Cingulate	0.94 (0.24)	0.81 (0.16)	0.75 (0.22)	
Hippocampus	1.11 (0.26)	0.99 (0.17)	0.88 (0.17)	
Caudate	1.57 (0.49)	1.46 (0.33)	1.38 (0.37)	
Putamen	2.25 (0.48)	2.02 (0.36)	2.02 (0.44)	
Thalamus	1.85 (0.51)	1.9 (0.42)	1.79 (0.39)	

Table 6-2: Mean (SD) [^{11}C] DASB binding potential in different brain regions by 5-HTTLPR gain of function triallelic genotypes

Region	S'S' (N=16)	S'L' (N=32)	L'L' (N=15)	RM ANOVA
Raphe	4.19 (1.02)	4.5 (1.65)	4.68 (1.31)	F=0.09, df 2,59, p=0.91
Amygdala	2.06 (0.38)	1.81 (0.32)	1.71 (0.42)	
Ant Cingulate	0.89 (0.21)	0.81 (0.16)	0.75 (0.24)	
Hippocampus	1.06 (0.22)	0.98 (0.18)	0.88 (0.17)	
Caudate	1.47 (0.48)	1.47 (0.32)	1.41 (0.38)	
Putamen	2.14 (0.43)	2.02 (0.36)	2.05 (0.48)	
Thalamus	1.83 (0.44)	1.91 (0.42)	1.77 (0.42)	

S'S' includes SS, SL_G & L_GL_G genotypes; S'L' includes SL_A & L_AL_G genotypes; L'L' includes L_AL_A genotype

Figure 6-1: Scatter plots of [^{11}C] DASB binding potentials in putamen and caudate by 5-HTTLPR biallelic and triallelic genotypes



Legend: S'S' includes SS, SL_G & L_GL_G genotypes; S'L' includes SL_A & L_AL_G genotypes; L'L' includes L_AL_A genotype; Horizontal lines show group mean values.

6.4 DISCUSSION

My data in a large group of healthy volunteers, suggest that polymorphic variation in the 5-HTTLPR does not alter the expression of the 5-HTT in adult human brain as measured by [^{11}C] DASB binding potential. The findings

remained the same whether the 5-HTTPLR was classified on a bialleleic or triallelic basis. I included among the brain regions examined, areas that previous reports have implicated as showing an effect of 5-HTTLPR genotype on 5-HTT expression, for example, putamen, caudate & midbrain/raphe. However, no effect of allelic variation on 5-HTT binding potential could be detected. Overall my findings support previous imaging studies that have not found significant effects of the 5-HTTLPR on 5-HTT availability (Parsey et al., 2006a; Shioe et al., 2003).

To date, three studies have reported the effect of 5-HTTLPR triallelic genotype on 5-HTT binding using [^{11}C]DASB and PET. Praschak-Reider et al (2007) in a group of 43 male and female subjects reported about 12% higher 5-HTT binding only in putamen in L_A/L_A genotype carriers compared with non L_A/L_A carriers. This finding was uncorrected for multiple-comparisons and the other five regions studied did not show any effect. The authors further noted that in a subset of 30 caucasians, the putamen remained significant after correction for multiple comparisons. Reimold et al (2007), in a relatively small group (N=19) of male and female subjects found about 21 % higher BP in midbrain in L_A/L_A carriers. However, they did not find any effect in amygdala or thalamus and they did not report putamen or other striatal regions. Kalbitzer et al, (2010) reported no significant difference in 5-HTT binding between L homozygotes and S-allele carriers (Kalbitzer et al., 2010). However they found increased BP_{ND} for [^{11}C]DASB only in the caudate nucleus ($p=0.04$, uncorrected) in the L_A/L_A genotype (N=50). The effect size was not reported in the manuscript. In

comparison to these three studies, my study included a larger sample size and also used metabolite corrected arterial input method to derive BP_{ND}.

While my data suggest that variation in the 5-HTTLPR does not affect the availability of 5-HTT to [^{11}C] DASB binding in the adult brain there is much evidence to indicate that 5-HTTLPR genotype influences aspects of brain function in healthy subjects. Perhaps the best described finding in this respect relates to studies using functional magnetic resonance imaging (fMRI) to measure the activity of the amygdala in response to negative emotional stimuli (Hariri et al., 2005; Munafo et al., 2007; Rhodes et al., 2007). Across a range of tasks and stimulus types, carriers of an S allele of the 5-HTTPLR consistently show greater amygdala activation. In addition, there are clinically-orientated investigations suggesting, for example, that carriers of the S allele are at greater risk of experiencing depression when exposed to stressful life events (Hariri et al., 2005; Roiser et al., 2005) and less likely when depressed to respond to treatment with SSRIs (Serretti et al., 2007). It should be noted, however, that much of this evidence has been contested (Kraft et al., 2007; Risch et al., 2009).

Taken together the data suggest that variation in the 5-HTTLPR does not influence brain function by changing availability of the 5-HTT to [^{11}C] DASB binding in the adult human brain but by other mechanisms. In the absence of 5-HTTLPR polymorphism related alterations in 5-HTT expression, how may the reported functional associations with brain structure, function and behaviour be

explained? A popular current view is that the 5-HTTLPR genotype may be important in neurodevelopment so that effects of genotypes on brain function in adults are likely attributable to earlier neurodevelopmental changes. It should be kept in mind that promoter variants of gene polymorphisms play a role in not only in the quantity of mRNA expression but also the timing and duration of expression, and each of these effects is tissue-specific. It could be that the L versus S promoter variants has their main effect on the overall biological function by influencing the formation of 5-HT circuitry in fetal or childhood development, and these connectivity or functional changes might then be relatively fixed in adulthood. The 5-HTT protein available to [^{11}C] DASB binding in adult brains may be restored and maintained by homeostatic mechanisms that are independent of 5-HTTLPR genotype, and thus the PET binding potential would show no difference between S versus L genetic status.

This neurodevelopmental view may be supported by the observation that carriers of the S allele reportedly have reduced grey matter volume in both anterior cingulate and amygdala (Pezawas et al., 2005) and decreased functional connectivity between these brain regions (Heinz et al., 2005; Pezawas et al., 2005). Such neuroanatomical correlates may underlie abnormal functional reactions in S carriers to probes of neural circuitry regulating emotion. Furthermore, inherited differences in 5-HT transporter expression may also be compensated for by changes in tryptophan hydroxylase synthetic activity, or monoamine oxidase catabolic activity.

It is worth noting that additional variants in the 5-HTTLPR have been described and it is possible that a more complete classification of the different genotypes may allow an effect on 5-HTT availability to be described. In addition my colleagues and I have obtained evidence that amygdala responses to negative facial expressions measured by fMRI are influenced by the level of 5-HTT binding in left amygdala as measured by [^{11}C] DASB (Rhodes et al., 2007). This suggests that other factors involved in the regulation of 5-HTT expression might be important in explaining individual variation in emotional regulation.

It is possible that there may be gender differences in 5-HTTLPR genotype mediated 5-HTT expression, which this study could not address because I included only male volunteers. There may also be power issues. Hu et al, (2006) noted approximately 3-fold difference in mRNA expression between L_AL_A and the SS group and while it is not known how such a large *in vitro* effect may translate in to *in vivo* 5-HTT expression, my large PET study had adequate power to detect a between group difference of approximately 15%.

Recently, Kalbitzer et al (2010) reported that cerebral 5-HTT binding was associated with daylight minutes at the time of the PET-scan. Therefore, I reanalysed our data using the amount of daylight in minutes (Kalbitzer et al., 2010) as a covariate. I did not find any significant main or interaction effect of daylight minutes on either genotype or regional 5-HTT binding in biallelic or triallelic or L_AL_A vs non L_AL_A carriers (all p values >0.5). Therefore I believe that my results are unlikely to be confounded by the effect of daylight. In summary, this PET study, in a large group of healthy male European caucasian

volunteers, shows that variations in 5-HTTLPR gene do not affect 5-HTT expression as measured by [^{11}C] DASB binding in the living human brain.

7 5-HTTLPR TRIALLELIC POLYMORPHISM AND BRAIN MORPHOMETRY

7.1 INTRODUCTION

The short (S) allele of an insertion/deletion variant in the promoter region of the human serotonin transporter (5-HTT) gene (SLC6A4) has been associated with increased risk of depression in stressful life circumstances (Caspi et al., 2003). The way in which this genetic variation influences brain function is the subject of intensive research. Despite suggestive in vitro evidence, current Positron Emission Tomography (PET) studies and my study (chapter 6) do not show a consistent effect of the promoter variant on the availability of the 5-HTT in the brain in vivo and attention has shifted to differential effects of the S allele on brain morphology (Jedema et al., 2010).

As discussed in the Introduction, brain morphology has been studied using a Region of Interest (ROI) based approach or automated morphometry based methods. In ROI models, the structures examined must be defined in advance and so this approach is driven by a priori hypotheses. Using the ROI approach, Frodl et al (2004) reported that depressed patients with a long allele 'L' had smaller hippocampal grey (GM) and white matter (WM) volumes when compared with patients with an S allele. This effect was however not seen in healthy controls. Taylor et al (2005) found similar results in elderly patients with late onset (50 years and above) depression where L homozygote carriers had smaller right hippocampal volumes than S homozygotes. In the same study, further post-hoc analysis revealed that patients with an earlier age of onset of depression (age below 50) and homozygous S/S genotype had smaller hippocampal volumes (Taylor et al., 2005). There are however negative

findings (Hickie et al., 2007; O'Hara et al., 2007). Hickie et al (2007), in a group of elderly depressed patients did not significant effect of 5-HTTLPR effect on hippocampus and amygdala but found low caudate volume in S allele carrier. O'Hara et al (2007) in a group of healthy older adults found no main effect of the 5-HTT S allele on hippocampal volume but reported an interactive effect; S carriers with high cortisol levels had low hippocampal volume (O'Hara et al., 2007). Finally, Scherk et al (2009) observed increased amygdala volume in S allele carriers in both bipolar disorder patients and healthy subjects (Scherk et al., 2009). The results of ROI based studies have been summarized in Table 7-1.

Voxel-based morphometry (VBM) is an objective, fully automated deterministic technique which allows the investigator to look for changes in volume in any part of the brain by applying statistics to the whole brain and examining significant changes at a voxel level (Ashburner and Friston, 2000; Good et al., 2001a). Voxel based morphology is an operator independent, bias-free approach to structural analysis of brain. Using the VBM approach, Pezawas et al (2005) found decreased volume in perigenual anterior cingulate cortex (pACC) and amygdala in 114 controls (LL= 35, S'= 79) classified according to the bialleleic promoter polymorphism (Pezawas et al., 2005). In contrast, Canli et al (2005) studying 41 healthy controls (LL= 13, S'= 28) found reductions in gray matter density in S' carriers (insula, left middle frontal gyrus and gyrus rectus, right inferior temporal gyrus, ACC and cerebellum). Frodl et al (2008), studying the tri-allelic 5HTT polymorphism in 77 healthy controls, found rather

more widespread reductions in gray matter in S' carriers (left amygdala, right hippocampus, left ACC and bilateral dorsolateral prefrontal cortex) (Frodl et al., 2008). However, in the latter study the morphometric comparisons appear to have been restricted to L'L' (n= 10) and S'S' (n= 23) homozygotes. Finally Rao et al (2007), in a small group of healthy controls (n=26; LL = 13), did not find any effect of genotype on amygdala or ventro-medial prefrontal cortex (VMPFC) (Rao et al., 2007) (Table 7-2).

As mentioned above, the differences among the morphometry studies may be due to several experimental variables including genotype (biallelic vs triallelic), sample size or technique (VBM or ROI) or diagnosis.

In this study I used both ROI and VBM analysis in a large sample of healthy control subjects to assess the effect of the triallelic 5-HTTLPR polymorphism on brain gray matter volume. This includes an embedded A/G substitution, rs25531 ($S/L_A/L_G$), where the L_G allele is considered functionally similar to and grouped together with the S allele (L'=L_A; S'=S and L_G).

7.2 METHODS

7.2.1 Study Participants

I studied 113 healthy volunteers who were free from any lifetime psychiatric or neurological disorder (females 43, males 70), mean age 37.6 years (range 18-60 years, SD 11.3). There were 22 S'-non-carriers (L'L' genotype) (mean age

32.7 years, SD 11.2) and 91 S' carriers (mean age 37.6 years, SD 11.2).

7.2.2 MRI Acquisition

All volunteers had a structural T1 MRI scan at the Robert Steiner MRI unit at the Hammersmith Hospital, London, UK. Structural MRI data were acquired at 3T (3T Intera Philips Medical Systems) MR scanners [TR=9.6ms, TE=4.6ms, flip angle=8, NSA=1, voxel dimensions 0 94 mm x 0.94 mm x 1.2 mm]. The scans were inspected by an independent clinical radiologist and found to be normal.

7.2.3 Regions of Interest (ROI) analysis

The regions of interest studied were bilateral amygdala, anterior cingulate cortex and hippocampus. The selection of ROI were restricted to those reported in previous published studies reporting the effects of the 5-HTTLPR on gray matter volume (Frodl et al., 2008; Pezawas et al., 2005). The ROIs were generated from a standard anatomic atlas (Harvard-Oxford cortical and subcortical atlas) available within FSL.

7.2.4 VBM preprocessing

Image preprocessing utilised an optimised VBM protocol (FSL v4.1.4). Structural data were analysed with FSL-VBM, a voxel-based morphometry style analysis (Ashburner and Friston, 2000; Good et al., 2001a) carried out with FSL

tools (Smith et al., 2004). First, structural images were brain-extracted using BET (Smith, 2002). MRI image quality was visually checked and poor quality images were excluded (n=3). Next, tissue-type segmentation was carried out using FAST4 (Zhang et al., 2001). The resulting grey matter partial volume images were then aligned to MNI152 standard space using the affine registration tool FLIRT (Jenkinson et al., 2002; Jenkinson and Smith, 2001), followed optionally by nonlinear registration using FNIRT (Andersson et al., 2007a, b), which uses a b-spline representation of the registration warp field (Rueckert et al., 1999). The resulting images were averaged to create a study-specific template, to which the native grey matter images were then non-linearly re-registered. The registered partial volume images were then modulated (to correct for local expansion or contraction) by dividing by the Jacobian determinant of the warp field. The modulated segmented images were then smoothed with an isotropic Gaussian kernel with a sigma of 12 mm. Finally, voxel wise GLM was applied using permutation-based non-parametric testing, correcting for multiple comparisons across space.

7.2.5 Genotyping

The genotyping procedures were described in chapter 6. The 5HTTLPR region of SLC6A4 was examined by amplifying with PCR using standard methods. The genotyping was carried out at the a) Dr. James L. Kennedy' lab, Psychiatric Neurogenetics Section, centre for addiction and mental Health, Toronto, Canada and; b) Psychopharmacology unit, university department of Psychiatry, Oxford, UK by Dr Beata Godlewska. The genetic variants of 5HTTLPR

rs25531polymorphism were determined by the PCR reaction, followed by digestion with MspI restriction enzyme (De Luca et al., 2005).

7.2.6 Statistics

Effects of the 5-HTTLPR on gray matter volume were examined using an analysis of covariance model with age and gender as covariates of no interest. Gray-matter volume changes were assessed statistically with one-tailed t-tests using a threshold free cluster-based approach with correction for multiple comparisons at the whole-brain level. Because the t contrast is a one-tailed test, the directions between the two conditions; (S' > L'L' homozygotes carriers or S' < L'L' homozygotes carriers) were tested. In addition, bilateral amygdala, ACC and hippocampus were also analysed separately as ROIs using two-tailed t tests. My primary hypothesis was that brain GM volume in limbic and frontal regions would be lower in S' carriers using the triallelic classification of S and L, where L alleles were classified as L_A and L_G. I first studied L' (S' non-carriers = L_AL_A) vs S' carriers and then L' and S'S' homozygotes. Age and gender were added as covariates.

7.3 RESULTS

The ROI based analysis using both biallelic and triallelic results did not show any significant differences between S' carriers and L'L' homozygotes in any of the a priori regions studied (all $p>0.05$)

Whole brain VBM analysis revealed significantly reduced gray matter volume in S' allele carriers vs L'L' homozygotes in 3 regions; (a) right inferior frontal gyrus (IFG) (*x*=54, *y*=18, *z*=22); (b) left dorsal ACC (*x*=-8, *y*=-16, *z*=36); and (c) superior temporal gyrus (STG) (*x*=62, *y*=-14, *z*=-4) (Figure 7-1 & 7-2). In addition, there were no regions that displayed greater volume in S' allele carriers vs L'L' homozygotes. Comparison of L'L' and S'S' homozygotes showed reduced gray matter volume in S'S' participants in right IFG (*x*=56, *y*=18, *z*=22) and right STG (*x*=62, *y*=-14, *z*=-4). There was no region that showed significant increased grey matter volume in S' allele carriers vs L'L' homozygotes.

7.4 DISCUSSION

My findings are broadly consistent with earlier observations using VBM showing decreased regional gray matter volume in S' carriers but the regional localisation of this effect shows variation (Table 1 and 2). The differences in the results among the above mentioned studies may be due to the use of different scanners, structural analysis techniques, genotyping (biallelic vs triallelelic association) or the play of chance. While there are some differences in the localisation of changes, in agreement with this study, most of the VBM investigations in healthy controls, found reductions in ACC volume in S' carriers. In addition, a recent study in non-human primates (4 L'L' vs 4 L'S') also reported widespread reductions in gray matter volume in S' carriers including ACC, medial prefrontal and orbitofrontal cortex as well as the amygdala (Jedema et al., 2010).

In contrast to Pezawas et al (2005) and Frodl et al (2008), we did not find any differences in amygdala grey matter volume between the 5-HTTLPR genotypes using either ROI or VBM methods. Scherk et al (2009), in a group of bipolar disorder and healthy subjects, using the ROI method, found increased amygdala volume in S' carriers in both groups (Scherk et al., 2009). However this effect became only of trend level significance when diagnosis was included in the analysis. It is possible that the lack of effect allele status on amygdala, in addition to technical differences, may be explained by interacting effect of other genotypes with the 5-HTT polymorphism. For example, Pezawas et al (2008) reported that the structural connectivity between amygdala and ACC was modulated by a polymorphism in the Brain Derived Neurotropic Factor (BDNF) gene (Pezawas et al., 2008). This may suggest a complex interplay of gene-gene interactions at neural systems level in the human brain.

We did not find any effect of genotype on hippocampus using either of the analytic approaches. This is not surprising as previous studies either only found changes in S carriers who were also depressed patients with (Frodl et al., 2004; Taylor et al., 2005) or modulated by cortisol (O'Hara et al., 2007) or no effect (Dutt et al., 2009). The reason why some 5-HTTLPR effects are seen only in patients is still unclear. It is possible that patients have other pathological processes induced by factors such as stress, elevated cortisol level changes or other aspects of the disease process. These factors might well themselves alter grey matter volume. Therefore the effect of S' carriage may be

obscured/confounded more readily in patient groups.

The reduction in volume in ACC in S' carriers is of interest because the ACC plays an important role in emotion, mood and the responses to stress (Devinsky et al., 1995) and has been implicated in several neuropsychiatric conditions (Baiano et al., 2007; Drevets et al., 2008; Riffkin et al., 2005; Seidman et al., 2006). In addition, the 5-HTTLPR is densely expressed in ACC. Overall the findings suggest that if S' carriage of the 5-HTT polymorphism does predispose to the development of depression this action may be exerted through effects on the volume and function of the ACC.

The structural changes observed may not be restricted to grey matter alone. For instance, Pacheco et al. (2009), using diffusion MRI, reported a negative correlation between S' carriage and white matter connectivity (as measured fractional anisotropy) in the left frontal uncinate fasciculus (Pacheco et al., 2009). In addition, there may be changes in smaller regions which are not detectable using the current imaging technology. For example, Young et al (2007) reported a postmortem tissue analyses in which they observed an association between 5-HTTLPR 'S' allele and enlargement of the pulvinar nucleus of thalamus (Young et al., 2007). The pulvinar relays visual information to subcortical and higher cortical brain regions (Young et al., 2007).

The reduction in GM volume seen in the VBM analysis in the present study could indicate a decreased number of neuronal numbers or size or density. It is

to be noted that MRI measurements may reflect alterations of neuronal and non-neuronal tissue compartments, physiological alterations in brain tissue or changes in other chemical constituents (Weinberger and McClure, 2002). Furthermore the exact nature of grey matter changes observed with VBM is not well understood. For instance, whether the changes in grey matter represent changes in grey matter thickness can only be addressed using histological techniques at present. Further advancements in high resolution MRIs may allow more in vivo visualization of the fine structure of the brain (Bridge and Clare, 2006).

It is now well known that serotonin plays an important regulatory role in neurodevelopment (Sodhi and Sanders-Bush, 2004). Studies using serotonin transporter knockout mice reported marked reduction in the thickness of the cortical layers (Altamura et al., 2007; Alvarez et al., 2002). Presumably then the changes seen in grey matter volume in 5-HTT S' carriers might be developmental in origin.

Taken together, the studies suggest that carriage of the S' allele may influence brain function through an effect on brain morphology, perhaps exerted during neurodevelopment. Studies with larger samples of subjects appear to have more restricted morphological changes; however, an effect of S' carriage on volume of the ACC appears a fairly reliable finding. This is of interest in view of the role of the anterior cingulate in integrating cognitive and emotional information as well as its frequent implication in functional imaging studies in depressed patents.

Table 7-1: Characteristics of Regions of Interest (ROI) based studies

Studies	N	Age Mean (SD)	L Carriers	Study main outcome
Frodl et al 2004	40 depressed	44.4 (11.7)	16	Depressed patients with L/L had smaller hippocampal GM & WM No effect in control subjects
Taylor et al 2005	83	69.4 (6.3)	29	Patients with a late onset of depression (n=63)and L /L genotype exhibited smaller right hippocampal volume Patients with an earlier age of onset (n=72) and S/S genotype had smaller hippocampal volumes No effect in control subjects
Taylor et al 2007	370 Combined	70 (7)	135	No effect of genotype on orbito frontal cortex volume in both depressed and control subjects
Wassink et al 2007	44 Autism	3.4 (0.3)	15	Autistic boys with S allele had greater cortical GM
Hickie et al 2007	45 Patients	52 (12.8)	15	Elderly depressed patients with S allele had smaller low caudate No effect in hippocampus
O' Hara et al 2007	154 (51:103F)	71.3 (8.8)	45	No genotypic effect on hippocampus Subjects with high cortisol & S allele had smaller hippocampus
Scherk et al 2009	74 Combined	41.9 (13)	26	S allele in a combined group of bipolar disorder and control subjects had greater amygdala volume
Raznahan et al 2009	43	-	-	No effect of genotype in a group of adolescents and adults with Autistic spectrum
Dutt et al 2009	57	40.8 (25.1)	16	No effect of genotype in hippocampus and ventricular volume group in controls. Also no effect in a large group patients with psychosis, their relatives and controls

Table 7-2: Characteristics of Voxel-based morphometry (VBM) based studies

Studies	Healthy control group			Covariates	Outcome
	N (M:F)	Age Mean (SD)	L carriers		
Pezawas et al 2005	114 (58:56)	32.8 (9.57)	35	A, Sx, TGM	ROIs in Limbic cortex only - S carriers had greater pACC & Amygdala
Canli et al 2005	41 (19:22)	34.8	13	A, Sx, TGM	L carriers had greater GM volume L SFG, LMFG, L ACC & R IFG GM L carriers had greater GM density bilateral INS, L MFG, GR, RIFG, ACC & CERE
Rao et al 2007	26 (13:13)	20.4 (2.1)	13	A, Sx, TGM	No Amygdala or VMPFC
Frodl et al 2008	77 (42:35)	40.5 (11.6)	L_AL_A 10	A, Sx	ROIs in Limbic and DL/DM PFC L_A had larger ACC, R DLPFC, R DMPFC, L Amygdala, L Hippocampus Patients L_AL_A had bilateral smaller hippocampus
Frodl et al 2010	27 (9:18)	41.9	-	**-**	S-allele and had a positive history for emotional neglect had smaller hippocampal volumes than patients Larger DLPFC in subjects homozygous for the L-allele with a history of emotional neglect

GM: grey matter; L: left; R: right; ACC: anterior cingulate cortex; pACC: peri anterior cingulate cortex; SFG: superior frontal gyrus; MFG: medial frontal gyrus; IFG: inferior

frontal gyrus; INS: insula; CERE: cerebellum; GR: gyrus rectus; VMPFC: ventro medial prefrontal cortex; DLPFC: dorsolateral prefrontal cortex; DMPFC: dorsomedial prefrontal cortex; A: age; Sx: Sex; TGM: total grey matter.

Figure 7-1: Displayed are axial, coronal and sagittal images depicting significantly reduced gray matter volume in S' allele carriers vs L'L' homozygotes in right inferior frontal gyrus.

Numerals refer to coordinates in Montreal Neurological Institute space. Images in radiological format

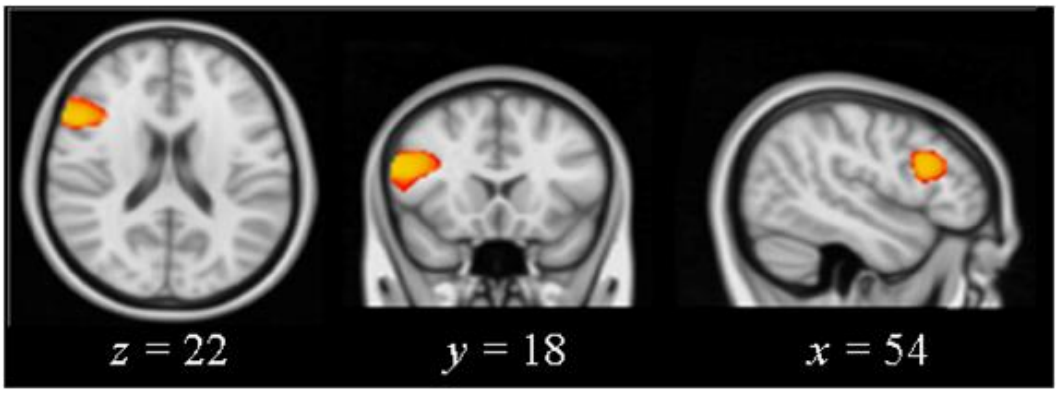
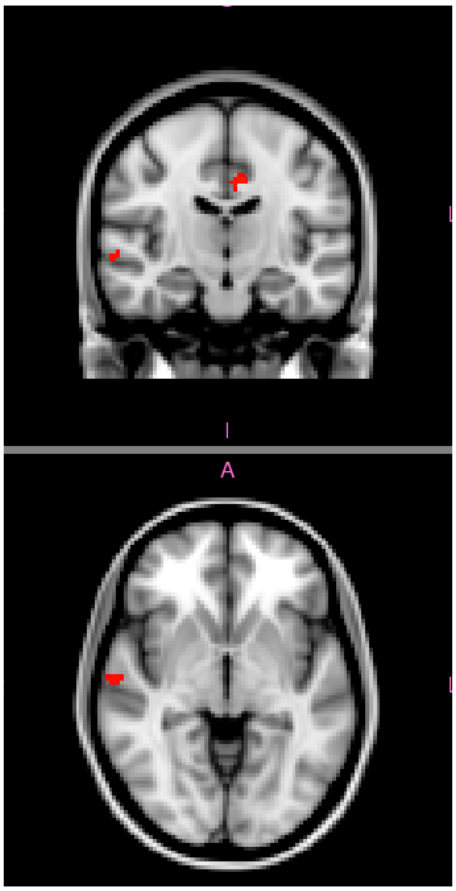


Figure 7-2: Axial and coronal depicting significantly reduced gray matter volume in S' allele carriers vs L'L' homozygotes in (a) left anterior cingulate and (b) superior temporal gyrus



8 SUMMARY AND DISCUSSION

8.1 SUMMARY OF MAIN FINDINGS

There were five main aims for this thesis, which were outlined in the Introduction. These aims are presented below together with a brief summary of the results of the study concerned.

8.1.1 Study 1:

Aim

To assess the effects of an intravenous infusion of 10mg citalopram, a selective serotonin reuptake inhibitor (SSRI), prior to PET scanning, on the kinetics of [^{11}C]DASB in arterial plasma and in selected brain regions.

Results

The citalopram infusion led to a substantial increase of the area under the curve of the metabolite-corrected arterial plasma input function. A mean reduction of the cerebellar V_T of [^{11}C]DASB binding of 19% with Logan analysis and of 24% with spectral analysis was observed after citalopram infusion, which confirms previous findings of displaceable 5-HTT binding in cerebellar grey matter. The 5-HTT occupancy by citalopram of six target regions with moderate to high DASB binding was 60% derived from BP_{ND} and 69% derived from BP_P.

8.1.2 Study 2:

Aim

To measure brain 5-HTT binding in a group of unmedicated acutely depressed patients in comparison to healthy controls using [^{11}C]DASB.

Results

The depressed patients had lowered 5-HTT binding in several brain regions including brain stem, thalamus, caudate, putamen, anterior cingulate cortex and frontal cortex. These results suggest diminished availability of the 5-HTT in the brain in unmedicated acutely depressed patients

8.1.3 Study 3:

Aim

To measure brain 5-HTT binding in a group of unmedicated recovered depressed patients in comparison to healthy subjects

Results

There was no significant difference in the binding potential of [^{11}C]DASB between the recovered depressed patients and healthy comparison subjects in any of the brain regions studied. The findings do not support the proposal that

recurrent depression is associated with long-standing deficits in 5-HTT, independent of clinical state.

8.1.4 Study 4:

Aim

To examine the availability of the 5-HTT in brain using positron emission tomography in conjunction with the selective 5-HTT ligand [^{11}C] DASB in healthy volunteers who were genotyped for short (S) and long (L) variants (SLC6A4 and rs25531) of the 5-HTTLPR

Results

[^{11}C] DASB binding potential was not influenced by allelic status of participants, whether classified on a biallelic or triallelic basis, in any of the regions studied. The findings suggest 5-HTTLPR polymorphic variation does not affect the availability of 5-HTT to [^{11}C] DASB binding in adult human brain.

8.1.5 Study 5:

Aim

To assess the effect of the triallelic 5-HTTLPR polymorphism on brain grey matter volume using Region of Interest (ROI) and Voxel-Based Morphometry

(VBM) analysis in a group of healthy subjects

Results

Whole brain VBM analysis revealed significantly reduced gray matter volume in S' allele carriers vs L'L' homozygotes in right inferior frontal gyrus, left anterior cingulate and superior temporal gyrus. The studies suggest that carriage of the S' allele may impact on brain morphology.

8.2 DISCUSSION

8.2.1 5-HTT in depression

As outlined in the Introduction, there is much evidence from a variety of sources that brain serotonin function is abnormal in depression (Cowen, 2008). The fact that acutely lowering serotonin levels by means of tryptophan depletion can cause depressive relapse in vulnerable people suggests that low availability of serotonin may be an important factor in causing depression in some circumstances (Booij et al., 2002; Delgado et al., 1990; Smith et al., 1997). The 5-HTT is a key target of antidepressant drug action and the present thesis aimed to explore the role of the 5-HTT in depression using PET imaging in conjunction with an appropriate 5-HTT ligand, [^{11}C]DASB.

My findings suggest that acutely depressed patients demonstrate reduced 5-HTT binding in several brain regions; however, judging from the lack of

change in the 5-HTT in recovered depressed patients, diminished 5-HTT binding is a state marker of depression, present during the acute illness but remitting when patients recover. However, some caveats are required for this conclusion. First, whether or not acutely depressed patients have diminished binding of the 5-HTT is controversial because the findings from different studies are inconsistent even when considering only the studies of [^{11}C]DASB (Cannon et al., 2007; Meyer et al., 2004a; Reimold et al., 2008). It is possible that this variation reflects heterogeneity in the characteristics of the patient group and certainly my patients were notable for a chronic course of illness and lack of response to treatment. Hence it is possible that low 5-HTT binding might be confined to a subgroup of patients with these features. In support of this possibility I found that [^{11}C]DASB binding correlated inversely with number of depressive episodes and early age of onset, both factors associated with a poorer long-term prognosis.

Another important issue is the functional meaning of a decrease in [^{11}C]DASB in patients with acute depression. It would be expected that diminished availability of the 5-HTT would result in decreased reuptake of serotonin into the nerve ending and hence greater levels of synaptic serotonin. After all this is presumably how SSRIs increase synaptic serotonin and relieve depression (Owens and Nemeroff, 1994). It seems unlikely therefore that lowered [^{11}C]DASB binding can explain low synaptic serotonin and thereby account for the depressed state. A possible explanation is that if the activity of serotonin neurons is low and the availability of serotonin decreased, the number of 5-HTT

sites may decrease to compensate for this. Some preclinical studies support this view that the 5-HTT subcellular distribution is affected by extracellular 5-HT levels (Blakely et al., 1998; Ramamoorthy and Blakely, 1999; Zahniser and Doolen, 2001). From this viewpoint low 5-HTT binding may be an adaptive response which is magnified by SSRI treatment.

It is possible that following recovery when serotonin neurotransmission is at a more normal level and antidepressant medication withdrawn, the number of 5-HTT binding sites is normalised. However, as noted earlier, is also possible that low 5-HTT binding might be associated with a poor response to treatment. Conceivably then, patients who do well with antidepressants may have normal 5-HTT binding when depressed and when recovered. This could be a clinically useful predictor in that it would be possible prospectively to study a range of depressed patients prior to treatment and see if low 5-HTT binding was associated with a worse clinical outcome, a possibility for which there is some preliminary evidence (Miller et al., 2008). However, even if such a study produced the predicted result, the expensive and specialised nature of PET probably makes it unsuitable to predict response to antidepressant treatment in routine practice.

8.2.2 Future directions

In a further study, because of the controversial nature of the PET literature and the small size of my acutely depressed sample, it would be worthwhile trying to confirm my observation that depressed patients with a chronic history and poor

response to treatment have lowered 5-HTT binding. In addition it would be important to extend my observations to female patients whom I was not able to study in the present investigations. If the primary abnormality in depressed patients is low serotonin availability from presynaptic nerve terminals it might be possible to test this using PET measure of serotonin release through ligand displacement. Such an approach has been applied with great success in the dopamine field but at present there is no analogous displacement test that seems widely applicable in the serotonin field (Laruelle, 2000; Talbot et al., 2005). There is some evidence that the binding of selective ligands to 5-HT_{1A} receptors in the raphe nuclei is decreased following SSRI challenge, perhaps representing displacement by endogenous serotonin of ligand bound to 5-HT_{1A} autoreceptors (Sibon et al., 2008). However the binding of [^{11}C]DASB in healthy volunteers does not seem sensitive to changing levels of endogenous serotonin as judged by studies that have employed tryptophan depletion (Praschak-Rieder et al., 2005; Talbot et al., 2005). Further work is needed to find suitably displaceable ligands that can be used to measure serotonin release in the human brain (Milak et al., 2010). This would be an important technical development leading to better understanding of the role of serotonin neurotransmission in psychiatric disorders.

8.2.3 PET Methodological issues

As has been noted in the Introduction and Chapters 4 and 5, other explanations for the differing results of [^{11}C]DASB PET studies in depression involve methodological issues (Cannon et al., 2007; Meyer et al., 2004a; Reimold et al.,

2008). Using a metabolite corrected arterial input and reference tissue method; I found decreases in ^{11}C-DASB V_T in cerebellar grey matter in depressed patients compared to healthy subjects. The cerebellum is a structure with reportedly small to negligible concentration of 5-HTT (Kish et al., 2005; Laruelle et al., 1988). The reduction in [^{11}C]DASB cerebellar V_T in depressed patients might reflect either the loss of some specific binding in cerebellum or differences in nonspecific binding between patients and controls. In fact, this apparent reduction in cerebellum V_T does not invalidate my finding of low 5-HTT binding in depression, as the magnitude of V_T values in target regions were very significantly decreased in patients compared to differences in the cerebellum as reference region. However, clearly in some circumstances changes in depressed patients in cerebellar V_T could confound a PET study which makes investigations using simplified scanning protocols without measurement of the plasma input function problematic.

Another caveat is that in my study it was not possible to measure reliably in all subjects the tracer free fraction which would give information about systematic differences in f_1 plasma free tracer. However in a subset of patients when values were corrected for the measured f_1, the study results remained significant. In addition, the f_1 plasma free tracer differences should affect global binding differences not region specific (Parsey et al., 2006b)

I found similar binding potential differences in cerebellum in my citalopram displacement experiment which illustrates the importance of plasma

quantification of tracer concentrations also in drug occupancy studies (Chapter 3). The interpretation of the change of 5-HTT would require some caution if there were any changes in nonspecific binding in the disease process (Ikoma et al 2002). The impact of protein binding and non-specific binding on drug distribution in brain tissue requires further research (Syvänen et al 2010).

8.2.4 5-HTT transporter gene, 5-HTT and brain morphology

The transcriptional activity of promoter region of serotonin transporter gene (SLC6A4) is differentially modulated by short and long variants, with differences in 5-HTT mRNA, protein density and 5-HT uptake activity in human lymphoblastoid cells (Heils et al., 1996; Lesch et al., 1996). A 5-HTT knockout mouse study indicated that 5-HTT binding sites in brain are absent in 5-HTT homozygous (-/-) null mutant mice and are reduced 50% in 5-HTT heterozygous (+/-) mutant mice (Bengel et al., 1998).

Despite the strong evidence that variations in the 5-HTTLPR influence expression and availability of the 5-HTT in vitro, the effect of the polymorphic variants on brain 5-HTT receptor binding has been inconsistent, as demonstrated, in both post-mortem (Little et al., 1998; Mann et al., 2000) and imaging studies (Jacobsen et al., 2000; Parsey et al., 2006a; Praschak-Rieder et al., 2007; Reimold et al., 2007; Shioe et al., 2003; van Dyck et al., 2004; Willeit et al., 2001). My data suggest that variation in the 5-HTTLPR does not influence the availability of the 5-HTT to [^{11}C] DASB binding in the adult human

brain. As argued in the chapter 6, it is possible that promoter variants of gene polymorphisms play a role in not only in the quantity of mRNA expression but also the timing and duration of expression, and each of these effects is tissue-specific. This may explain why a straightforward relationship between [^{11}C] DASB binding in the brain and the 5-HTTLPR polymorphism has been hard to demonstrate.

Despite this, there is much evidence both direct and indirect that the promoter polymorphism can influence brain *function*. Thus individuals with the S or short allele variant of 5-HTTLPR show anxious and dysphoric traits (Lesch et al., 1996), increased amygdala response to fear (Hariri et al., 2002) and are at increased risk for depression in the presence of stressful life events (Caspi et al., 2003). However, it should be noted that even with these fairly well-established findings there are numerous failures to replicate (Kraft et al., 2007; Munafo et al., 2008; Munafo et al., 2009; Willis-Owen et al., 2005). This may be because the effect size of the promoter polymorphism is small. Another possibility is that other genes interact with the 5-HTTLPR to influence whether or not its effect is expressed, so called epistasis (Pezawas et al., 2008).

If the variation in the 5-HTTLPR does not influence brain function directly through changes in the availability of the 5-HTT binding, how might the probable influence of the 5-HTTLPR on brain function and behaviour be explained?

One possibility could be that the L and S promoter variants have their main effect on the overall brain function by influencing the formation of 5-HT circuitry in fetal or childhood development, and these connectivity or functional changes might then be relatively fixed in adulthood. The 5-HTT protein available to [11C] DASB binding in adult brains may be restored and maintained by homeostatic mechanisms that are independent of 5-HTTLPR genotype, and thus the PET binding potential would show no difference between S versus L genetic status. There is some evidence for such a mechanism. For instance, transient pharmacological inhibition of 5-HTT in adult mice during early development produced abnormal emotional behaviours (Ansorge et al., 2004; Riccio et al., 2009). In addition, 5-HTT knockout mice show altered neocortical morphology (Altamura et al 2007). The results suggest that a developmental mechanism might explain how altered 5-HTTT activity at one point during development can increase vulnerability to psychiatric disorders. This neurodevelopmental view may be supported by the observation that carriers of the S allele reportedly have reduced grey matter volume in both anterior cingulate and amygdala (Pezawas et al., 2005) and decreased functional connectivity between these brain regions (Heinz et al., 2005; Pezawas et al., 2005).

My findings provide some support for this view in that I found that carriers of the S allele did have reduced grey matter volume in a number of brain regions. However, there was relatively little overlap between the regions implicated in my study and those reported by others with the exception of anterior cingulate cortex. This suggests that while the S allele might be associated with reduced

grey matter volume, the brain region affected shows much individual variation, perhaps as result of interaction of the S allele with other genetic or environmental factors. It is possible that such neuroanatomical correlates may underlie abnormal functional reactions in S carriers to probes of neural circuitry regulating emotion (and perhaps explain some of their inconsistency).

Due to relatively small sample sizes and unavailability of DNA samples, the effect of the 5-HTTLPR on 5-HTT binding and brain morphology was not investigated in the depressed patients in my study. However an effect of 5-HTTLPR variation on brain morphological changes in depressed patients has been reported albeit in different brain regions (Frodl et al., 2008; Frodl et al., 2004; Taylor et al., 2005). High intensity MRI or other techniques will be required to clarify the nature of brain grey matter changes observed (Bridge and Clare, 2006) (Chapter 7). Clearly further study of depressed patients and comparison with healthy subjects would be important in this respect.

8.2.5 Conclusion

In conclusion my studies have shown that at least in a subgroup of depressed patients acute depression is associated with decreased availability of the 5-HTT as measured by ligand PET. The evidence I have indicates that this abnormality is a state marker of depression but this suggestion that needs to be confirmed by following the *same* group of patients through depression, treatment and its resolution. It seems unlikely that the decrease in 5-HTT availability can account for the likely abnormality in serotonin in depression that is decreased serotonin

neurotransmission. To establish the underlying serotonin abnormality with greater precision would be greatly helped by development of techniques for measuring serotonin release in vivo by PET ligand displacement.

My studies also suggest that if the 5-HTT promoter polymorphism does exert a reliable effect on the risk of depression it is not exerted through changes in the 5-HTT but more probably through changes in brain morphology perhaps neurodevelopmental in origin and perhaps involving the anterior cingulate cortex. It should be noted however that the majority of participants in my study were carriers of the S allele so perhaps it is not useful to think of the S allele as vulnerability factor. It may, for example, makes more sense to think of LL homozygotes as being a minority who are to some extent protected from the risk of depression.

REFERENCES

Abi-Dargham, A., Laruelle, M., Seibyl, J., Rattner, Z., Baldwin, R.M., Zoghbi, S.S., Zea-Ponce, Y., Bremner, J.D., Hyde, T.M., Charney, D.S., et al., 1994. SPECT measurement of benzodiazepine receptors in human brain with iodine-123-iomazenil: kinetic and equilibrium paradigms. J Nucl Med 35, 228-238.

Aghajanian, G.K., Marek, G.J., 1999. Serotonin and hallucinogens. Neuropsychopharmacology 21, 16S-23S.

Akiskal, H.S., Bourgeois, M.L., Angst, J., Post, R., Moller, H., Hirschfeld, R., 2000. Re-evaluating the prevalence of and diagnostic composition within the broad clinical spectrum of bipolar disorders. J Affect Disord 59 Suppl 1, S5-S30.

Alonso, J., Angermeyer, M.C., Bernert, S., Bruffaerts, R., Brugha, T.S., Bryson, H., de Girolamo, G., Graaf, R., Demyttenaere, K., Gasquet, I., Haro, J.M., Katz, S.J., Kessler, R.C., Kovess, V., Lepine, J.P., Ormel, J., Polidori, G., Russo, L.J., Vilagut, G., Almansa, J., Arbabzadeh-Bouchez, S., Autonell, J., Bernal, M., Buist-Bouwman, M.A., Codony, M., Domingo-Salvany, A., Ferrer, M., Joo, S.S., Martinez-Alonso, M., Matschinger, H., Mazzi, F., Morgan, Z., Morosini, P., Palacin, C., Romera, B., Taub, N., Vollebergh, W.A., 2004. Prevalence of mental disorders in Europe: results from the European Study of the Epidemiology of Mental Disorders (ESEMeD) project. Acta Psychiatr Scand Suppl, 21-27.

Altamura, C., Dell'Acqua, M.L., Moessner, R., Murphy, D.L., Lesch, K.P., Persico, A.M., 2007. Altered neocortical cell density and layer thickness in serotonin transporter knockout mice: a quantitation study. Cereb Cortex 17, 1394-1401.

Alvarez, C., Vitalis, T., Fon, E.A., Hanoun, N., Hamon, M., Seif, I., Edwards, R., Gaspar, P., Cases, O., 2002. Effects of genetic depletion of monoamines on somatosensory cortical development. Neuroscience 115, 753-764.

Anderson, I.M., 2000. Selective serotonin reuptake inhibitors versus tricyclic antidepressants: a meta-analysis of efficacy and tolerability. J Affect Disord 58, 19-36.

Anderson, I.M., Cowen, P.J., 1991. Prolactin response to the dopamine antagonist, metoclopramide, in depression. Biol Psychiatry 30, 313-316.

Anderson, I.M., Ferrier, I.N., Baldwin, R.C., Cowen, P.J., Howard, L., Lewis, G., Matthews, K., McAllister-Williams, R.H., Peveler, R.C., Scott, J., Tylee, A., 2008. Evidence-based guidelines for treating depressive disorders with antidepressants: a revision of the 2000 British Association for Psychopharmacology guidelines. J Psychopharmacol 22, 343-396.

Anderson, I.M., Parry-Billings, M., Newsholme, E.A., Fairburn, C.G., Cowen, P.J., 1990. Dieting reduces plasma tryptophan and alters brain 5-HT function in women. Psychol Med 20, 785-791.

Anderson, I.M., Ware, C.J., da Roza Davis, J.M., Cowen, P.J., 1992. Decreased 5-HT-mediated prolactin release in major depression. Br J Psychiatry 160, 372-378.

Andersson, J.L.R., Jenkinson, M., Smith, S., 2007a. Non-linear optimisation. . FMRIB technical report TR07JA1 from www.fmrib.ox.ac.uk/analysis/techrep

Andersson, J.L.R., Jenkinson, M., Smith, S., 2007b. Non-linear registration, aka Spatial normalisation FMRIB technical report TR07JA2 from www.fmrib.ox.ac.uk/analysis/techrep

Angold, A., Costello, E.J., Worthman, C.M., 1998. Puberty and depression: the roles of age, pubertal status and pubertal timing. Psychol Med 28, 51-61.

Angst, J., 1998. The emerging epidemiology of hypomania and bipolar II disorder. J Affect Disord 50, 143-151.

Ansorge, M.S., Zhou, M., Lira, A., Hen, R., Gingrich, J.A., 2004. Early-life blockade of the 5-HT transporter alters emotional behavior in adult mice. Science 306, 879-881.

Arango, V., Ernsberger, P., Marzuk, P.M., Chen, J.S., Tierney, H., Stanley, M., Reis, D.J., Mann, J.J., 1990. Autoradiographic demonstration of increased serotonin 5-HT2 and beta-adrenergic receptor binding sites in the brain of suicide victims. Arch Gen Psychiatry 47, 1038-1047.

Arango, V., Underwood, M.D., Boldrini, M., Tamir, H., Kassir, S.A., Hsiung, S., Chen, J.J., Mann, J.J., 2001. Serotonin 1A receptors, serotonin transporter binding and serotonin transporter mRNA expression in the brainstem of depressed suicide victims. Neuropsychopharmacology 25, 892-903.

Arango, V., Underwood, M.D., Gubbi, A.V., Mann, J.J., 1995. Localized alterations in pre- and postsynaptic serotonin binding sites in the ventrolateral prefrontal cortex of suicide victims. Brain Res 688, 121-133.

Arora, R.C., Meltzer, H.Y., 1989a. 3H-imipramine binding in the frontal cortex of suicides. Psychiatry Res 30, 125-135.

Arora, R.C., Meltzer, H.Y., 1989b. Increased serotonin2 (5-HT2) receptor binding as measured by 3H-lysergic acid diethylamide (3H-LSD) in the blood platelets of depressed patients. Life Sci 44, 725-734.

Arranz, B., Eriksson, A., Mellerup, E., Plenge, P., Marcusson, J., 1994. Brain 5-HT1A, 5-HT1D, and 5-HT2 receptors in suicide victims. Biol Psychiatry 35, 457-463.

Asberg, M., Thoren, P., Traskman, L., Bertilsson, L., Ringberger, V., 1976a. "Serotonin depression"--a biochemical subgroup within the affective disorders? Science 191, 478-480.

Asberg, M., Traskman, L., Thoren, P., 1976b. 5-HIAA in the cerebrospinal fluid. A biochemical suicide predictor? Arch Gen Psychiatry 33, 1193-1197.

Ashburner, J., 2009. Computational anatomy with the SPM software. Magn Reson Imaging 27, 1163-1174.

Ashburner, J., Friston, K.J., 2000. Voxel-based morphometry--the methods. Neuroimage 11, 805-821.

Asselin, M.C., Montgomery, A.J., Grasby, P.M., Hume, S.P., 2007. Quantification of PET studies with the very high-affinity dopamine D2/D3 receptor ligand [11C]FLB 457: re-evaluation of the validity of using a cerebellar reference region. J Cereb Blood Flow Metab 27, 378-392.

Attar-Levy, D., Martinot, J.L., Blin, J., Dao-Castellana, M.H., Crouzel, C., Mazoyer, B., Poirier, M.F., Bourdel, M.C., Aymard, N., Syrota, A., Feline, A., 1999. The cortical serotonin2 receptors studied with positron-emission tomography and [18F]-setoperone during depressive illness and antidepressant treatment with clomipramine. Biol Psychiatry 45, 180-186.

Attenburrow, M.J., Mitter, P.R., Whale, R., Terao, T., Cowen, P.J., 2001. Low-dose citalopram as a 5-HT neuroendocrine probe. Psychopharmacology (Berl)

155, 323-326.

Badawi, R.D., 1998. Aspects of Optimisation and Quantification in Three-Dimensional Positron Emission Tomography. Unliversity of London, London.

Baiano, M., David, A., Versace, A., Churchill, R., Balestrieri, M., Brambilla, P., 2007. Anterior cingulate volumes in schizophrenia: a systematic review and a meta-analysis of MRI studies. Schizophr Res 93, 1-12.

Barnes, N.M., Sharp, T., 1999. A review of central 5-HT receptors and their function. Neuropharmacology 38, 1083-1152.

Beck, A.T., Ward, C.H., Mendelson, M., Mock, J., Erbaugh, J., 1961. An inventory for measuring depression. Arch Gen Psychiatry 4, 561-571.

Belanger, M.J., Simpson, N.R., Wang, T., Van Heertum, R.L., Mann, J.J., Parsey, R.V., 2004. Biodistribution and radiation dosimetry of [11C]DASB in baboons. Nucl Med Biol 31, 1097-1102.

Bengel, D., Murphy, D.L., Andrews, A.M., Wichems, C.H., Feltner, D., Heils, A., Mossner, R., Westphal, H., Lesch, K.P., 1998. Altered brain serotonin homeostasis and locomotor insensitivity to 3, 4-methylenedioxymethamphetamine ("Ecstasy") in serotonin transporter-deficient mice. Mol Pharmacol 53, 649-655.

Benmansour, S., Cecchi, M., Morilak, D.A., Gerhardt, G.A., Javors, M.A., Gould, G.G., Frazer, A., 1999. Effects of chronic antidepressant treatments on serotonin transporter function, density, and mRNA level. J Neurosci 19, 10494-10501.

Bergouignan, L., Chupin, M., Czechowska, Y., Kinkingnehun, S., Lemogne, C., Le Bastard, G., Lepage, M., Garnero, L., Colliot, O., Fossati, P., 2009. Can voxel based morphometry, manual segmentation and automated segmentation equally detect hippocampal volume differences in acute depression? Neuroimage 45, 29-37.

Bhagwagar, Z., Cowen, P.J., 2008. 'It's not over when it's over': persistent neurobiological abnormalities in recovered depressed patients. Psychol Med 38, 307-313.

Bhagwagar, Z., Hafizi, S., Cowen, P.J., 2002a. Acute citalopram administration

produces correlated increases in plasma and salivary cortisol. Psychopharmacology (Berl) 163, 118-120.

Bhagwagar, Z., Hinz, R., Taylor, M., Fancy, S., Cowen, P., Grasby, P., 2006. Increased 5-HT(2A) receptor binding in euthymic, medication-free patients recovered from depression: a positron emission study with [(11)C]MDL 100,907. Am J Psychiatry 163, 1580-1587.

Bhagwagar, Z., Rabiner, E.A., Sargent, P.A., Grasby, P.M., Cowen, P.J., 2004. Persistent reduction in brain serotonin1A receptor binding in recovered depressed men measured by positron emission tomography with [11C]WAY-100635. Mol Psychiatry 9, 386-392.

Bhagwagar, Z., Whale, R., Cowen, P.J., 2002b. State and trait abnormalities in serotonin function in major depression. Br J Psychiatry 180, 24-28.

Bienvenu, O.J., Davydow, D.S., Kendler, K.S., 2010. Psychiatric 'diseases' versus behavioral disorders and degree of genetic influence. Psychol Med, 1-8.

Bifulco, A., Brown, G.W., Adler, Z., 1991. Early sexual abuse and clinical depression in adult life. Br J Psychiatry 159, 115-122.

Biggio, G., Fadda, F., Fanni, P., Tagliamonte, A., Gessa, G.L., 1974. Rapid depletion of serum tryptophan, brain tryptophan, serotonin and 5-hydroxyindoleacetic acid by a tryptophan-free diet. Life Sci 14, 1321-1329.

Biver, F., Wikler, D., Lotstra, F., Damhaut, P., Goldman, S., Mendlewicz, J., 1997. Serotonin 5-HT2 receptor imaging in major depression: focal changes in orbito-insular cortex. Br J Psychiatry 171, 444-448.

Blakely, R.D., Ramamoorthy, S., Schroeter, S., Qian, Y., Apparsundaram, S., Galli, A., DeFelice, L.J., 1998. Regulated phosphorylation and trafficking of antidepressant-sensitive serotonin transporter proteins. Biol Psychiatry 44, 169-178.

Bligh-Glover, W., Kolli, T.N., Shapiro-Kulnane, L., Dilley, G.E., Friedman, L., Balraj, E., Rajkowska, G., Stockmeier, C.A., 2000. The serotonin transporter in the midbrain of suicide victims with major depression. Biol Psychiatry 47, 1015-1024.

Booij, L., Van der Does, W., Benkelfat, C., Bremner, J.D., Cowen, P.J., Fava,

M., Gillin, C., Leyton, M., Moore, P., Smith, K.A., Van der Kloot, W.A., 2002. Predictors of mood response to acute tryptophan depletion. A reanalysis. Neuropsychopharmacology 27, 852-861.

Bridge, H., Clare, S., 2006. High-resolution MRI: in vivo histology? Philos Trans R Soc Lond B Biol Sci 361, 137-146.

Briley, M.S., Langer, S.Z., Raisman, R., Sechter, D., Zarifian, E., 1980. Tritiated imipramine binding sites are decreased in platelets of untreated depressed patients. Science 209, 303-305.

Brown, G.L., Ebert, M.H., Goyer, P.F., Jimerson, D.C., Klein, W.J., Bunney, W.E., Goodwin, F.K., 1982. Aggression, suicide, and serotonin: relationships to CSF amine metabolites. Am J Psychiatry 139, 741-746.

Bunney, W.E., Jr., Davis, J.M., 1965. Norepinephrine in depressive reactions. A review. Arch Gen Psychiatry 13, 483-494.

Cahill, L., 2006. Why sex matters for neuroscience. Nat Rev Neurosci 7, 477-484.

Cannon, D.M., Ichise, M., Fromm, S.J., Nugent, A.C., Rollis, D., Gandhi, S.K., Klaver, J.M., Charney, D.S., Manji, H.K., Drevets, W.C., 2006. Serotonin transporter binding in bipolar disorder assessed using [11C]DASB and positron emission tomography. Biol Psychiatry 60, 207-217.

Cannon, D.M., Ichise, M., Rollis, D., Klaver, J.M., Gandhi, S.K., Charney, D.S., Manji, H.K., Drevets, W.C., 2007. Elevated serotonin transporter binding in major depressive disorder assessed using positron emission tomography and [11C]DASB; comparison with bipolar disorder. Biol Psychiatry 62, 870-877.

Carson, R.E., Channing, M.A., Blasberg, R.G., Dunn, B.B., Cohen, R.M., Rice, K.C., Herscovitch, P., 1993. Comparison of bolus and infusion methods for receptor quantitation: application to [18F]cyclofoxy and positron emission tomography. J Cereb Blood Flow Metab 13, 24-42.

Caspi, A., Sugden, K., Moffitt, T.E., Taylor, A., Craig, I.W., Harrington, H., McClay, J., Mill, J., Martin, J., Braithwaite, A., Poulton, R., 2003. Influence of life stress on depression: moderation by a polymorphism in the 5-HTT gene. Science 301, 386-389.

Cipriani, A., Furukawa, T.A., Salanti, G., Geddes, J.R., Higgins, J.P., Churchill, R., Watanabe, N., Nakagawa, A., Omori, I.M., McGuire, H., Tansella, M., Barbui, C., 2009. Comparative efficacy and acceptability of 12 new-generation antidepressants: a multiple-treatments meta-analysis. Lancet 373, 746-758.

Coppen, A., Eccleston, E.G., Peet, M., 1973. Total and free tryptophan concentration in the plasma of depressive patients. Lancet 2, 60-63.

Coppen, A., Shaw, D.M., Malleson, A., Eccleston, E., Gundy, G., 1965. Tryptamine metabolism in depression. Br J Psychiatry 111, 993-998.

Coppen, A., Swade, C., Wood, K., 1978. Platelet 5-hydroxytryptamine accumulation in depressive illness. Clin Chim Acta 87, 165-168.

Coppen, A.J., 1969. Biochemical aspects of depression. Int Psychiatry Clin 6, 53-81.

Cowen, P.J., 2008. Serotonin and depression: pathophysiological mechanism or marketing myth? Trends Pharmacol Sci 29, 433-436.

Cowen, P.J., Charig, E.M., 1987. Neuroendocrine responses to intravenous tryptophan in major depression. Arch Gen Psychiatry 44, 958-966.

Cowen, P.J., Parry-Billings, M., Newsholme, E.A., 1989. Decreased plasma tryptophan levels in major depression. J Affect Disord 16, 27-31.

Crow, T.J., Cross, A.J., Cooper, S.J., Deakin, J.F., Ferrier, I.N., Johnson, J.A., Joseph, M.H., Owen, F., Poulter, M., Lofthouse, R., et al., 1984. Neurotransmitter receptors and monoamine metabolites in the brains of patients with Alzheimer-type dementia and depression, and suicides. Neuropharmacology 23, 1561-1569.

Cunningham, V.J., Ashburner, J., Byrne, H., Jones, T., 1993. Use of spectral analysis to obtain parametric images from dynamic PET studies. . In: Uemura, K., Jones, T., Lassem, N.A., Kanno, I. (Eds.), In quantification of brain function: tracer kinetics and image analysis in brain PET. Excerpta Medica, Amsterdam., pp. 101-111.

Cunningham, V.J., Gunn, R.N., Byrne, H., Matthews, J.C., 1998. Suppression of noise artifacts in spectral analysis of dynamic PET data. . Academic Press., San Diego, CA.

Cunningham, V.J., Jones, T., 1993. Spectral analysis of dynamic PET studies. J Cereb Blood Flow Metab 13, 15-23.

Cunningham, V.J., Lammertsma, A.A., 1995a. Radioligand studies in brain: kinetic analysis of PET data. Med Chem Res, 79-96.

Cunningham, V.J., Lammertsma, A.A., 1995b. Radioligand studies in brain: kinetic analysis of PET data. . Med Chem Res 79 - 96.

Cunningham, V.J., Rabiner, E.A., Slifstein, M., Laruelle, M., Gunn, R.N., 2010. Measuring drug occupancy in the absence of a reference region: the Lassen plot re-visited. J Cereb Blood Flow Metab 30, 46-50.

D'Haenen, H., Bossuyt, A., Mertens, J., Bossuyt-Piron, C., Gijsemans, M., Kaufman, L., 1992. SPECT imaging of serotonin2 receptors in depression. Psychiatry Res 45, 227-237.

Dahlstrom, M., Ahonen, A., Ebeling, H., Torniainen, P., Heikkila, J., Moilanen, I., 2000. Elevated hypothalamic/midbrain serotonin (monoamine) transporter availability in depressive drug-naive children and adolescents. Mol Psychiatry 5, 514-522.

Davidson, K.M., Ritson, E.B., 1993. The relationship between alcohol dependence and depression. Alcohol Alcohol 28, 147-155.

De Luca, V., Tharmalingam, S., King, N., Strauss, J., Bulgin, N., Kennedy, J.L., 2005. Association study of a novel functional polymorphism of the serotonin transporter gene in bipolar disorder and suicidal behaviour. Psychopharmacology (Berl) 182, 128-131.

Delgado, P.L., Charney, D.S., Price, L.H., Aghajanian, G.K., Landis, H., Heninger, G.R., 1990. Serotonin function and the mechanism of antidepressant action. Reversal of antidepressant-induced remission by rapid depletion of plasma tryptophan. Arch Gen Psychiatry 47, 411-418.

Devinsky, O., Morrell, M.J., Vogt, B.A., 1995. Contributions of anterior cingulate cortex to behaviour. Brain 118 (Pt 1), 279-306.

Dillon, K.A., Gross-Isseroff, R., Israeli, M., Biegon, A., 1991. Autoradiographic analysis of serotonin 5-HT1A receptor binding in the human brain postmortem: effects of age and alcohol. Brain Res 554, 56-64.

Drevets, W.C., Savitz, J., Trimble, M., 2008. The subgenual anterior cingulate cortex in mood disorders. CNS Spectr 13, 663-681.

Drevets, W.C., Thase, M.E., Moses-Kolko, E.L., Price, J., Frank, E., Kupfer, D.J., Mathis, C., 2007. Serotonin-1A receptor imaging in recurrent depression: replication and literature review. Nucl Med Biol 34, 865-877.

Dutt, A., McDonald, C., Dempster, E., Prata, D., Shaikh, M., Williams, I., Schulze, K., Marshall, N., Walshe, M., Allin, M., Collier, D., Murray, R., Bramon, E., 2009. The effect of COMT, BDNF, 5-HTT, NRG1 and DTNBP1 genes on hippocampal and lateral ventricular volume in psychosis. Psychol Med 39, 1783-1797.

Edwards, J.G., Anderson, I., 1999. Systematic review and guide to selection of selective serotonin reuptake inhibitors. Drugs 57, 507-533.

Ellis, P.M., Salmond, C., 1994. Is platelet imipramine binding reduced in depression? A meta-analysis. Biol Psychiatry 36, 292-299.

Endres, C.J., Carson, R.E., 1998. Assessment of dynamic neurotransmitter changes with bolus or infusion delivery of neuroreceptor ligands. J Cereb Blood Flow Metab 18, 1196-1210.

First, M.B., Spitzer, R.L., Gibbon, M., Wiliam, J.B.W., 1996. Structured Clinical Interview for DSM-IV-TR Axis I Disorders, Clinical Version (SCID-CV). American Psychiatric Press, Inc., Washington, D.C.

Frank, E., Prien, R.F., Jarrett, R.B., Keller, M.B., Kupfer, D.J., Lavori, P.W., Rush, A.J., Weissman, M.M., 1991. Conceptualization and rationale for consensus definitions of terms in major depressive disorder. Remission, recovery, relapse, and recurrence. Arch Gen Psychiatry 48, 851-855.

Frankle, W.G., Huang, Y., Hwang, D.R., Talbot, P.S., Slifstein, M., Van Heertum, R., Abi-Dargham, A., Laruelle, M., 2004. Comparative evaluation of serotonin transporter radioligands 11C-DASB and 11C-McN 5652 in healthy humans. J Nucl Med 45, 682-694.

Frankle, W.G., Slifstein, M., Gunn, R.N., Huang, Y., Hwang, D.R., Darr, E.A., Narendran, R., Abi-Dargham, A., Laruelle, M., 2006. Estimation of serotonin transporter parameters with 11C-DASB in healthy humans: reproducibility and comparison of methods. J Nucl Med 47, 815-826.

Frodl, T., Koutsouleris, N., Bottlender, R., Born, C., Jager, M., Morgenthaler, M., Scheuerecker, J., Zill, P., Baghai, T., Schule, C., Rupprecht, R., Bondy, B., Reiser, M., Moller, H.J., Meisenzahl, E.M., 2008. Reduced gray matter brain volumes are associated with variants of the serotonin transporter gene in major depression. Mol Psychiatry 13, 1093-1101.

Frodl, T., Meisenzahl, E.M., Zill, P., Baghai, T., Rujescu, D., Leinsinger, G., Bottlender, R., Schule, C., Zwanzger, P., Engel, R.R., Rupprecht, R., Bondy, B., Reiser, M., Moller, H.J., 2004. Reduced hippocampal volumes associated with the long variant of the serotonin transporter polymorphism in major depression. Arch Gen Psychiatry 61, 177-183.

Gaddum, J.H., 1953. Antagonism between Lysergic Acid Diethylamide and 5-Hydroxytryptamine. Journal of Physiology-London 121, P15-P15.

Gartlehner, G., Gaynes, B.N., Hansen, R.A., Thieda, P., DeVeaugh-Geiss, A., Krebs, E.E., Moore, C.G., Morgan, L., Lohr, K.N., 2008. Comparative benefits and harms of second-generation antidepressants: background paper for the American College of Physicians. Ann Intern Med 149, 734-750.

Geday, J., Hermansen, F., Rosenberg, R., Smith, D.F., 2005. Serotonin modulation of cerebral blood flow measured with positron emission tomography (PET) in humans. Synapse 55, 224-229.

Gelder, M., Harrison P, Cowen P, 2006. The Oxford Textbook of Psychiatry. Oxford University Press, Oxford 2006, pp246.

Gijsbers van Wijk, C.M., Huisman, H., Kolk, A.M., 1999. Gender differences in physical symptoms and illness behavior. A health diary study. Soc Sci Med 49, 1061-1074.

Ginovart, N., Wilson, A.A., Meyer, J.H., Hussey, D., Houle, S., 2001. Positron emission tomography quantification of [(11)C]-DASB binding to the human serotonin transporter: modeling strategies. J Cereb Blood Flow Metab 21, 1342-1353.

Giuliani, N.R., Calhoun, V.D., Pearlson, G.D., Francis, A., Buchanan, R.W., 2005. Voxel-based morphometry versus region of interest: a comparison of two methods for analyzing gray matter differences in schizophrenia. Schizophr Res 74, 135-147.

Goldberg, R.J., Capone, R.J., Hunt, J.D., 1985. Cardiac complications following tricyclic antidepressant overdose. Issues for monitoring policy. JAMA 254, 1772-1775.

Golden, R.N., Ekstrom, D., Brown, T.M., Ruegg, R., Evans, D.L., Haggerty, J.J., Jr., Garbutt, J.C., Pedersen, C.A., Mason, G.A., Browne, J., et al., 1992. Neuroendocrine effects of intravenous clomipramine in depressed patients and healthy subjects. Am J Psychiatry 149, 1168-1175.

Good, C.D., Johnsrude, I., Ashburner, J., Henson, R.N., Friston, K.J., Frackowiak, R.S., 2001a. Cerebral asymmetry and the effects of sex and handedness on brain structure: a voxel-based morphometric analysis of 465 normal adult human brains. Neuroimage 14, 685-700.

Good, C.D., Johnsrude, I.S., Ashburner, J., Henson, R.N., Friston, K.J., Frackowiak, R.S., 2001b. A voxel-based morphometric study of ageing in 465 normal adult human brains. Neuroimage 14, 21-36.

Greenberg, B.D., Tolliver, T.J., Huang, S.J., Li, Q., Bengel, D., Murphy, D.L., 1999. Genetic variation in the serotonin transporter promoter region affects serotonin uptake in human blood platelets. Am J Med Genet 88, 83-87.

Gross-Isseroff, R., Israeli, M., Biegon, A., 1989. Autoradiographic analysis of tritiated imipramine binding in the human brain post mortem: effects of suicide. Arch Gen Psychiatry 46, 237-241.

Gross-Isseroff, R., Salama, D., Israeli, M., Biegon, A., 1990. Autoradiographic analysis of age-dependent changes in serotonin 5-HT2 receptors of the human brain postmortem. Brain Res 519, 223-227.

Gunn, R.N., Gunn, S.R., Cunningham, V.J., 2001. Positron emission tomography compartmental models. J Cereb Blood Flow Metab 21, 635-652.

Hagnell, O., Lanke, J., Rorsman, B., Ojesjo, L., 1982. Are we entering an age of melancholy? Depressive illnesses in a prospective epidemiological study over 25 years: the Lundby Study, Sweden. Psychol Med 12, 279-289.

Hamilton, M., 1960. A rating scale for depression. J Neurol Neurosurg Psychiatry 23, 56-62.

Hammers, A., Allom, R., Koepp, M.J., Free, S.L., Myers, R., Lemieux, L.,

Mitchell, T.N., Brooks, D.J., Duncan, J.S., 2003. Three-dimensional maximum probability atlas of the human brain, with particular reference to the temporal lobe. Hum Brain Mapp 19, 224-247.

Hammers, A., Asselin, M.C., Hinz, R., Kitchen, I., Brooks, D.J., Duncan, J.S., Koepp, M.J., 2007. Upregulation of opioid receptor binding following spontaneous epileptic seizures. Brain 130, 1009-1016.

Hammers, A., Koepp, M.J., Free, S.L., Brett, M., Richardson, M.P., Labbe, C., Cunningham, V.J., Brooks, D.J., Duncan, J., 2002. Implementation and application of a brain template for multiple volumes of interest. Hum Brain Mapp 15, 165-174.

Hariri, A.R., Drabant, E.M., Munoz, K.E., Kolachana, B.S., Mattay, V.S., Egan, M.F., Weinberger, D.R., 2005. A susceptibility gene for affective disorders and the response of the human amygdala. Arch Gen Psychiatry 62, 146-152.

Hariri, A.R., Drabant, E.M., Weinberger, D.R., 2006. Imaging genetics: perspectives from studies of genetically driven variation in serotonin function and corticolimbic affective processing. Biol Psychiatry 59, 888-897.

Hariri, A.R., Mattay, V.S., Tessitore, A., Kolachana, B., Fera, F., Goldman, D., Egan, M.F., Weinberger, D.R., 2002. Serotonin transporter genetic variation and the response of the human amygdala. Science 297, 400-403.

Harris, E.C., Barraclough, B., 1998. Excess mortality of mental disorder. Br J Psychiatry 173, 11-53.

Healy, D., 1997. Let Them Eat Prozac: The Unhealthy Relationship Between the Pharmaceutical Industry and Depression, New edition edition (15 Oct 2006) ed. New York University Press; .

Heils, A., Teufel, A., Petri, S., Stober, G., Riederer, P., Bengel, D., Lesch, K.P., 1996. Allelic variation of human serotonin transporter gene expression. J Neurochem 66, 2621-2624.

Heinz, A., Braus, D.F., Smolka, M.N., Wrase, J., Puls, I., Hermann, D., Klein, S., Grusser, S.M., Flor, H., Schumann, G., Mann, K., Buchel, C., 2005. Amygdala-prefrontal coupling depends on a genetic variation of the serotonin transporter. Nat Neurosci 8, 20-21.

Heise L, Ellsberg M, M, G., 1999. Ending violence against women. Vol. XXVII, No 4, Population reports, Johns Hopkins University, 1999.

Heninger, G.R., Charney, D.S., Sternberg, D.E., 1984. Serotonergic function in depression. Prolactin response to intravenous tryptophan in depressed patients and healthy subjects. Arch Gen Psychiatry 41, 398-402.

Herold, N., Uebelhack, K., Franke, L., Amthauer, H., Luedemann, L., Bruhn, H., Felix, R., Uebelhack, R., Plotkin, M., 2006. Imaging of serotonin transporters and its blockade by citalopram in patients with major depression using a novel SPECT ligand [123I]-ADAM. J Neural Transm 113, 659-670.

Hickie, I.B., Naismith, S.L., Ward, P.B., Scott, E.M., Mitchell, P.B., Schofield, P.R., Scimone, A., Wilhelm, K., Parker, G., 2007. Serotonin transporter gene status predicts caudate nucleus but not amygdala or hippocampal volumes in older persons with major depression. J Affect Disord 98, 137-142.

Hinz, R., Bhagwagar, Z., Cowen, P.J., Cunningham, V.J., Grasby, P.M., 2007. Validation of a tracer kinetic model for the quantification of 5-HT(2A) receptors in human brain with [(11)C]MDL 100,907. J Cereb Blood Flow Metab 27, 161-172.

Hinz, R., Murthy, V., Selvaraj, S., Taylor, M., Cowen, P.J., Bhagwagar, Z., Grasby, P.M., 2006. Changes of [^{11}C]DASB binding in human brain after citalopram infusion. . VIth International Symposium on Functional Neuroreceptor Mapping: NeuroReceptor Mapping 2006. . Neuroimage, Vol 31, (Suppl, 2). Copenhagen, Denmark., p. T26.

Hinz, R., Turkheimer, F.E., 2006. Determination of tracer arrival delay with spectral analysis. Ieee Transactions on Nuclear Science 53, 212-219.

Hirvonen, J., Karlsson, H., Kajander, J., Lepola, A., Markkula, J., Rasi-Hakala, H., Nagren, K., Salminen, J.K., Hietala, J., 2008. Decreased brain serotonin 5-HT1A receptor availability in medication-naive patients with major depressive disorder: an in-vivo imaging study using PET and [carbonyl-11C]WAY-100635. Int J Neuropsychopharmacol 11, 465-476.

Hornung, J.P., 2003. The human raphe nuclei and the serotonergic system. J Chem Neuroanat 26, 331-343.

Houle, S., Ginovart, N., Hussey, D., Meyer, J.H., Wilson, A.A., 2000. Imaging the serotonin transporter with positron emission tomography: initial human

studies with [11C]DAPP and [11C]DASB. Eur J Nucl Med 27, 1719-1722.

Hoyer, D., Hannon, J.P., Martin, G.R., 2002. Molecular, pharmacological and functional diversity of 5-HT receptors. Pharmacol Biochem Behav 71, 533-554.

Hrdina, P.D., Demeter, E., Vu, T.B., Sotonyi, P., Palkovits, M., 1993. 5-HT uptake sites and 5-HT2 receptors in brain of antidepressant-free suicide victims/depressives: increase in 5-HT2 sites in cortex and amygdala. Brain Res 614, 37-44.

Hu, X., Oroszi, G., Chun, J., Smith, T.L., Goldman, D., Schuckit, M.A., 2005. An expanded evaluation of the relationship of four alleles to the level of response to alcohol and the alcoholism risk. Alcohol Clin Exp Res 29, 8-16.

Hu, X.Z., Lipsky, R.H., Zhu, G., Akhtar, L.A., Taubman, J., Greenberg, B.D., Xu, K., Arnold, P.D., Richter, M.A., Kennedy, J.L., Murphy, D.L., Goldman, D., 2006. Serotonin transporter promoter gain-of-function genotypes are linked to obsessive-compulsive disorder. Am J Hum Genet 78, 815-826.

Huang, Y., Hwang, D.R., Narendran, R., Sudo, Y., Chatterjee, R., Bae, S.A., Mawlawi, O., Kegeles, L.S., Wilson, A.A., Kung, H.F., Laruelle, M., 2002. Comparative evaluation in nonhuman primates of five PET radiotracers for imaging the serotonin transporters: [11C]McN 5652, [11C]ADAM, [11C]DASB, [11C]DAPA, and [11C]AFM. J Cereb Blood Flow Metab 22, 1377-1398.

Hyttel, J., 1982. Citalopram--pharmacological profile of a specific serotonin uptake inhibitor with antidepressant activity. Prog Neuropsychopharmacol Biol Psychiatry 6, 277-295.

Ichimiya, T., Suhara, T., Sudo, Y., Okubo, Y., Nakayama, K., Nankai, M., Inoue, M., Yasuno, F., Takano, A., Maeda, J., Shibuya, H., 2002. Serotonin transporter binding in patients with mood disorders: a PET study with [11C](+)McN5652. Biol Psychiatry 51, 715-722.

Ichise, M., Ballinger, J.R., 1996. From graphical analysis to multilinear regression analysis of reversible radioligand binding. J Cereb Blood Flow Metab 16, 750-752.

Ichise, M., Liow, J.S., Lu, J.Q., Takano, A., Model, K., Toyama, H., Suhara, T., Suzuki, K., Innis, R.B., Carson, R.E., 2003. Linearized reference tissue parametric imaging methods: application to [11C]DASB positron emission

tomography studies of the serotonin transporter in human brain. J Cereb Blood Flow Metab 23, 1096-1112.

Ikoma, Y., Suhara, T., Toyama, H., Ichimiya, T., Takano, A., Sudo, Y., Inoue, M., Yasuno, F., Suzuki, K., 2002. Quantitative analysis for estimating binding potential of the brain serotonin transporter with [11 C]McN5652. J Cereb Blood Flow Metab 22, 490-501.

Innis, R.B., Cunningham, V.J., Delforge, J., Fujita, M., Gjedde, A., Gunn, R.N., Holden, J., Houle, S., Huang, S.C., Ichise, M., Iida, H., Ito, H., Kimura, Y., Koeppe, R.A., Knudsen, G.M., Knuuti, J., Lammertsma, A.A., Laruelle, M., Logan, J., Maguire, R.P., Mintun, M.A., Morris, E.D., Parsey, R., Price, J.C., Slifstein, M., Sossi, V., Suhara, T., Votaw, J.R., Wong, D.F., Carson, R.E., 2007. Consensus nomenclature for in vivo imaging of reversibly binding radioligands. J Cereb Blood Flow Metab 27, 1533-1539.

Jacobsen, L.K., Staley, J.K., Zoghbi, S.S., Seibyl, J.P., Kosten, T.R., Innis, R.B., Gelernter, J., 2000. Prediction of dopamine transporter binding availability by genotype: a preliminary report. Am J Psychiatry 157, 1700-1703.

Jedema, H.P., Gianaros, P.J., Greer, P.J., Kerr, D.D., Liu, S., Higley, J.D., Suomi, S.J., Olsen, A.S., Porter, J.N., Lopresti, B.J., Hariri, A.R., Bradberry, C.W., 2010. Cognitive impact of genetic variation of the serotonin transporter in primates is associated with differences in brain morphology rather than serotonin neurotransmission. Mol Psychiatry 15, 512-522, 446.

Jenkinson, M., Bannister, P., Brady, M., Smith, S., 2002. Improved optimization for the robust and accurate linear registration and motion correction of brain images. Neuroimage 17, 825-841.

Jenkinson, M., Smith, S., 2001. A global optimisation method for robust affine registration of brain images. Med Image Anal 5, 143-156.

Joensuu, M., Tolmunen, T., Saarinen, P.I., Tiihonen, J., Kuikka, J., Ahola, P., Vanninen, R., Lehtonen, J., 2007. Reduced midbrain serotonin transporter availability in drug-naive patients with depression measured by SERT-specific [(123)I] nor-beta-CIT SPECT imaging. Psychiatry Res 154, 125-131.

Joyce, J.N., Shane, A., Lexow, N., Winokur, A., Casanova, M.F., Kleinman, J.E., 1993. Serotonin uptake sites and serotonin receptors are altered in the limbic system of schizophrenics. Neuropsychopharmacology 8, 315-336.

Kalbitzer, J., Erritzoe, D., Holst, K.K., Nielsen, F.A., Marner, L., Lehel, S., Arentzen, T., Jernigan, T.L., Knudsen, G.M., 2010. Seasonal Changes in Brain Serotonin Transporter Binding in Short Serotonin Transporter Linked Polymorphic Region-Allele Carriers but Not in Long-Allele Homozygotes. Biol Psychiatry.

Kapitany, T., Schindl, M., Schindler, S.D., Hesselmann, B., Fureder, T., Barnas, C., Sieghart, W., Kasper, S., 1999. The citalopram challenge test in patients with major depression and in healthy controls. Psychiatry Res 88, 75-88.

Keller, M.B., Lavori, P.W., Mueller, T.I., Endicott, J., Coryell, W., Hirschfeld, R.M., Shea, T., 1992. Time to recovery, chronicity, and levels of psychopathology in major depression. A 5-year prospective follow-up of 431 subjects. Arch Gen Psychiatry 49, 809-816.

Kendler, K.S., Gatz, M., Gardner, C.O., Pedersen, N.L., 2006a. A Swedish national twin study of lifetime major depression. Am J Psychiatry 163, 109-114.

Kendler, K.S., Gatz, M., Gardner, C.O., Pedersen, N.L., 2006b. Personality and major depression: a Swedish longitudinal, population-based twin study. Arch Gen Psychiatry 63, 1113-1120.

Kendler, K.S., Karkowski, L.M., Prescott, C.A., 1999. Causal relationship between stressful life events and the onset of major depression. Am J Psychiatry 156, 837-841.

Kendler, K.S., Prescott, C.A., 1999. A population-based twin study of lifetime major depression in men and women. Arch Gen Psychiatry 56, 39-44.

Kendler, K.S., Thornton, L.M., Gardner, C.O., 2001. Genetic risk, number of previous depressive episodes, and stressful life events in predicting onset of major depression. Am J Psychiatry 158, 582-586.

Kent, J.M., Coplan, J.D., Lombardo, I., Hwang, D.R., Huang, Y., Mawlawi, O., Van Heertum, R.L., Slifstein, M., Abi-Dargham, A., Gorman, J.M., Laruelle, M., 2002. Occupancy of brain serotonin transporters during treatment with paroxetine in patients with social phobia: a positron emission tomography study with 11C McN 5652. Psychopharmacology (Berl) 164, 341-348.

Kessler, R.C., 1997. The effects of stressful life events on depression. Annu Rev Psychol 48, 191-214.

Kessler, R.C., Berglund, P., Demler, O., Jin, R., Koretz, D., Merikangas, K.R., Rush, A.J., Walters, E.E., Wang, P.S., 2003. The epidemiology of major depressive disorder: results from the National Comorbidity Survey Replication (NCS-R). JAMA 289, 3095-3105.

Kessler, R.C., Berglund, P., Demler, O., Jin, R., Merikangas, K.R., Walters, E.E., 2005. Lifetime prevalence and age-of-onset distributions of DSM-IV disorders in the National Comorbidity Survey Replication. Arch Gen Psychiatry 62, 593-602.

Kim, D.Y., Camilleri, M., 2000. Serotonin: a mediator of the brain-gut connection. Am J Gastroenterol 95, 2698-2709.

Kim, J.S., Ichise, M., Sangare, J., Innis, R.B., 2006. PET imaging of serotonin transporters with [11C]DASB: test-retest reproducibility using a multilinear reference tissue parametric imaging method. J Nucl Med 47, 208-214.

Kinahan, P.E., Rogers, J.G., 1989. Analytic 3d Image-Reconstruction Using All Detected Events. Ieee Transactions on Nuclear Science 36, 964-968.

Kish, S.J., Furukawa, Y., Chang, L.J., Tong, J., Ginovart, N., Wilson, A., Houle, S., Meyer, J.H., 2005. Regional distribution of serotonin transporter protein in postmortem human brain: is the cerebellum a SERT-free brain region? Nucl Med Biol 32, 123-128.

Klimek, V., Roberson, G., Stockmeier, C.A., Ordway, G.A., 2003. Serotonin transporter and MAO-B levels in monoamine nuclei of the human brainstem are normal in major depression. J Psychiatr Res 37, 387-397.

Kraft, J.B., Peters, E.J., Slager, S.L., Jenkins, G.D., Reinalda, M.S., McGrath, P.J., Hamilton, S.P., 2007. Analysis of association between the serotonin transporter and antidepressant response in a large clinical sample. Biol Psychiatry 61, 734-742.

Kretzschmar, M., Brust, P., Zessin, J., Cumming, P., Bergmann, R., Johannsen, B., 2003. Autoradiographic imaging of the serotonin transporter in the brain of rats and pigs using S-([18F]fluoromethyl)-(+)-McN5652. Eur Neuropsychopharmacol 13, 387-397.

Lammertsma, A.A., Hume, S.P., 1996. Simplified reference tissue model for PET receptor studies. Neuroimage 4, 153-158.

Lapin, I.P., Oxenkrug, G.F., 1969. Intensification of the central serotoninergic processes as a possible determinant of the thymoleptic effect. Lancet 1, 132-136.

Larisch, R., Klimke, A., Mayoral, F., Hamacher, K., Herzog, H.R., Vosberg, H., Tosch, M., Gaebel, W., Rivas, F., Coenen, H.H., Muller-Gartner, H.W., 2001. Disturbance of serotonin 5HT2 receptors in remitted patients suffering from hereditary depressive disorder. Nuklearmedizin 40, 129-134.

Laruelle, M., 2000. Imaging synaptic neurotransmission with in vivo binding competition techniques: a critical review. J Cereb Blood Flow Metab 20, 423-451.

Laruelle, M., Abi-Dargham, A., Casanova, M.F., Toti, R., Weinberger, D.R., Kleinman, J.E., 1993a. Selective abnormalities of prefrontal serotonergic receptors in schizophrenia. A postmortem study. Arch Gen Psychiatry 50, 810-818.

Laruelle, M., Baldwin, R.M., Malison, R.T., Zea-Ponce, Y., Zoghbi, S.S., al-Tikriti, M.S., Sybirska, E.H., Zimmermann, R.C., Wisniewski, G., Neumeyer, J.L., et al., 1993b. SPECT imaging of dopamine and serotonin transporters with [123I]beta-CIT: pharmacological characterization of brain uptake in nonhuman primates. Synapse 13, 295-309.

Laruelle, M., Giddings, S.S., Zea-Ponce, Y., Charney, D.S., Neumeyer, J.L., Baldwin, R.M., Innis, R.B., 1994. Methyl 3 beta-(4-[125I]iodophenyl)tropane-2 beta-carboxylate in vitro binding to dopamine and serotonin transporters under "physiological" conditions. J Neurochem 62, 978-986.

Laruelle, M., Slifstein, M., Huang, Y., 2002. Positron emission tomography: imaging and quantification of neurotransporter availability. Methods 27, 287-299.

Laruelle, M., Vanisberg, M.A., Maloteaux, J.M., 1988. Regional and subcellular localization in human brain of [3H]paroxetine binding, a marker of serotonin uptake sites. Biol Psychiatry 24, 299-309.

Lassen, N.A., Bartenstein, P.A., Lammertsma, A.A., Prevett, M.C., Turton, D.R., Luthra, S.K., Osman, S., Bloomfield, P.M., Jones, T., Patsalos, P.N., et al., 1995. Benzodiazepine receptor quantification in vivo in humans using [11C]flumazenil and PET: application of the steady-state principle. J Cereb Blood Flow Metab 15, 152-165.

Lawrence, K.M., De Paermentier, F., Cheetham, S.C., Crompton, M.R., Katona, C.L., Horton, R.W., 1990. Brain 5-HT uptake sites, labelled with [3H]paroxetine, in antidepressant-free depressed suicides. Brain Res 526, 17-22.

Leake, A., Fairbairn, A.F., McKeith, I.G., Ferrier, I.N., 1991. Studies on the serotonin uptake binding site in major depressive disorder and control post-mortem brain: neurochemical and clinical correlates. Psychiatry Res 39, 155-165.

Lehto, S., Tolmunen, T., Joensuu, M., Saarinen, P.I., Vanninen, R., Ahola, P., Tiihonen, J., Kuikka, J., Lehtonen, J., 2006. Midbrain binding of [123I]nor-beta-CIT in atypical depression. Prog Neuropsychopharmacol Biol Psychiatry 30, 1251-1255.

Lesch, K.P., Bengel, D., Heils, A., Sabol, S.Z., Greenberg, B.D., Petri, S., Benjamin, J., Muller, C.R., Hamer, D.H., Murphy, D.L., 1996. Association of anxiety-related traits with a polymorphism in the serotonin transporter gene regulatory region. Science 274, 1527-1531.

Lesch, K.P., Wolozin, B.L., Murphy, D.L., Reiderer, P., 1993. Primary structure of the human platelet serotonin uptake site: identity with the brain serotonin transporter. J Neurochem 60, 2319-2322.

Little, K.Y., McLaughlin, D.P., Zhang, L., Livermore, C.S., Dalack, G.W., McFinton, P.R., DelProposto, Z.S., Hill, E., Cassin, B.J., Watson, S.J., Cook, E.H., 1998. Cocaine, ethanol, and genotype effects on human midbrain serotonin transporter binding sites and mRNA levels. Am J Psychiatry 155, 207-213.

Little, K.Y., McLauglin, D.P., Ranc, J., Gilmore, J., Lopez, J.F., Watson, S.J., Carroll, F.I., Butts, J.D., 1997. Serotonin transporter binding sites and mRNA levels in depressed persons committing suicide. Biol Psychiatry 41, 1156-1164.

Logan, J., Fowler, J.S., Volkow, N.D., Wang, G.J., Ding, Y.S., Alexoff, D.L., 1996. Distribution volume ratios without blood sampling from graphical analysis of PET data. J Cereb Blood Flow Metab 16, 834-840.

Logan, J., Fowler, J.S., Volkow, N.D., Wolf, A.P., Dewey, S.L., Schlyer, D.J., MacGregor, R.R., Hitzemann, R., Bendriem, B., Gatley, S.J., et al., 1990. Graphical analysis of reversible radioligand binding from time-activity measurements applied to [N-11C-methyl]-(-)-cocaine PET studies in human subjects. J Cereb Blood Flow Metab 10, 740-747.

Lotrich, F.E., Bies, R., Muldoon, M.F., Manuck, S.B., Smith, G.S., Pollock, B.G., 2005. Neuroendocrine response to intravenous citalopram in healthy control subjects: pharmacokinetic influences. Psychopharmacology (Berl) 178, 268-275.

Lowther, S., De Paermentier, F., Cheetham, S.C., Crompton, M.R., Katona, C.L., Horton, R.W., 1997. 5-HT1A receptor binding sites in post-mortem brain samples from depressed suicides and controls. J Affect Disord 42, 199-207.

Lu, J.Q., Ichise, M., Liow, J.S., Ghose, S., Vines, D., Innis, R.B., 2004. Biodistribution and radiation dosimetry of the serotonin transporter ligand 11C-DASB determined from human whole-body PET. J Nucl Med 45, 1555-1559.

Lundberg, J., Halldin, C., Farde, L., 2006. Measurement of serotonin transporter binding with PET and [11C]MADAM: a test-retest reproducibility study. Synapse 60, 256-263.

Luthra, S.K., Osman, S., Turton, D.R., Vaja, V., Dowsett, K., Brady, F., 1993. An automated system based on solid phase extraction and HPLC for the routine determination in plasma of unchanged [11C]-L-deprenyl; [11C]diprenrophine; [11C]flumazenil; [11C]raclopride; and [11C]Scherring 23390. . J Lab Comp Radiopharm. 32, 518 - 520.

Maj, M., Veltro, F., Pirozzi, R., Lobrace, S., Magliano, L., 1992. Pattern of recurrence of illness after recovery from an episode of major depression: a prospective study. Am J Psychiatry 149, 795-800.

Malison, R.T., Price, L.H., Berman, R., van Dyck, C.H., Pelton, G.H., Carpenter, L., Sanacora, G., Owens, M.J., Nemeroff, C.B., Rajeevan, N., Baldwin, R.M., Seibyl, J.P., Innis, R.B., Charney, D.S., 1998. Reduced brain serotonin transporter availability in major depression as measured by [123I]-2 beta-carbomethoxy-3 beta-(4-iodophenyl)tropane and single photon emission computed tomography. Biol Psychiatry 44, 1090-1098.

Malizia, A.L., Melichar, J.M., Brown, D.J., Gunn, R.N., Reynolds, A., Jones, T., Nutt, D.J., 1997. Demonstration of clomipramine and venlafaxine occupation at serotonin reuptake sites in man in vivo. J Psychopharmacol 11, 279-281.

Mann, J.J., Huang, Y.Y., Underwood, M.D., Kassir, S.A., Oppenheim, S., Kelly, T.M., Dwork, A.J., Arango, V., 2000. A serotonin transporter gene promoter polymorphism (5-HTTLPR) and prefrontal cortical binding in major depression and suicide. Arch Gen Psychiatry 57, 729-738.

Mann, J.J., Stanley, M., McBride, P.A., McEwen, B.S., 1986. Increased serotonin2 and beta-adrenergic receptor binding in the frontal cortices of suicide victims. Arch Gen Psychiatry 43, 954-959.

Marcusson, J.O., Ross, S.B., 1990. Binding of some antidepressants to the 5-hydroxytryptamine transporter in brain and platelets. Psychopharmacology (Berl) 102, 145-155.

Matsubara, S., Arora, R.C., Meltzer, H.Y., 1991. Serotonergic measures in suicide brain: 5-HT1A binding sites in frontal cortex of suicide victims. J Neural Transm Gen Sect 85, 181-194.

Mechelli, A., Price, C.J., Friston, K.J., Ashburner, J., 2005. Voxel-based morphometry of the human brain: Methods and applications. Current Medical Imaging Reviews 1, 105-113.

Medical Research Council, 1965. Report by its Clinical Committee: clinical trial of the treatment of depressive illness. Br Med J 1965;i:881-6.

Meltzer, C.C., Price, J.C., Mathis, C.A., Butters, M.A., Ziolko, S.K., Moses-Kolko, E., Mazumdar, S., Mulsant, B.H., Houck, P.R., Lopresti, B.J., Weissfeld, L.A., Reynolds, C.F., 2004. Serotonin 1A receptor binding and treatment response in late-life depression. Neuropsychopharmacology 29, 2258-2265.

Meltzer, C.C., Price, J.C., Mathis, C.A., Greer, P.J., Cantwell, M.N., Houck, P.R., Mulsant, B.H., Ben-Eliezer, D., Lopresti, B., DeKosky, S.T., Reynolds, C.F., 3rd, 1999. PET imaging of serotonin type 2A receptors in late-life neuropsychiatric disorders. Am J Psychiatry 156, 1871-1878.

Meltzer, H.Y., Arora, R.C., Baber, R., Tricou, B.J., 1981. Serotonin uptake in blood platelets of psychiatric patients. Arch Gen Psychiatry 38, 1322-1326.

Messa, C., Colombo, C., Moresco, R.M., Gobbo, C., Galli, L., Lucignani, G., Gilardi, M.C., Rizzo, G., Smeraldi, E., Zanardi, R., Artigas, F., Fazio, F., 2003. 5-HT(2A) receptor binding is reduced in drug-naive and unchanged in SSRI-responder depressed patients compared to healthy controls: a PET study. Psychopharmacology (Berl) 167, 72-78.

Meyer, J.H., 2007. Imaging the serotonin transporter during major depressive disorder and antidepressant treatment. J Psychiatry Neurosci 32, 86-102.

Meyer, J.H., Houle, S., Sagrati, S., Carella, A., Hussey, D.F., Ginovart, N., Goulding, V., Kennedy, J., Wilson, A.A., 2004a. Brain serotonin transporter binding potential measured with carbon 11-labeled DASB positron emission tomography: effects of major depressive episodes and severity of dysfunctional attitudes. Arch Gen Psychiatry 61, 1271-1279.

Meyer, J.H., Kapur, S., Houle, S., DaSilva, J., Owczarek, B., Brown, G.M., Wilson, A.A., Kennedy, S.H., 1999. Prefrontal cortex 5-HT2 receptors in depression: an [18F]setoperone PET imaging study. Am J Psychiatry 156, 1029-1034.

Meyer, J.H., McMain, S., Kennedy, S.H., Korman, L., Brown, G.M., DaSilva, J.N., Wilson, A.A., Blak, T., Eynan-Harvey, R., Goulding, V.S., Houle, S., Links, P., 2003. Dysfunctional attitudes and 5-HT2 receptors during depression and self-harm. Am J Psychiatry 160, 90-99.

Meyer, J.H., Wilson, A.A., Ginovart, N., Goulding, V., Hussey, D., Hood, K., Houle, S., 2001. Occupancy of serotonin transporters by paroxetine and citalopram during treatment of depression: a [(11)C]DASB PET imaging study. Am J Psychiatry 158, 1843-1849.

Meyer, J.H., Wilson, A.A., Sagrati, S., Hussey, D., Carella, A., Potter, W.Z., Ginovart, N., Spencer, E.P., Cheok, A., Houle, S., 2004b. Serotonin transporter occupancy of five selective serotonin reuptake inhibitors at different doses: an [11C]DASB positron emission tomography study. Am J Psychiatry 161, 826-835.

Milak, M.S., Severance, A.J., Prabhakaran, J., Kumar, J.S., Majo, V.J., Ogden, R.T., Mann, J.J., Parsey, R.V., 2010. In vivo serotonin-sensitive binding of [(11)C]CUMI-101: a serotonin 1A receptor agonist positron emission tomography radiotracer. J Cereb Blood Flow Metab.

Miller, J.M., Brennan, K.G., Ogden, T.R., Oquendo, M.A., Sullivan, G.M., Mann, J.J., Parsey, R.V., 2009. Elevated serotonin 1A binding in remitted major depressive disorder: evidence for a trait biological abnormality. Neuropsychopharmacology 34, 2275-2284.

Mintun, M.A., Raichle, M.E., Kilbourn, M.R., Wooten, G.F., Welch, M.J., 1984. A quantitative model for the in vivo assessment of drug binding sites with positron emission tomography. Ann Neurol 15, 217-227.

Mintun, M.A., Sheline, Y.I., Moerlein, S.M., Vlassenko, A.G., Huang, Y., Snyder,

A.Z., 2004. Decreased hippocampal 5-HT2A receptor binding in major depressive disorder: in vivo measurement with [18F]altanserin positron emission tomography. Biol Psychiatry 55, 217-224.

Mueller, T.I., Leon, A.C., 1996. Recovery, chronicity, and levels of psychopathology in major depression. Psychiatr Clin North Am 19, 85-102.

Munafo, M.R., Brown, S.M., Hariri, A.R., 2007. Serotonin Transporter (5-HTTLPR) Genotype and Amygdala Activation: A Meta-Analysis. Biol Psychiatry.

Munafo, M.R., Brown, S.M., Hariri, A.R., 2008. Serotonin transporter (5-HTTLPR) genotype and amygdala activation: a meta-analysis. Biol Psychiatry 63, 852-857.

Munafo, M.R., Durrant, C., Lewis, G., Flint, J., 2009. Gene X environment interactions at the serotonin transporter locus. Biol Psychiatry 65, 211-219.

Murphy, J.M., Laird, N.M., Monson, R.R., Sobol, A.M., Leighton, A.H., 2000. A 40-year perspective on the prevalence of depression: the Stirling County Study. Arch Gen Psychiatry 57, 209-215.

Murray, C.J., Lopez, A.D., 1997. Global mortality, disability, and the contribution of risk factors: Global Burden of Disease Study. Lancet 349, 1436-1442.

Nelson, L.D., Stern, S.L., Cicchetti, D.V., 1992. The Dysfunctional Attitude Scale - How Well Can It Measure Depressive Thinking. Journal of Psychopathology and Behavioral Assessment 14, 217-223.

Neumeister, A., Bain, E., Nugent, A.C., Carson, R.E., Bonne, O., Luckenbaugh, D.A., Eckelman, W., Herscovitch, P., Charney, D.S., Drevets, W.C., 2004. Reduced serotonin type 1A receptor binding in panic disorder. J Neurosci 24, 589-591.

Newberg, A.B., Amsterdam, J.D., Wintering, N., Ploessl, K., Swanson, R.L., Shults, J., Alavi, A., 2005. 123I-ADAM binding to serotonin transporters in patients with major depression and healthy controls: a preliminary study. J Nucl Med 46, 973-977.

NICE, 2004. Depression: management of depression in primary and secondary care - NICE guidance.

NICE, Guidelines, 2009. Depression: the treatment and management of depression in adults (update). Clinical Guidelines CG 90.

Ninan, P.T., van Kammen, D.P., Scheinin, M., Linnoila, M., Bunney, W.E., Jr., Goodwin, F.K., 1984. CSF 5-hydroxyindoleacetic acid levels in suicidal schizophrenic patients. Am J Psychiatry 141, 566-569.

O'Hara, R., Schroder, C.M., Mahadevan, R., Schatzberg, A.F., Lindley, S., Fox, S., Weiner, M., Kraemer, H.C., Noda, A., Lin, X., Gray, H.L., Hallmayer, J.F., 2007. Serotonin transporter polymorphism, memory and hippocampal volume in the elderly: association and interaction with cortisol. Mol Psychiatry 12, 544-555.

Ogden, R.T., Ojha, A., Erlandsson, K., Oquendo, M.A., Mann, J.J., Parsey, R.V., 2007. In vivo quantification of serotonin transporters using [(11)C]DASB and positron emission tomography in humans: modeling considerations. J Cereb Blood Flow Metab 27, 205-217.

Oquendo, M.A., Hastings, R.S., Huang, Y.Y., Simpson, N., Ogden, R.T., Hu, X.Z., Goldman, D., Arango, V., Van Heertum, R.L., Mann, J.J., Parsey, R.V., 2007. Brain serotonin transporter binding in depressed patients with bipolar disorder using positron emission tomography. Arch Gen Psychiatry 64, 201-208.

Owen, F., Chambers, D.R., Cooper, S.J., Crow, T.J., Johnson, J.A., Lofthouse, R., Poulter, M., 1986. Serotonergic mechanisms in brains of suicide victims. Brain Res 362, 185-188.

Owens, M.J., Nemeroff, C.B., 1994. Role of serotonin in the pathophysiology of depression: focus on the serotonin transporter. Clin Chem 40, 288-295.

Pacheco, J., Beevers, C.G., Benavides, C., McGeary, J., Stice, E., Schnyer, D.M., 2009. Frontal-limbic white matter pathway associations with the serotonin transporter gene promoter region (5-HTTLPR) polymorphism. J Neurosci 29, 6229-6233.

Parsey, R.V., Hastings, R.S., Oquendo, M.A., Hu, X., Goldman, D., Huang, Y.Y., Simpson, N., Arcement, J., Huang, Y., Ogden, R.T., Van Heertum, R.L., Arango, V., Mann, J.J., 2006a. Effect of a triallelic functional polymorphism of the serotonin-transporter-linked promoter region on expression of serotonin transporter in the human brain. Am J Psychiatry 163, 48-51.

Parsey, R.V., Hastings, R.S., Oquendo, M.A., Huang, Y.Y., Simpson, N., Arcement, J., Huang, Y., Ogden, R.T., Van Heertum, R.L., Arango, V., Mann, J.J., 2006b. Lower serotonin transporter binding potential in the human brain during major depressive episodes. Am J Psychiatry 163, 52-58.

Parsey, R.V., Kegeles, L.S., Hwang, D.R., Simpson, N., Abi-Dargham, A., Mawlawi, O., Slifstein, M., Van Heertum, R.L., Mann, J.J., Laruelle, M., 2000. In vivo quantification of brain serotonin transporters in humans using [11C]McN 5652. J Nucl Med 41, 1465-1477.

Parsey, R.V., Kent, J.M., Oquendo, M.A., Richards, M.C., Pratap, M., Cooper, T.B., Arango, V., Mann, J.J., 2006c. Acute occupancy of brain serotonin transporter by sertraline as measured by [11C]DASB and positron emission tomography. Biol Psychiatry 59, 821-828.

Parsey, R.V., Ogden, R.T., Mann, J.J., 2003. Determination of volume of distribution using likelihood estimation in graphical analysis: elimination of estimation bias. J Cereb Blood Flow Metab 23, 1471-1478.

Parsey, R.V., Oquendo, M.A., Ogden, R.T., Olvet, D.M., Simpson, N., Huang, Y.Y., Van Heertum, R.L., Arango, V., Mann, J.J., 2006d. Altered serotonin 1A binding in major depression: a [carbonyl-C-11]WAY100635 positron emission tomography study. Biol Psychiatry 59, 106-113.

Paul, S.M., Rehavi, M., Skolnick, P., Ballenger, J.C., Goodwin, F.K., 1981. Depressed patients have decreased binding of tritiated imipramine to platelet serotonin "transporter". Arch Gen Psychiatry 38, 1315-1317.

Paykel, E.S., 2000. Not an age of depression after all? Incidence rates may be stable over time. Psychol Med 30, 489-490.

Perry, E.K., Marshall, E.F., Blessed, G., Tomlinson, B.E., Perry, R.H., 1983. Decreased imipramine binding in the brains of patients with depressive illness. Br J Psychiatry 142, 188-192.

Pezawas, L., Meyer-Lindenberg, A., Drabant, E.M., Verchinski, B.A., Munoz, K.E., Kolachana, B.S., Egan, M.F., Mattay, V.S., Hariri, A.R., Weinberger, D.R., 2005. 5-HTTLPR polymorphism impacts human cingulate-amygdala interactions: a genetic susceptibility mechanism for depression. Nat Neurosci 8, 828-834.

Pezawas, L., Meyer-Lindenberg, A., Goldman, A.L., Verchinski, B.A., Chen, G., Kolachana, B.S., Egan, M.F., Mattay, V.S., Hariri, A.R., Weinberger, D.R., 2008. Evidence of biologic epistasis between BDNF and SLC6A4 and implications for depression. Mol Psychiatry 13, 709-716.

Piccinelli, M., Wilkinson, G., 1994. Outcome of depression in psychiatric settings. Br J Psychiatry 164, 297-304.

Piccinelli, M., Wilkinson, G., 2000. Gender differences in depression. Critical review. Br J Psychiatry 177, 486-492.

Pike, V.W., 2009. PET radiotracers: crossing the blood-brain barrier and surviving metabolism. Trends Pharmacol Sci 30, 431-440.

Praschak-Rieder, N., Kennedy, J., Wilson, A.A., Hussey, D., Boovariwala, A., Willeit, M., Ginovart, N., Tharmalingam, S., Masellis, M., Houle, S., Meyer, J.H., 2007. Novel 5-HTTLPR allele associates with higher serotonin transporter binding in putamen: a [(11)C] DASB positron emission tomography study. Biol Psychiatry 62, 327-331.

Praschak-Rieder, N., Wilson, A.A., Hussey, D., Carella, A., Wei, C., Ginovart, N., Schwarz, M.J., Zach, J., Houle, S., Meyer, J.H., 2005. Effects of tryptophan depletion on the serotonin transporter in healthy humans. Biol Psychiatry 58, 825-830.

Ramamoorthy, S., Bauman, A.L., Moore, K.R., Han, H., Yang-Feng, T., Chang, A.S., Ganapathy, V., Blakely, R.D., 1993. Antidepressant- and cocaine-sensitive human serotonin transporter: molecular cloning, expression, and chromosomal localization. Proc Natl Acad Sci U S A 90, 2542-2546.

Ramamoorthy, S., Blakely, R.D., 1999. Phosphorylation and sequestration of serotonin transporters differentially modulated by psychostimulants. Science 285, 763-766.

Ranicar, A.S., Williams, C.W., Schnorr, L., Clark, J.C., Rhodes, C.G., Bloomfield, P.M., Jones, T., 1991. The on-line monitoring of continuously withdrawn arterial blood during PET studies using a single BGO/photomultiplier assembly and non-stick tubing. Med Prog Technol 17, 259-264.

Rao, H., Gillihan, S.J., Wang, J., Korczykowski, M., Sankoorikal, G.M., Kaercher, K.A., Brodkin, E.S., Detre, J.A., Farah, M.J., 2007. Genetic variation

in serotonin transporter alters resting brain function in healthy individuals. Biol Psychiatry 62, 600-606.

Rapport, M.M., Green, A.A., Page, I.H., 1948a. Crystalline Serotonin. Science 108, 329-330.

Rapport, M.M., Green, A.A., Page, I.H., 1948b. Partial Purification of the Vasoconstrictor in Beef Serum. Journal of Biological Chemistry 174, 735-741.

Reimold, M., Batra, A., Knobel, A., Smolka, M.N., Zimmer, A., Mann, K., Solbach, C., Reischl, G., Schwarzler, F., Grunder, G., Machulla, H.J., Bares, R., Heinz, A., 2008. Anxiety is associated with reduced central serotonin transporter availability in unmedicated patients with unipolar major depression: a [11C]DASB PET study. Mol Psychiatry 13, 606-613, 557.

Reimold, M., Smolka, M.N., Schumann, G., Zimmer, A., Wrase, J., Mann, K., Hu, X.Z., Goldman, D., Reischl, G., Solbach, C., Machulla, H.J., Bares, R., Heinz, A., 2007. Midbrain serotonin transporter binding potential measured with [11C]DASB is affected by serotonin transporter genotype. J Neural Transm 114, 635-639.

Reivich, M., Amsterdam, J.D., Brunswick, D.J., Shiue, C.Y., 2004. PET brain imaging with [11C](+)McN5652 shows increased serotonin transporter availability in major depression. J Affect Disord 82, 321-327.

Rhodes, R.A., Murthy, N.V., Dresner, M.A., Selvaraj, S., Stavrakakis, N., Babar, S., Cowen, P.J., Grasby, P.M., 2007. Human 5-HT transporter availability predicts amygdala reactivity in vivo. J Neurosci 27, 9233-9237.

Riccio, O., Potter, G., Walzer, C., Vallet, P., Szabo, G., Vutskits, L., Kiss, J.Z., Dayer, A.G., 2009. Excess of serotonin affects embryonic interneuron migration through activation of the serotonin receptor 6. Mol Psychiatry 14, 280-290.

Riffkin, J., Yucel, M., Maruff, P., Wood, S.J., Soulsby, B., Olver, J., Kyrios, M., Velakoulis, D., Pantelis, C., 2005. A manual and automated MRI study of anterior cingulate and orbito-frontal cortices, and caudate nucleus in obsessive-compulsive disorder: comparison with healthy controls and patients with schizophrenia. Psychiatry Res 138, 99-113.

Risch, N., Herrell, R., Lehner, T., Liang, K.Y., Eaves, L., Hoh, J., Griem, A., Kovacs, M., Ott, J., Merikangas, K.R., 2009. Interaction between the serotonin

transporter gene (5-HTTLPR), stressful life events, and risk of depression: a meta-analysis. JAMA 301, 2462-2471.

Robins, L.N., Helzer, J.E., Weissman, M.M., Orvaschel, H., Gruenberg, E., Burke, J.D., Jr., Regier, D.A., 1984. Lifetime prevalence of specific psychiatric disorders in three sites. Arch Gen Psychiatry 41, 949-958.

Rochat, B., Baumann, P., Audus, K.L., 1999. Transport mechanisms for the antidepressant citalopram in brain microvessel endothelium. Brain Res 831, 229-236.

Roiser, J.P., Cook, L.J., Cooper, J.D., Rubinsztein, D.C., Sahakian, B.J., 2005. Association of a functional polymorphism in the serotonin transporter gene with abnormal emotional processing in ecstasy users. Am J Psychiatry 162, 609-612.

Rosel, P., Arranz, B., San, L., Vallejo, J., Crespo, J.M., Urretavizcaya, M., Navarro, M.A., 2000. Altered 5-HT(2A) binding sites and second messenger inositol trisphosphate (IP(3)) levels in hippocampus but not in frontal cortex from depressed suicide victims. Psychiatry Res 99, 173-181.

Rueckert, D., Sonoda, L.I., Hayes, C., Hill, D.L., Leach, M.O., Hawkes, D.J., 1999. Nonrigid registration using free-form deformations: application to breast MR images. IEEE Trans Med Imaging 18, 712-721.

Ruhe, H.G., Booij, J., Reitsma, J.B., Schene, A.H., 2009. Serotonin transporter binding with [123I]beta-CIT SPECT in major depressive disorder versus controls: effect of season and gender. Eur J Nucl Med Mol Imaging 36, 841-849.

Santana, N., Bortolozzi, A., Serrats, J., Mengod, G., Artigas, F., 2004. Expression of serotonin1A and serotonin2A receptors in pyramidal and GABAergic neurons of the rat prefrontal cortex. Cereb Cortex 14, 1100-1109.

Sargent, P.A., Kjaer, K.H., Bench, C.J., Rabiner, E.A., Messa, C., Meyer, J., Gunn, R.N., Grasby, P.M., Cowen, P.J., 2000. Brain serotonin1A receptor binding measured by positron emission tomography with [11C]WAY-100635: effects of depression and antidepressant treatment. Arch Gen Psychiatry 57, 174-180.

Scherk, H., Gruber, O., Menzel, P., Schneider-Axmann, T., Kemmer, C., Usher,

J., Reith, W., Meyer, J., Falkai, P., 2009. 5-HTTLPR genotype influences amygdala volume. Eur Arch Psychiatry Clin Neurosci 259, 212-217.

Schildkraut, J.J., 1965. The catecholamine hypothesis of affective disorders: a review of supporting evidence. Am J Psychiatry 122, 509-522.

Schildkraut, J.J., Kety, S.S., 1967. Biogenic amines and emotion. Science 156, 21-37.

Schins, A., Van Kroonenburgh, M., Van Laere, K., D'Haenen, H., Lousberg, R., Crijns, H., Eersels, J., Honig, A., 2005. Increased cerebral serotonin-2A receptor binding in depressed patients with myocardial infarction. Psychiatry Res 139, 155-163.

Schneider, L.S., Lyness, S.A., 1995. Is platelet imipramine binding reduced in depression? A meta-analysis by Ellis and Salmond. Biol Psychiatry 38, 775-776.

Seidman, L.J., Valera, E.M., Makris, N., Monuteaux, M.C., Boriel, D.L., Kelkar, K., Kennedy, D.N., Caviness, V.S., Bush, G., Aleardi, M., Faraone, S.V., Biederman, J., 2006. Dorsolateral prefrontal and anterior cingulate cortex volumetric abnormalities in adults with attention-deficit/hyperactivity disorder identified by magnetic resonance imaging. Biol Psychiatry 60, 1071-1080.

Serretti, A., Kato, M., De Ronchi, D., Kinoshita, T., 2007. Meta-analysis of serotonin transporter gene promoter polymorphism (5-HTTLPR) association with selective serotonin reuptake inhibitor efficacy in depressed patients. Mol Psychiatry 12, 247-257.

Sheline, Y.I., Mintun, M.A., Barch, D.M., Wilkins, C., Snyder, A.Z., Moerlein, S.M., 2004. Decreased hippocampal 5-HT(2A) receptor binding in older depressed patients using [18F]altanserin positron emission tomography. Neuropsychopharmacology 29, 2235-2241.

Shioe, K., Ichimiya, T., Suhara, T., Takano, A., Sudo, Y., Yasuno, F., Hirano, M., Shinohara, M., Kagami, M., Okubo, Y., Nankai, M., Kanba, S., 2003. No association between genotype of the promoter region of serotonin transporter gene and serotonin transporter binding in human brain measured by PET. Synapse 48, 184-188.

Sibille, E., Lewis, D.A., 2006. SERT-ainly involved in depression, but when? Am

J Psychiatry 163, 8-11.

Sibon, I., Benkelfat, C., Gravel, P., Aznavour, N., Costes, N., Mzengeza, S., Booij, L., Baker, G., Soucy, J.P., Zimmer, L., Descarries, L., 2008. Decreased [18F]MPPF binding potential in the dorsal raphe nucleus after a single oral dose of fluoxetine: a positron-emission tomography study in healthy volunteers. Biol Psychiatry 63, 1135-1140.

Skre, I., Onstad, S., Torgersen, S., Kringlen, E., 1991. High interrater reliability for the Structured Clinical Interview for DSM-III-R Axis I (SCID-I). Acta Psychiatr Scand 84, 167-173.

Slifstein, M., Laruelle, M., 2000. Effects of statistical noise on graphic analysis of PET neuroreceptor studies. J Nucl Med 41, 2083-2088.

Smith, G.S., Kramer, E., Hermann, C.R., Goldberg, S., Ma, Y., Dhawan, V., Barnes, A., Chaly, T., Belakhleff, A., Laghrissi-Thode, F., Greenwald, B., Eidelberg, D., Pollock, B.G., 2002. Acute and chronic effects of citalopram on cerebral glucose metabolism in geriatric depression. Am J Geriatr Psychiatry 10, 715-723.

Smith, K.A., Fairburn, C.G., Cowen, P.J., 1997. Relapse of depression after rapid depletion of tryptophan. Lancet 349, 915-919.

Smith, S.M., 2002. Fast robust automated brain extraction. Hum Brain Mapp 17, 143-155.

Smith, S.M., Jenkinson, M., Woolrich, M.W., Beckmann, C.F., Behrens, T.E., Johansen-Berg, H., Bannister, P.R., De Luca, M., Drobnjak, I., Flitney, D.E., Niazy, R.K., Saunders, J., Vickers, J., Zhang, Y., De Stefano, N., Brady, J.M., Matthews, P.M., 2004. Advances in functional and structural MR image analysis and implementation as FSL. Neuroimage 23 Suppl 1, S208-219.

Snyder, S.H., Glowinski, J., Axelrod, J., 1965. The Storage of Norepinephrine and Some of Its Derivatives in Brain Synaptosomes. Life Sci 4, 797-807.

Sodhi, M.S., Sanders-Bush, E., 2004. Serotonin and brain development. Int Rev Neurobiol 59, 111-174.

Soucy, J.P., Lafaille, F., Lemoine, P., Mrini, A., Descarries, L., 1994. Validation of the transporter ligand cyanoimipramine as a marker of serotonin innervation

density in brain. J Nucl Med 35, 1822-1830.

Spinks, T.J., Jones, T., Bloomfield, P.M., Bailey, D.L., Miller, M., Hogg, D., Jones, W.F., Vaigneur, K., Reed, J., Young, J., Newport, D., Moyers, C., Casey, M.E., Nutt, R., 2000. Physical characteristics of the ECAT EXACT3D positron tomograph. Phys Med Biol 45, 2601-2618.

Spinks, T.J., Miller, M.P., Bailey, D.L., Bloomfield, P.M., Livieratos, L., Jones, T., 1998. The effect of activity outside the direct field of view in a 3D-only whole-body positron tomograph. Phys Med Biol 43, 895-904.

Stahl, S.M., 1977. The human platelet. A diagnostic and research tool for the study of biogenic amines in psychiatric and neurologic disorders. Arch Gen Psychiatry 34, 509-516.

Staley, J.K., Sanacora, G., Tamagnan, G., Maciejewski, P.K., Malison, R.T., Berman, R.M., Vythilingam, M., Kugaya, A., Baldwin, R.M., Seibyl, J.P., Charney, D., Innis, R.B., 2006. Sex differences in diencephalon serotonin transporter availability in major depression. Biol Psychiatry 59, 40-47.

Stanley, B., Molcho, A., Stanley, M., Winchel, R., Gameroff, M.J., Parsons, B., Mann, J.J., 2000. Association of aggressive behavior with altered serotonergic function in patients who are not suicidal. Am J Psychiatry 157, 609-614.

Stanley, M., Mann, J.J., 1983. Increased serotonin-2 binding sites in frontal cortex of suicide victims. Lancet 1, 214-216.

Stanley, M., Virgilio, J., Gershon, S., 1982. Tritiated imipramine binding sites are decreased in the frontal cortex of suicides. Science 216, 1337-1339.

Stockmeier, C.A., 2003. Involvement of serotonin in depression: evidence from postmortem and imaging studies of serotonin receptors and the serotonin transporter. J Psychiatr Res 37, 357-373.

Stockmeier, C.A., Dilley, G.E., Shapiro, L.A., Overholser, J.C., Thompson, P.A., Meltzer, H.Y., 1997. Serotonin receptors in suicide victims with major depression. Neuropsychopharmacology 16, 162-173.

Stockmeier, C.A., Shapiro, L.A., Dilley, G.E., Kolli, T.N., Friedman, L., Rajkowska, G., 1998. Increase in serotonin-1A autoreceptors in the midbrain of suicide victims with major depression-postmortem evidence for decreased

serotonin activity. J Neurosci 18, 7394-7401.

Suehiro, M., Scheffel, U., Ravert, H.T., Dannals, R.F., Wagner, H.N., Jr., 1993. [11C](+)McN5652 as a radiotracer for imaging serotonin uptake sites with PET. Life Sci 53, 883-892.

Sullivan, P.F., Neale, M.C., Kendler, K.S., 2000. Genetic epidemiology of major depression: review and meta-analysis. Am J Psychiatry 157, 1552-1562.

Szabo, Z., Kao, P.F., Scheffel, U., Suehiro, M., Mathews, W.B., Ravert, H.T., Musachio, J.L., Marenco, S., Kim, S.E., Ricaurte, G.A., et al., 1995. Positron emission tomography imaging of serotonin transporters in the human brain using [11C](+)McN5652. Synapse 20, 37-43.

Szabo, Z., McCann, U.D., Wilson, A.A., Scheffel, U., Owonikoko, T., Mathews, W.B., Ravert, H.T., Hilton, J., Dannals, R.F., Ricaurte, G.A., 2002. Comparison of (+)-(11)C-McN5652 and (11)C-DASB as serotonin transporter radioligands under various experimental conditions. J Nucl Med 43, 678-692.

Tadokoro, M., Jones, A.K.P., Cunningham, V.J., Sashin, D., Grootoonk, S., Ashburner, J., Jones, T., 1998. Parametric images of 11C-diprenorphine binding using spectral analysis of dynamic PET images acquired in 3D. . In: Uemura, K., Jones, T., Lassen, N.A., Kanno, I. (Eds.), Quantification of brain function: tracer kinetics and image analysis in brain PET. Excerpta Medica, New York, pp. 289 - 294.

Talbot, P.S., Frankle, W.G., Hwang, D.R., Huang, Y., Suckow, R.F., Slifstein, M., Abi-Dargham, A., Laruelle, M., 2005. Effects of reduced endogenous 5-HT on the in vivo binding of the serotonin transporter radioligand 11C-DASB in healthy humans. Synapse 55, 164-175.

Taylor, M.J., Sen, S., Bhagwagar, Z., 2010. Antidepressant Response and the Serotonin Transporter Gene-Linked Polymorphic Region. Biol Psychiatry.

Taylor, W.D., Steffens, D.C., Payne, M.E., MacFall, J.R., Marchuk, D.A., Svenson, I.K., Krishnan, K.R., 2005. Influence of serotonin transporter promoter region polymorphisms on hippocampal volumes in late-life depression. Arch Gen Psychiatry 62, 537-544.

Testa, C., Laakso, M.P., Sabattoli, F., Rossi, R., Beltramello, A., Soininen, H., Frisoni, G.B., 2004. A comparison between the accuracy of voxel-based

morphometry and hippocampal volumetry in Alzheimer's disease. J Magn Reson Imaging 19, 274-282.

Tipre, D.N., Lu, J.Q., Fujita, M., Ichise, M., Vines, D., Innis, R.B., 2004. Radiation dosimetry estimates for the PET serotonin transporter probe 11C-DASB determined from whole-body imaging in non-human primates. Nucl Med Commun 25, 81-86.

Turecki, G., Briere, R., Dewar, K., Antonetti, T., Lesage, A.D., Seguin, M., Chawky, N., Vanier, C., Alda, M., Joober, R., Benkelfat, C., Rouleau, G.A., 1999. Prediction of level of serotonin 2A receptor binding by serotonin receptor 2A genetic variation in postmortem brain samples from subjects who did or did not commit suicide. Am J Psychiatry 156, 1456-1458.

Turner, R., Jones, T., 2003. Techniques for imaging neuroscience. Br Med Bull 65, 3-20.

Twarog, B.M., Page, I.H., Bailey, H., 1953. Serotonin Content of Some Mammalian Tissues and Urine and a Method for Its Determination. American Journal of Physiology 175, 157-161.

Uebelhack, R., Franke, L., Herold, N., Plotkin, M., Amthauer, H., Felix, R., 2006. Brain and platelet serotonin transporter in humans-correlation between [123I]-ADAM SPECT and serotonergic measurements in platelets. Neurosci Lett 406, 153-158.

Uher, R., McGuffin, P., 2008. The moderation by the serotonin transporter gene of environmental adversity in the aetiology of mental illness: review and methodological analysis. Mol Psychiatry 13, 131-146.

Ustun, T.B., Ayuso-Mateos, J.L., Chatterji, S., Mathers, C., Murray, C.J., 2004. Global burden of depressive disorders in the year 2000. Br J Psychiatry 184, 386-392.

van Dyck, C.H., Malison, R.T., Staley, J.K., Jacobsen, L.K., Seibyl, J.P., Laruelle, M., Baldwin, R.M., Innis, R.B., Gelernter, J., 2004. Central serotonin transporter availability measured with [123I]beta-CIT SPECT in relation to serotonin transporter genotype. Am J Psychiatry 161, 525-531.

Vanhoutte, P.M., 1991. Platelet-derived serotonin, the endothelium, and cardiovascular disease. J Cardiovasc Pharmacol 17 Suppl 5, S6-12.

Watson, C.C., Newport, D., Casey, M.E., 1996. A single scatter simulation technique for scatter correction in 3D pet. Three-Dimensional Image Reconstruction in Radiology and Nuclear Medicine 4, 255-268
317.

Weinberger, D.R., McClure, R.K., 2002. Neurotoxicity, neuroplasticity, and magnetic resonance imaging morphometry: what is happening in the schizophrenic brain? Arch Gen Psychiatry 59, 553-558.

Weissman, A.N., Beck, A.T., 1978. Development and validation of the Dysfunctional Attitude Scale., Association for Advancement of Behavior Therapy., Chicago, IL.

Weissman, M.M., Bland, R., Joyce, P.R., Newman, S., Wells, J.E., Wittchen, H.U., 1993. Sex differences in rates of depression: cross-national perspectives. J Affect Disord 29, 77-84.

Weissman, M.M., Bland, R.C., Canino, G.J., Faravelli, C., Greenwald, S., Hwu, H.G., Joyce, P.R., Karam, E.G., Lee, C.K., Lellouch, J., Lepine, J.P., Newman, S.C., Rubio-Stipec, M., Wells, J.E., Wickramaratne, P.J., Wittchen, H., Yeh, E.K., 1996. Cross-national epidemiology of major depression and bipolar disorder. JAMA 276, 293-299.

Weissman, M.M., Olfson, M., 1995. Depression in women: implications for health care research. Science 269, 799-801.

Whitaker-Azmitia, P.M., 1999. The discovery of serotonin and its role in neuroscience. Neuropsychopharmacology 21, S2-S8.

Willeit, M., Praschak-Rieder, N., Neumeister, A., Pirker, W., Asenbaum, S., Vitouch, O., Tauscher, J., Hilger, E., Stastny, J., Brucke, T., Kasper, S., 2000. [123I]-beta-CIT SPECT imaging shows reduced brain serotonin transporter availability in drug-free depressed patients with seasonal affective disorder. Biol Psychiatry 47, 482-489.

Willeit, M., Stastny, J., Pirker, W., Praschak-Rieder, N., Neumeister, A., Asenbaum, S., Tauscher, J., Fuchs, K., Sieghart, W., Hornik, K., Aschauer, H.N., Brucke, T., Kasper, S., 2001. No evidence for in vivo regulation of midbrain serotonin transporter availability by serotonin transporter promoter gene polymorphism. Biol Psychiatry 50, 8-12.

Williams, J.B., Spitzer, R.L., Gibbon, M., 1992. International reliability of a diagnostic intake procedure for panic disorder. Am J Psychiatry 149, 560-562.

Willis-Owen, S.A., Turri, M.G., Munafo, M.R., Surtees, P.G., Wainwright, N.W., Brixey, R.D., Flint, J., 2005. The serotonin transporter length polymorphism, neuroticism, and depression: a comprehensive assessment of association. Biol Psychiatry 58, 451-456.

Wilson, A.A., Ginovart, N., Hussey, D., Meyer, J., Houle, S., 2002. In vitro and in vivo characterisation of [11C]-DASB: a probe for in vivo measurements of the serotonin transporter by positron emission tomography. Nucl Med Biol 29, 509-515.

Wilson, A.A., Ginovart, N., Schmidt, M., Meyer, J.H., Threlkeld, P.G., Houle, S., 2000. Novel radiotracers for imaging the serotonin transporter by positron emission tomography: synthesis, radiosynthesis, and in vitro and ex vivo evaluation of (11)C-labeled 2-(phenylthio)araalkylamines. J Med Chem 43, 3103-3110.

Woolley, D.W., Shaw, E., 1954. Some Neurophysiological Aspects of Serotonin. British Medical Journal 2, 122-126.

Xu, M., Luk, W.K., Cutler, P.D., Digby, W.M., 1994. Local Threshold for Segmented Attenuation Correction of Pet Imaging of the Thorax. Ieee Transactions on Nuclear Science 41, 1532-1537.

Yatham, L.N., Liddle, P.F., Shiah, I.S., Scarrow, G., Lam, R.W., Adam, M.J., Zis, A.P., Ruth, T.J., 2000. Brain serotonin2 receptors in major depression: a positron emission tomography study. Arch Gen Psychiatry 57, 850-858.

Yau, J.L., Kelly, P.A., Olsson, T., Noble, J., Seckl, J.R., 1999. Chronic amitriptyline administration increases serotonin transporter binding sites in the hippocampus of aged rats. Neurosci Lett 261, 183-185.

Young, K.A., Holcomb, L.A., Bonkale, W.L., Hicks, P.B., Yazdani, U., German, D.C., 2007. 5HTTLPR polymorphism and enlargement of the pulvinar: unlocking the backdoor to the limbic system. Biol Psychiatry 61, 813-818.

Young, S.N., Smith, S.E., Pihl, R.O., Ervin, F.R., 1985. Tryptophan depletion causes a rapid lowering of mood in normal males. Psychopharmacology (Berl) 87, 173-177.

Zahniser, N.R., Doolen, S., 2001. Chronic and acute regulation of Na+/Cl- -dependent neurotransmitter transporters: drugs, substrates, presynaptic receptors, and signaling systems. Pharmacol Ther 92, 21-55.

Zhang, Y., Brady, M., Smith, S., 2001. Segmentation of brain MR images through a hidden Markov random field model and the expectation-maximization algorithm. IEEE Trans Med Imaging 20, 45-57.